Comparative assessment of a novel photo-anthropometric landmark-positioning approach for the analysis of facial structures on two-dimensional images

Text pages: 25 pages

Figures: 4

Tables: 4 (pp. 21-24)

Supporting information: one document (SI, 70 pages)

ABSTRACT

Positioning landmarks in facial photo-anthropometry (FPA) applications remains today a highly variable procedure, as traditional cephalometric definitions are used as guidelines. Herein, a novel landmark-positioning approach, specifically adapted for FPA applications, is introduced and, in particular, assessed against the conventional cephalometric definitions for the analysis of 16 landmarks on ten frontal images by two groups of examiners (with and without professional knowledge of anatomy). Results showed that positioning reproducibility was significantly better using the novel method. Indeed, in contrast to the classic approach, very low landmark dispersions were observed for both groups of examiners, which were usually below the strictest clinical standards (i.e., 0.575 mm). Furthermore, the comparison between the two groups of examiners highlighted higher dispersion consistencies, which supported a higher robustness. Thus, the use of an adapted landmark-positioning approach proved to be highly advantageous in FPA analysis and future work in this field should consider adopting similar methodologies.

KEYWORDS: forensic science, facial analysis, anthropometry, cephalometry, facial identification, facial image

Facial photo-anthropometry (FPA) is the sub-field of physical anthropology that deals with the systematic study and measurement of human facial traits from two-dimensional images (1-3). Since facial measurements have been correlated with several individual characteristics, FPA has found large applications in a number of scientific fields in which the analysis of faces on two dimensional images is of interest (1, 3, 4). In legal medicine and forensic science, in particular, different studies reported the possibility of using FPA to estimate the age of individuals (5-7), to predict their sex or ancestry (8, 9), to simulate facial growth or age progression (7, 10), as well as to support human identification by comparing captured facial images to reference ones, i.e. forensic facial identification (FFI) (1, 11, 12).

The first step in every FPA application involves the placement of a number of reference points (i.e., landmarks) on the facial images of the analyzed individuals, which is a process conventionally performed by following definitions used in classic facial anthropometry (or, as it is also called, cephalometry) (1, 3, 13). Traditional cephalometric definitions, however, merely describe a series of purely anatomical structures lying on the skin surface and/or the underlying bones and were primarily established for the purpose of directly mapping actual living subjects or their lateral-view X-ray image for medical purposes (14-16). Consequently, their adoption in FPA applications usually leads to a high positioning variability within and between examiners (17-22). The main reason for this arises from the fact that different examiners may have different interpretations of where a specific cephalometric landmark should be placed on a two-dimensional, frontal view, facial image, without any three-dimensional reference and/or the possibility to touch the subject's actual facial surface. As a result of this, the general reliability of FPA has been recently challenged by the scientific community (17-19, 23). One significant aftermath, in particular, has been the recommendation from the Facial

Identification Scientific Working Group (FISWG) to avoid using FPA-based methodologies as proof of evidence in FFI (21).

Even if it is acknowledged that the application of FPA-based methodologies may be difficult and inadequate in a number of situations, such as those involving low resolution and/or non-frontal facial images, in several others it is not and may actually be beneficial. This is the case, for example, in those situations where images are acquired under sufficiently standardized conditions, such as in the detection of identity document fraud or age estimation from portrait images (17, 20, 23, 24). To guarantee highly reliable results, however, a high reproducibility in landmark location is still essential and improvements would therefore be necessary (22, 23, 25). In particular, it is advised that the aforementioned reproducibility issues may be reduced through the use of proper landmark descriptions and/or locating procedures optimized for FPA applications, which thus take into account the specific problems encountered when positioning landmarks on two-dimensional facial images.

Despite the numerous works in FPA, however, none have previously proposed this kind of adapted protocol, leaving a gap in the specialized literature. Recently, a novel FPA-specific landmark approach was suggested by Flores et al. (28). In addition to a complete series of descriptions for landmarks based on visual references, the work also included optimized operational procedures and illustrations to locate each landmark of interest on two-dimensional images. These are intended to better assist examiners in FPA analysis and thus improve both the reproducibility and robustness of the landmark placement procedure. The approach has nonetheless never been assessed. Consequently, the current work aimed to undertake this and, in particular, to evaluate the improvement in reliability from using this adapted approach (hereafter, AdMet) over the classic, cephalometry-based one (hereafter, ClMet).

In order to achieve these aims, the two approaches were applied to a set of ten frontal view facial images and variability of the placement of specific landmarks between different examiners (i.e., reproducibility) investigated through their spatial dispersions around the grand means. Two groups of examiners, composed of individuals with and without specific knowledge of anatomy, respectively, took part in the experiment. This was done in order to assess the robustness of the approaches with respect to the experience level of the examiner. Observed landmark dispersions were finally compared to clinical standards currently accepted in cephalometry, by converting pixel-based values to millimeters through iris ratio calibration (7, 26, 27). To our knowledge, this is the first time that the adapted, FPA-optimized landmark-positioning previously reported by Flores et al. (28) has been evaluated in published literature. It is also the first time that a comparative study between different landmark-positioning approaches for FPA analysis has been carried out, as well as that their relative reliabilities have been investigated and validated against previously reported clinical standards.

Materials and methods

Reference facial images

Ten frontal view facial images (from five male and five female subjects) were randomly selected from a larger database composed of 500 Brazilian frontal view images. For capture, subjects were asked to adopt a neutral facial expression and their faces were aligned with the Frankfurt plane. All the two-dimensional images were acquired using a Geometrix FaceVision® FV802 Series Biometric Camera (ALIVE Tech, Cumming, GA), with no interchangeable lenses, and positioned at 1.2 m from the individual's face, at a resolution of 1,200 x 1,600 pixels.

FPA analysis

Two groups of examiners were selected. The first group, named experts group (EG), was composed of five examiners with specific knowledge of anatomy (master or doctoral students in medical or dental areas), as well as previous experience in anthropometry and/or cephalometry. The second group, named non-experts group (NG), was composed of five examiners with higher education in scientific fields out of medical sciences, with neither training or specific knowledge of anatomy nor previous experience in anthropometry and/or cephalometry.

Both groups were asked to map the previously selected facial images according to two different landmark-positioning approaches: a classic method (ClMet) and a newly developed adapted method (AdMet). Generally, the mapping involved placing 16 specific landmarks on facial images, 8 odd (medians) and 8 even (laterals), as shown in Fig. 1. For ClMet, examiners were provided with a list of definitions for the 16 landmarks, previously compiled from a set of particularly influential works in craniofacial anthropometry (29-31) (Table 1). For AdMet, examiners were provided with the respective definitions and operational marking procedures obtained from the work of Flores et al. (28). This approach has been translated into a manual that is publicly available at http://facisgroup.org/facial_landmarks and included in Supporting Information (SI).

The AdMet approach provides the examiner with clearer reference points that explicitly mention visible facial features instead of being solely based on anatomical structures. Furthermore, each described facial landmark includes a brief operational procedure and graphical illustrations, intended to better support locating it on images. The difference between ClMet and AdMet can easily be highlighted through an example. The ectocanthion landmark is conventionally defined as: "*the lateral corner (angle) of the eye*" (29-31). The newly adapted approach (28), on the contrary, reports the following definition: "*The most lateral landmark in the corner of the eye (distant from the midline),*

where the upper and lower ciliary implantation lines meet" (p. 07). The following positioning procedure is also provided: "*Move the vertical line from lateral to medial side of the face to the landmark where the upper and lower ciliary lines meet in the region of lateral angle of the eye. Then, move the horizontal line until the point of convergence of those lines. Mark ectocanthion in the intersection region between the two auxiliary lines*" (p. 07). See Fig. 2 for an illustration of the corresponding page of the manual (SI). The manual describes a total of 36 landmarks. For the sake of comparison, however, only the 16 for which cephalometric definitions could be applied were selected in this work.

The FPA analyses with the two different landmark-positioning approaches were carried out by the same participants, with a month interval in between (starting from ClMet), in order to minimize memory effects on landmark placement. For each approach, examiners were asked to analyze the same 10 facial images in triplicate, again with a week interval in between. For mapping, a non-commercial software package for two-dimensional facial analysis was used, i.e. SAFF-2D® (Forensic Facial Analysis System, Department of Federal Police, Brazil). The software allows examiners to locate the facial landmarks on images and to automatically register them through Cartesian coordinates (X, Y).

Data treatment

Initially, for each replicate experiment, average coordinates for all 16 landmarks were calculated for the three analyses. Then, differences (in pixels, px) on both the horizontal and vertical axes were determined between these average coordinates and the grand between-faces means. Location dispersions were defined as the mean differences on the horizontal axis (D_X) and mean differences on the vertical axis (D_Y). The arithmetic mean between these two values, i.e. the mean dispersion (D_{MXY}), was also determined as summary statistics (17).

Values for D_X, D_Y and D_{MXY} were then converted into an actual physical scale (i.e., from px to mm) by applying a scaling factor of 4.35 px mm^{-1}, in order to allow comparison of observed dispersions with previously published clinical standards. This scaling factor was previously determined by size comparison of a reference anatomical structure measured from images and real persons. The iris diameter was used for this purpose, as it has previously been proved to be an adequate reference for facial image calibration (7, 26, 27). Considering that the average iris diameter in images was calculated to be around 50 pixels and that the maximum population value of the horizontal visible iris diameter (HVID) is described in specific literature as around 11.5 mm (32-34), a ratio of 4.35 px mm^{-1} was determined. Converted dispersions were referred to as "estimated real dispersions" (ERD), i.e. ERD_X, ERD_Y and ERD_{MXY} (17).

Results assessment

The normality of the data was initially assessed by the Shapiro-Wilk test and the intra-examiner marking reliability by the intra-class correlation coefficient (ICC). Analysis of variance was applied to assess any significant differences between the dispersion values resulting from the tested factors (i.e., the expert groups and FPA protocols). This was performed using marginal linear regressions with gamma distribution for the errors. Results of all these statistical analyses were assessed against a statistical significance level of 5% ($\alpha = 0.05$).

For clinical validation, ERD values were compared against reference thresholds previously reported in the literature. In this respect, values smaller than 0.575 mm were considered ideal, based on the most strict references in cephalometry (13) (mean between 0.59 mm and 0.56 mm), while values between 0.575 and 1 mm were considered acceptable (14, 25, 35-38). ERD values greater than 1 mm were considered undesirable.

Results

General statistical analysis

Firstly, the normality of the data was assessed. The Shapiro-Wilk test indicated that the data were not normally distributed and, thus, a non-parametric statistical analysis was subsequently conducted. The ICC test results showed that the intra-examiner scores were reliable (ICC > 0.75) for both EG and NG (i.e., the groups of expert and non-expert examiners, respectively) using both tested FPA approaches, i.e. ClMet and AdMet.

Application of ClMet

Location dispersions for the 16 landmarks were calculated for both positioning approaches and were reported in Table 2 (values in px, i.e. D_x, D_y, and D_{MXY}), and Table 3 (values converted in mm, i.e. ERD_x, ERD_y and ERD_{MXY}). A graphical comparison of D_{MXY} and the analysis of effects are furthermore displayed in Fig. 3 and 4, respectively.

Using ClMet, the two groups of examiners performed the landmark positionings very differently, with EG showing significantly better results than NG. In fact, the mean D_{MXY} values were 3.244 px (0.746 mm) and 9.160 px (2.106 mm) for NG and EG, respectively, which corresponds to a difference greater than 2.8 times. The highest D_{MXY} for NG (i.e., 39.221 px or 9.016 mm for G) was almost 4 times larger than the highest D_{MXY} for EG (i.e., 10.517 px or 2.418 mm for Go). Furthermore, 12 of the 16 landmarks (Al, Ch, En, G, Gn, Go, Il, Im, Li, N, Sn, and Zy) were significantly more dispersed for NG than for EG. Consequently, positioning performances with ClMet were proved to be strongly dependent on the previous anatomical knowledge and/or experience of the examiners, with more experienced examiners providing significantly more reproducible results.

More generally, Go, G, Zy, and N showed the largest dispersions in both groups of examiners and were thus the most difficult landmarks to positioning. On the contrary, En, Sn, and Sto were generally within the 5 least dispersed landmarks overall.

Adoption of AdMet

Adoption of AdMet resulted in a significant decrease in the dispersion of landmark placement for both groups of examiners. This was particularly true for NG. Indeed, its mean D_{MXY} passed from 9.160 px (2.106 mm) to 1.754 px (0.403mm), compared to a decrease from 3.244 px (0.746 mm) to 1.616 px (0.372 mm) for EG. A statistically significant decrease was furthermore observed in the positioning dispersion of 13 of the 16 landmarks (Al, Ch, Ec, G, Gn, Go, Il, Im, Li, Ls, N, Sto, and Zy) for NG, and in that of 10 of the 16 landmarks (Al, Ec, G, Go, Il, Im, Lm, Ls, N, and Zy) for EG. These results together proved that the use of AdMet actually significantly improved reproducibility in landmark positioning, independent from previous anatomical knowledge and/or experience of the examiner. A simultaneous increase in the positioning dispersion of 2 of the 16 landmarks (Sn and Ch) was, nevertheless, detected for EG. Even if statistically significant, however, this was still really small on a physical scale and thus considered negligible from a practical point of view (Fig. 4).

Comparison of the results obtained by the two groups of examiners between themselves showed that, on average, they performed very similarly when the novel landmark-positioning approach was used. In fact, the respective mean D_{MXY} values were largely consistent (1.616 px or 0.372 mm for EG, and 1.754 px or 0.403 mm for NG). Perhaps surprising, however, was that dispersion results for the single landmarks showed that, from a statistical point of view, a higher number of landmarks were more reproducibly positioned by NG compared to EG. Indeed, 7 over 16 landmarks (Ch, Gn, Go, Li, Ls, N, and Sto) showed significantly lower D_{MXY} values for NG than for EG when

AdMet was used, while only 1 of 16 (Zy) showed a significantly larger D_{MXY}. Again, the differences in dispersion for all these landmarks (but Zy) were very small on a physical scale and, thus, considered inconsequential from a practical point of view (Fig. 4). Hence, it could be concluded that AdMet allowed for a higher degree of robustness in landmark positioning between examiners with different anatomical knowledge and/or experience. The only exception was the placement of Zy, for which previous knowledge and/or experience seemed particularly important.

More generally, the positioning of Zy resulted in relatively high D_{MXY} values for both groups of examiners, especially when compared to the other landmarks. This was particularly true for NG, as the D_{MXY} for this landmark was 8.104 px (1.863 mm) against 3.939 px (0.906 mm) for EG. The dispersions of the other 3 landmarks that showed particularly high D_{MXY} using ClMet (i.e., G, N, and Go) were significantly decreased through the use of AdMet.

Clinical validation

In order to validate the approach against clinically accepted standards, estimated real mean dispersion (ERD_{MXY}) values were compared to reference thresholds previously reported in the cephalometric literature (Table 4). A complete comparison for all ERD values (i.e., ERD_x, ERD_y, and ERD_{MXY}) is further available in Table 3.

ClMet led to ERD_{MXY} within ideal or acceptable limits (i.e., ≤ 1 mm) for several landmarks when used by both groups of examiners (12 landmarks for EG and 9 for NG). A significant number of landmarks, however, showed ERD_{MXY} above acceptable limits (i.e., > 1 mm); these were, namely, 4 landmarks for EG (i.e., G, Go, N, and Zy) and 7 for NG (i.e., G, Go, Il, Im, Li, N, and Zy). For NG, in particular, G, Go, N, and Zy showed ERD_{MXY} larger than 3 mm, which were considered especially high. When AdMet was used, none of the landmarks showed ERD_{MXY} above acceptable limits for either group of

examiners, except 1 for NG (i.e., Zy). More specifically, 14 landmarks were generally within the ideal range (i.e., < 0.575 mm). This showed the higher validity of AdMet when compared with previously reported clinical standards.

Discussion

Physical anthropology is a well-established tool for the extraction, interpretation, and classification of the human body within industrial, medical, orthodontic and forensic applications (14, 25, 30, 31). In recent decades, the increasingly widespread use of digital imaging devices has highlighted the necessity of bringing its precepts to indirect, 2D-image contexts. Starting from the assumption that all FPA-based analyses (e.g. establishment of measures, angles, ratios, and indexes) rely on the previous determination of landmarks, evaluating the particular variation regarding their positioning is a necessary step for its safe and reliable application (1, 2, 12, 13).

Although landmark-positioning variability has been a commonly addressed issue in the scientific community, its assessment and improvement for uses on photographs have been scarce. In particular, no studies have ever proposed conceptual adaptations to the definition of landmarks for image-based applications, while those that have addressed FPA-positioning variability used non-specific landmark-positioning approaches (i.e., cephalometric definitions). As a consequence, doubts can be raised concerning the proper and reliable attribution of the investigated landmarks (6, 17, 19). Recently, an alternative nomenclature (i.e., capulometric landmarks) has been tentatively proposed for the analysis of 2D images (22). Again, nonetheless, no visual references were implemented, resulting in a set of definitions very similar to the classic cephalometric ones. The lack of a standardized set of landmarks and protocols specific to FPA analysis should be viewed with concern because, depending on the scientific field

of interest, errors may lead to misunderstandings in diagnosis/treatment or even to improper characterization and/or classification of a specific population or individual (3, 7).

Classifying human features into class or individual characteristic is a constant practice in forensic science. A proper population survey of a specific facial feature, whether morphological or photo-anthropometrical, is necessary to determine its importance in the human individualization process and to statistically support the quantification and decision of an identification match (20, 39, 40). As a result of its inherent potential to make image-based facial analysis more objective, systematic and reproducible, FPA has promising capabilities for the analytical survey of facial structures along with the high possibility of automatization. This is a step forward for the evaluation of large databases, as well for understanding human facial variation. In this sense, generating landmark-specific variability information according to the adopted methodology is of utmost importance, by determining the extent to which each one can provide reliable facial relationships to support forthcoming statistical associations.

In the present study, as expected, the use of classical cephalometric descriptions led to low reproducibilities between the examiners in positioning the 16 investigated landmarks on facial images. Indeed, ERD_{MXY} values for most of them were above an ideal limit threshold, and this was true not only for non-expert examiners, but also for expert ones. More specifically, only 9 of the 16 landmarks showed ERD_{MXY} values within an ideal error range when positioned by expert examiners, and 4 of 16 had ERD_{MXY} values above an acceptable threshold.

Observed dispersions, furthermore, showed an overall low consistency between the two groups of examiners, with non-experts particularly struggling with placing landmarks on facial images in a reproducible way, as demonstrated by their significantly bigger inter-variability. This suggests a low robustness of the classic landmark-positioning method with respect to the experience level of the examiners and, in

particular, that previous anatomical knowledge and/or experience in the procedure are necessary in order to properly understand traditional cephalometric descriptions and locate the corresponding structures on facial images.

The positioning of Go, G, Zy, and N on frontal facial images proved to be particularly challenging following the traditional cephalometric descriptions, as proved by their very high dispersions amongst all the examiners (especially non-experts). This is a serious problem that may affect the usefulness of the traditional landmark method in many FPA applications. Indeed, these four specific landmarks are involved in the establishment of some of the most characteristic facial measurements and indices (14, 29), such as the facial height (N - Gn), facial width (Zy - Zy), mandibular width (Go - Go), facial length index (N - Gn / Zy - Zy), mandibulo-facial index (Go - Go / Zy - Zy) and naso-chelion angle (Ch - N - Ch). The same observation has, nonetheless, already been reported in a number of previous studies (6, 17, 22, 35, 41, 42) and may be explained by the fact that the traditional cephalometric descriptions for these four landmarks largely rely on physical and/or bone structures, which are particularly difficult to detect on frontal images. As a proof, the opposite trend could actually be seen for landmarks such as Ch and Sto, for which traditional cephalometric definitions rely more strongly on facial structures visible on images (6, 22).

The adoption of adapted and FPA-specific landmark definitions positively enhanced the performance of positioning the 16 investigated landmarks on facial images and, thus, of the general FPA procedure. Undeniably, placement reproducibility between examiners was significantly improved. All the landmarks showed ERD_{MXY} within acceptable limit thresholds when placed by expert examiners, contrary to that observed when classic cephalometric definitions were used. Even more notably, 14 of 16 landmarks showed ERD_{MXY} values within ideal limit thresholds. In contrast, landmark dispersions showed a better consistency between experts and non-experts. This finding

supports the higher robustness of the adapted landmark approach with respect to the experience level of the examiners. Furthermore, it is also consistent with the conclusion that the most relevant factor in the correct positioning of landmarks on facial images is not necessarily the examiner's previous knowledge in facial anatomy or their experience in the procedure, but rather the accuracy of the landmark descriptions themselves. In this regard, an FPA-optimized approach is more helpful than a cephalometry-based one, as the latter is essentially based on descriptions of underlying anatomical structures.

The use of adapted landmark definitions also solved the high positioning variability of G, N and Go that is observed when using the classic cephalometric approach; an improvement that, by itself, is prone to significantly enhance the general reliability of FPA in most applications. Placement of Zy, however, still resulted in high ERD_{MXY} for both groups of examiners, which confirms its particular complexity in being positioned on facial images. Nonetheless, after a more detailed inspection, it can be observed that its dispersion on the vertical axis (ERD_Y) more significantly contributes to ERD_{MXY} than its dispersion on the horizontal axis (ERD_X), and that the latter is almost negligible and within an ideal threshold after using an adapted landmark-positioning approach. In this regard, it is important to highlight that errors in the vertical and horizontal directions may be of substantial importance depending on the specific application and/or landmark. Zy, in particular, is most frequently used in horizontal measurements (e.g., facial width) and related indices (e.g., facial length index) (14, 29), and thus the use of an adapted approach may actually allow a more efficient use of this landmark. In any case, further improvements to the landmark descriptions may be implemented in order to also take into account the variability on the vertical axis and bring ERD_Y to within an acceptable dispersion range.

Conclusion

In this work, the use of an adapted approach for landmark facial images based on descriptions and locating procedures optimized for FPA analysis has been assessed and compared against a traditional approach based on classic cephalometric descriptions. Results showed that the use of conventional cephalometric descriptions led to a low reproducibility between examiners in positioning landmarks and, more importantly, to a low consistency in the positioning dispersions between experts and non-experts. This suggested that previous anatomical knowledge and/or experience is necessary in order to correctly apply traditional cephalometric descriptions. The use of adapted landmark definitions, on the contrary, significantly decreased the landmark dispersion between examiners, whilst also reducing the differences arising from experience level. This second observation, in particular, supported the conclusion that the most relevant factor in the correct positioning of landmarks on facial images is not necessarily the examiner's knowledge about facial anatomy, but instead the accuracy of landmark descriptions and the application of an approach based on clear visual references.

Thus, the use of an adapted landmark-positioning approach proved to be highly advantageous in FPA analysis and future work in this field should consider adopting similar methodologies. In particular, the adapted approach specifically used in this research performed well and may be implemented in future FPA applications.

References

1. Davis J, Valentine T, Davis R. Computer assisted photo-anthropometric analyses of full-face and profile facial images. Forensic Sci Int 2010 Jul;200(1-3):165–76.

2. İşcan M. Introduction to techniques for photographic comparison: potentials and problems. In: İşcan M, Helmer R, editors. Forensic Analysis of the Skull: Craniofacial Analysis, Reconstruction, and Identification. New York, NY: Wiley-Liss; 1993;57–70.

3. Stavrianos C, Papadopoulos C, Pantelidou O, Emmanouil J, Pentalotis N, Tatsis

D. The use of photoanthropometry in facial mapping. Research J Medical Sci 2012;6(4):4.

4. Moreton R, Morley J. Investigation into the use of photoanthropometry in facial image comparison. Forensic Sci Int 2011 Oct;212(1-3):231–7.

5. Borges DL, Vidal FB, Flores MRP, Melani RFH, Guimarães MA, Machado CEP. Photoanthropometric face iridial proportions for age estimation: An investigation using features selected via a joint mutual information criterion. Forensic Sci Int 2018 Mar;284:9–14.

6. Cattaneo C, Obertová Z, Ratnayake M, Marasciuolo L, Tutkuviene J, Poppa P, et al. Can facial proportions taken from images be of use for ageing in cases of suspected child pornography? A pilot study. Int J Legal Med 2012 Jan;126(1):139–44.

7. Machado CEP, Flores MRP, Lima LNC, Tinoco RLR, Franco A, Bezerra ACB, et al. A new approach for the analysis of facial growth and age estimation: Iris ratio. PLoS One 2017;12(7):e0180330.

8. Adamu L, Ojo S, Danborno B, Adebisi S, Taura M. Sex determination using facial linear dimensions and angles among Hausa population of Kano State, Nigeria. Egyptian J Forensic Sci 2016;6:28.

9. Packiriswamy V, Bashour M, Nayak S. Anthropometric Analysis of the South Indian Woman's Nose. Facial Plast Surg 2016 Jun;32(3):304–8.

10. Ramanathan N, Chellappa R. Modeling age progression in young faces. IEEE Computer Society Conference on Computer Vision and Pattern Recognition, 2006; New York, NY: CVPR, 2006;387–94.

11. Porter G, Doran G. An anatomical and photographic technique for forensic facial identification. Forensic Sci Int 2000 Nov;114(2):97–105.

12. Halberstein RA. The application of anthropometric indices in forensic photography: three case studies. J Forensic Sci 2001 Nov;46(6):1438–41.

13. Trpkova B, Major P, Prasad N, Nebbe B. Cephalometric landmarks identification and reproducibility: a meta analysis. Am J Orthod Dentofacial Orthop 1997 Aug;112(2):165–70.

14. Farkas L. Anthropometry of the Head and Face. 2nd ed. New York, NY: Raven Press, 1994.

15. Shishkin KM, Arsenina OI, Shishkin MK, Popova NV. Cephalometry efficacy in orthodontic treatment planning: correlations of cephalometric values and their changes in the course of treatment. Stomatologia 2017;96(4):36–7.

16. Esenlik E, Plana NM, Grayson BH, Flores RL. Cephalometric Predictors of Clinical Severity in Treacher Collins Syndrome. Plast Reconstr Surg 2017 Dec;140(6):1240–9.

17. Campomanes-Álvarez B, Ibáñez O, Navarro F, Alemán I, Cordón O, Damas S. Dispersion assessment in the location of facial landmarks on photographs. Int J Legal Med 2015 Jan;129(1):227–36.

18. Cattaneo C, Ritz-Timme S, Gabriel P, Gibelli D, Giudici E, Poppa P, et al. The difficult issue of age assessment on pedo-pornographic material. Forensic Sci Int 2009 Jan;183(1-3):21–4.

19. Lucas T, Kumaratilake J, Henneber M. Metric Identification of the Same People from Images: How Reliable Is It? J Anthropology 2016 June;2016(1):1–10.

20. Cummaudo M, Guerzoni M, Marasciuolo L, Gibelli D, Cigada A, Obertovà Z, et al. Pitfalls at the root of facial assessment on photographs: a quantitative study of accuracy in positioning facial landmarks. Int J Legal Med 2013 May;127(3):699–706.

21. FISWG. Guidelines for Facial Comparison Methods; www.fiswg.org (accessed July 22, 2018).

22. Caple J, Stephan CN. A standardized nomenclature for craniofacial and facial anthropometry. Int J Legal Med 2016 May;130(3):863–79.

23. Lee WJ, Kim DM, Lee UY, Cho JH, Kim MS, Hong JH, et al. A Preliminary Study

of the Reliability of Anatomical Facial Landmarks Used in Facial Comparison. J Forensic Sci 2018 Aug:1–9.

24. Wilkinson C, Evans R. Are facial image analysis experts any better than the general public at identifying individuals from CCTV images? Sci Justice 2009 Sep;49(3):191–6.

25. Farkas L. Accuracy of Anthropometric Measurements: Past, Present, and Future. Cleft Palate-Craniofacial J 1996;33:10–22.

26. Driessen J, Vuyk H, Borgstein J. New insights into facial anthropometry in digital photographs using iris dependent calibration. Int J Pediatr Otorhinolaryngol 2011 Apr;75(4):579–84.

27. Miot H, Pivotto D, Jorge E, Mazeto G. Evaluation of oculometric parameters by facial digital photography: use of iris diameter as a reference. Arq Bras Oftalmol 2008 Sep-Oct;71(5):679–83.

28. Flores MRP, Machado CEP, Silva RHA. Proposta de Análise Facial Fotoantropométrica em norma frontal: Metodologia descritiva dos pontos anatômicos de referência [Photo-anthropometric facial analysis in frontal view images: descriptive methodology proposal for anatomical landmarks]. Novas Edições Acadêmicas, 2017; http://facisgroup.org/facial_landmarks (accessed August 11, 2018).

29. George R. Facial Geometry: Graphic Facial Analysis for Forensic Artists. Springfield, MO: Charles C Thomas Publisher, 2007.

30. Kolar J, Salter E. Craniofacial anthropometry: practical measurement of the head and face for clinical, surgical, and research use. Springfield, MO: Charles C Thomas Publisher, 1997.

31. Zimbler M, Ham J. Aesthetic Facial Analysis. Cummings Otolaryngology Head and Neck Surgery 2005:517–8.

32. Hickson-Curran S, Young G, Brennan N, Hunt C. Chinese and Caucasian ocular

topography and soft contact lens fit. Clin Exp Optom 2016 Mar;99(2):149–56.

33. Ronneburger A, Basarab J, Howland H. Growth of the cornea from infancy to adolescence. Ophthalmic Physiol Opt 2006 Jan;26(1):80–7.

34. Martin D, Holden B. A new method for measuring the diameter of the in vivo human cornea. Am J Optom Physiol Opt 1982 May;59(5):436–41.

35. Aksu M, Kaya D, Kocadereli I. Reliability of reference distances used in photogrammetry. Angle Orthod 2010 Jul;80(4):482–9.

36. Forsyth D, Davis D. Assessment of an automated cephalometric analysis system. Eur J Orthod 1996 Oct;18(5):471–8.

37. Richardson A. A comparison of traditional and computerized methods of cephalometric analysis. Eur J Orthod 1981;3(1):15–20.

38. Strauss R, Weis B, Lindauer S, Rebellato J, Isaacson R. Variability of facial photographs for use in treatment planning for orthodontics and orthognathic surgery. Int J Adult Orthodon Orthognath Surg 1997;12(3):197–203.

39. Mallett XD, Dryden I, Bruegge RV, Evison M. An exploration of sample representativeness in anthropometric facial comparison. J Forensic Sci 2010 Jul;55(4):1025–31.

40. Evison M, Dryden I, Fieller N, Mallett X, Morecroft L, Schofield D, et al. Key parameters of face shape variation in 3D in a large sample. J Forensic Sci 2010 Jan;55(1):159–62.

41. Bishara S, Cummins D, Jorgensen G, Jakobsen J. A computer assisted photogrammetric analysis of soft tissue changes after orthodontic treatment. Part I: Methodology and reliability. Am J Orthod Dentofacial Orthop 1995 Jun;107(7):633–9.

42. Farkas L, Bryson W, Klotz J. Is photogrammetry of the face reliable? Plast Reconstr Surg 1980 Sep;66(3):346–55.

TABLE 1—*List of the 16 investigated facial landmarks, with the corresponding sets of adopted cephalometric and facial photo-anthropometric (FPA) descriptions (used in the ClMet and AdMet landmark-positioning approaches, respectively). Cephalometric descriptions were compiled from those reported by George (29), Kolar and Salter (30), and Zimbler and Ham (31). FPA-specific descriptions were extracted from the FPA manual provided in the Supplementary Information (SI) and the corresponding pages are reported in the table.*

#	*Landmark*	*Abbr.*	*Cephalometric description (ClMet)*	*FPA description (AdMet)*
1	Ectocanthion	Ec	The lateral corner (angle) of the eye.	Pg. 07
2	Endocanthion	En	The medial angle of the eye. Medial corner of the eye where the eyelids meet, not in the caruncles (reddish eminence in the medial region of the eye).	Pg. 10
3	Iridion laterale	Il	The most lateral point of the iris rim.	Pg. 13
4	Iridion mediale	Im	The most medial point of the iris rim.	Pg. 14
5	Glabella	G	The most prominent region in the midsagittal plane between supraorbital arches.	Pg. 65
6	Nasion	N	Median point at the nasal root (apex of the frontonasal angle).	Pg. 66
7	Subnasal	Sn	Midpoint of the base of the columella, underneath the nasal spine.	Pg. 33
8	Alare	Al	The most lateral point of the nose wing. The most lateral point of the curvature of the nasal wing.	Pg. 35
9	Chelion	Ch	The corner of the mouth. The region of encounter of upper and lower lip vermilion border.	Pg. 42
10	Labiale superius	Ls	The midpoint (at the midsagittal plane) of the upper lip vermilion border.	Pg. 40
11	Stomion	Sto	The encounter of upper and lower lip at the midsagittal plane when lips are naturally closed.	Pg. 46
12	Labiale inferius	Li	The midpoint (at the midsagittal plane) of the lower lip vermilion border.	Pg. 47
13	Labiomentale	Lm	Point of greatest depression between the lower lip and the menton (at the mentolabial sulcus).	Pg. 48
14	Gnathion	Gn	The lowest point of menton edge, at the midsagittal plane.	Pg. 49
15	Gonion	Go	The most lateral point of the mandible angle. The widest point of the mandible.	Pg. 50
16	Zygion	Zy	The most lateral point (greater width) of the zygomatic bone (cheek).	Pg. 52

TABLE 2—*Summary dispersion statistics (in px) for the 16 investigated landmarks according to the group of examiners (EG vs. NG) and the applied landmark-positioning approach (ClMet vs. AdMet).*

Landmark	D	ClMet						AdMet					
		EG			NG			EG			NG		
		Mean	SD	Rank	Mean	SD	Rank	Mean	SD	Rank	Mean	SD	Rank
Al	D_X	0.812	0.731	14	1.057	0.871	16	0.548	0.440	14	0.681	0.602	14
	D_Y	2.411	1.859	7	3.502	2.722	8	1.440	1.161	7	1.588	1.530	7
	D_{MXY}	1.609	1.027	9	2.281	1.534	13	1.031	0.651	12	1.126	0.847	11
Ch	D_X	1.842	1.455	8	4.590	4.017	5	3.182	2.238	1	2.313	1.946	1
	D_Y	0.637	0.536	16	1.056	0.831	15	1.018	0.842	11	0.678	0.588	14
	D_{MXY}	1.239	0.812	11	2.832	2.113	10	2.102	1.255	3	1.521	1.031	5
Ec	D_X	3.858	2.433	2	4.166	2.676	6	2.088	1.784	3	2.041	1.587	3
	D_Y	1.321	0.938	9	1.678	1.217	13	1.340	1.017	8	1.887	1.611	4
	D_{MXY}	2.593	1.422	7	2.922	1.503	9	1.721	1.128	6	1.966	1.212	3
En	D_X	1.304	1.061	12	2.286	1.930	12	1.366	1.304	8	1.790	1.621	4
	D_Y	0.860	0.704	14	1.144	0.855	14	1.024	0.773	10	1.069	1.037	9
	D_{MXY}	1.077	0.688	14	1.723	1.222	15	1.202	0.826	11	1.426	1.207	7
G	D_X	2.839	2.492	3	2.718	1.856	10	1.267	1.077	9	0.762	0.806	12
	D_Y	14.423	8.488	2	75.721	18.755	1	1.921	1.521	4	2.033	1.887	3
	D_{MXY}	8.632	4.751	2	39.221	9.611	1	1.600	1.028	8	1.385	1.061	8
Gn	D_X	2.066	1.570	5	3.133	2.202	8	2.214	2.170	2	1.111	1.780	9
	D_Y	1.087	0.847	11	2.431	2.911	11	1.477	2.512	6	1.750	2.377	5
	D_{MXY}	1.579	0.930	10	2.758	1.777	11	1.853	1.611	5	1.453	1.437	6
Go	D_X	6.403	4.526	1	7.970	5.682	4	1.018	1.030	13	0.721	0.555	13
	D_Y	14.650	11.382	1	20.869	14.567	4	0.820	0.693	14	0.856	0.627	13
	D_{MXY}	10.517	7.804	1	14.417	9.877	4	0.917	0.646	14	0.775	0.479	13
Il	D_X	0.617	0.543	16	10.543	8.670	2	0.491	0.381	15	0.522	0.441	15
	D_Y	1.059	0.782	12	2.674	3.732	10	0.982	0.770	12	1.051	0.943	10
	D_{MXY}	0.838	0.480	16	6.606	4.579	5	0.727	0.433	15	0.771	0.564	14
Im	D_X	0.804	1.672	15	8.427	6.073	3	0.449	0.371	16	0.460	0.317	16
	D_Y	1.210	1.631	10	1.739	1.363	12	0.946	0.813	13	0.968	0.866	12
	D_{MXY}	1.032	1.586	15	5.093	3.013	6	0.702	0.458	16	0.703	0.455	15
Li	D_X	1.722	1.289	9	2.330	1.820	11	1.730	1.366	5	1.040	1.122	10
	D_Y	1.527	1.414	8	7.676	6.637	5	1.627	1.624	5	1.342	1.226	8
	D_{MXY}	1.627	0.991	8	5.011	3.403	7	1.681	1.077	7	1.185	0.789	9
Lm	D_X	1.952	1.728	6	3.069	2.179	9	1.766	1.232	4	1.155	1.304	7
	D_Y	6.465	5.030	5	5.548	4.252	6	3.864	4.845	2	5.568	9.725	2
	D_{MXY}	4.208	2.692	5	4.313	2.423	8	2.816	2.563	2	3.371	4.828	2
Ls	D_X	1.579	1.111	11	1.430	1.126	14	1.268	0.923	10	1.221	0.951	6
	D_Y	4.111	3.614	6	3.524	3.140	7	2.688	2.414	3	1.047	0.830	11
	D_{MXY}	2.838	2.017	6	2.478	1.588	12	1.982	1.376	4	1.131	0.673	10
N	D_X	1.876	1.322	7	3.141	2.363	7	1.220	1.070	11	0.786	0.792	11
	D_Y	7.542	6.868	4	58.842	50.286	2	0.709	0.583	16	0.615	0.660	15
	D_{MXY}	4.706	3.603	4	30.989	25.664	2	0.955	0.555	13	0.729	0.512	16
Sn	D_X	1.209	0.930	13	1.210	0.851	15	1.611	1.210	7	1.380	1.285	5
	D_Y	0.976	0.848	13	2.943	4.945	9	1.245	1.121	9	1.742	1.559	6
	D_{MXY}	1.101	0.662	13	2.067	2.504	14	1.416	0.857	9	1.555	1.033	4
Sto	D_X	1.640	1.211	10	1.869	1.548	13	1.727	1.280	6	1.133	1.137	8
	D_Y	0.711	0.683	15	0.981	0.931	16	0.710	0.466	15	0.611	0.488	16
	D_{MXY}	1.185	0.727	12	1.428	0.890	16	1.218	0.702	10	0.866	0.676	12
Zy	D_X	2.588	2.072	4	23.311	13.214	1	1.061	0.832	12	2.094	2.065	2
	D_Y	11.656	8.201	3	21.532	13.007	3	6.833	6.023	1	14.122	12.127	1
	D_{MXY}	7.117	4.327	3	22.423	10.628	3	3.939	3.051	1	8.104	6.666	1
Global	D_X	2.069	-	-	5.078	-	-	1.438	-	-	1.201	-	-
	D_Y	4.415	-	-	13.241	-	-	1.790	-	-	2.308	-	-
	D_{MXY}	3.244	-	-	9.160	-	-	1.616	-	-	1.754	-	-

D: dispersion statistics; SD: standard deviation.

TABLE 3—*Summary dispersion statistics (after conversion to mm) for the 16 investigated landmarks according to the group of examiners (EG vs. NG) and the applied landmark-positioning approach (ClMet vs. AdMet). A comparison of the values with reference clinical thresholds previously reported in the literature is also given in the columns headed "T.".*

Landmark	ERD	ClMet						AdMet					
		EG			NG			EG			NG		
		Mean	SD	T.	Mean	SD	T.	Mean	SD	T.	Mean	SD	T.
Al	ERD_X	0.187	0.168		0.243	0.200		0.126	0.101		0.157	0.138	
	ERD_Y	0.554	0.427		0.805	0.626	x	0.331	0.267		0.365	0.352	
	ERD_{MXY}	0.370	0.236		0.524	0.353		0.237	0.150		0.259	0.195	
Ch	ERD_X	0.423	0.334		1.055	0.923	xx	0.731	0.514	x	0.532	0.447	
	ERD_Y	0.146	0.123		0.243	0.191		0.234	0.194		0.156	0.135	
	ERD_{MXY}	0.285	0.187		0.651	0.486	x	0.483	0.289		0.350	0.237	
Ec	ERD_X	0.887	0.559	x	0.958	0.615	x	0.480	0.410		0.469	0.365	
	ERD_Y	0.304	0.216		0.386	0.280		0.308	0.234		0.434	0.370	
	ERD_{MXY}	0.596	0.327	x	0.672	0.346	x	0.396	0.259		0.452	0.279	
En	ERD_X	0.300	0.244		0.526	0.444		0.314	0.300		0.411	0.373	
	ERD_Y	0.198	0.162		0.263	0.197		0.235	0.178		0.246	0.238	
	ERD_{MXY}	0.248	0.158		0.396	0.281		0.276	0.190		0.328	0.277	
G	ERD_X	0.653	0.573	x	0.625	0.427	x	0.291	0.248		0.175	0.185	
	ERD_Y	3.316	1.951	xx	17.407	4.311	xx	0.442	0.350		0.467	0.434	
	ERD_{MXY}	1.984	1.092	xx	9.016	2.209	xx	0.368	0.236		0.318	0.244	
Gn	ERD_X	0.475	0.361		0.720	0.506	x	0.509	0.499		0.255	0.409	
	ERD_Y	0.250	0.195		0.559	0.669		0.340	0.577		0.402	0.546	
	ERD_{MXY}	0.363	0.214		0.634	0.409	x	0.426	0.370		0.334	0.330	
Go	ERD_X	1.472	1.040	xx	1.832	1.306	xx	0.234	0.237		0.166	0.128	
	ERD_Y	3.368	2.617	xx	4.797	3.349	xx	0.189	0.159		0.197	0.144	
	ERD_{MXY}	2.418	1.794	xx	3.314	2.271	xx	0.211	0.149		0.178	0.110	
Il	ERD_X	0.142	0.125		2.424	1.993	xx	0.113	0.088		0.120	0.101	
	ERD_Y	0.243	0.180		0.615	0.858	x	0.226	0.177		0.242	0.217	
	ERD_{MXY}	0.193	0.110		1.519	1.053	xx	0.167	0.100		0.177	0.130	
Im	ERD_X	0.185	0.384		1.937	1.396	xx	0.103	0.085		0.106	0.073	
	ERD_Y	0.278	0.375		0.400	0.313		0.217	0.187		0.223	0.199	
	ERD_{MXY}	0.237	0.365		1.171	0.693	xx	0.161	0.105		0.162	0.105	
Li	ERD_X	0.396	0.296		0.536	0.418		0.398	0.314		0.239	0.258	
	ERD_Y	0.351	0.325		1.765	1.526	xx	0.374	0.373		0.309	0.282	
	ERD_{MXY}	0.374	0.228		1.152	0.782	xx	0.386	0.248		0.272	0.181	
Lm	ERD_X	0.449	0.397		0.706	0.501	x	0.406	0.283		0.266	0.300	
	ERD_Y	1.486	1.156	xx	1.275	0.977	xx	0.888	1.114	x	1.280	2.236	xx
	ERD_{MXY}	0.967	0.619	x	0.991	0.557	x	0.647	0.589	x	0.775	1.110	x
Ls	ERD_X	0.363	0.255		0.329	0.259		0.291	0.212		0.281	0.219	
	ERD_Y	0.945	0.831	x	0.810	0.722	x	0.618	0.555	x	0.241	0.191	
	ERD_{MXY}	0.652	0.464	x	0.570	0.365		0.456	0.316		0.260	0.155	
N	ERD_X	0.431	0.304		0.722	0.543	x	0.280	0.246		0.181	0.182	
	ERD_Y	1.734	1.579	xx	13.527	11.560	xx	0.163	0.134		0.141	0.152	
	ERD_{MXY}	1.082	0.828	xx	7.124	5.900	xx	0.220	0.128		0.168	0.118	
Sn	ERD_X	0.278	0.214		0.278	0.196		0.370	0.278		0.317	0.295	
	ERD_Y	0.224	0.195		0.677	1.137	x	0.286	0.258		0.400	0.358	
	ERD_{MXY}	0.253	0.152		0.475	0.576		0.326	0.197		0.357	0.237	
Sto	ERD_X	0.377	0.278		0.430	0.356		0.397	0.294		0.260	0.261	
	ERD_Y	0.163	0.157		0.226	0.214		0.163	0.107		0.140	0.112	
	ERD_{MXY}	0.272	0.167		0.328	0.205		0.280	0.161		0.199	0.155	
Zy	ERD_X	0.595	0.476	x	5.359	3.038	xx	0.244	0.191		0.481	0.475	
	ERD_Y	2.680	1.885	xx	4.950	2.990	xx	1.571	1.385	xx	3.246	2.788	xx
	ERD_{MXY}	1.636	0.995	xx	5.155	2.443	xx	0.906	0.701	x	1.863	1.532	xx
Global	ERD_X	0.476	-		1.167	-	xx	0.331	-		0.276	-	
	ERD_Y	1.015	-	xx	3.044	-	xx	0.412	-		0.531	-	
	ERD_{MXY}	0.746	-	x	2.106	-	xx	0.372	-		0.403	-	

ERD: estimated real mean dispersion; SD: standard deviation; T.: reference threshold. For thresholds: "xx" = above acceptable limits (> 1 mm), "x" = within the range of acceptability (0.575 and 1 mm), values without crosses were within an ideal average dispersion (< 0.575 mm).

TABLE 4—*Comparison of the estimated real mean dispersions (ERD_{MXY}) with reference clinical thresholds previously reported in the literature.*

Landmark	ClMet				AdMet			
	EG		NG		EG		NG	
	ERD_{MXY}	Thres.	ERD_{MXY}	Thres.	ERD_{MXY}	Thres.	ERD_{MXY}	Thres.
Al	0.370		0.524		0.237		0.259	
Ch	0.285		0.651	x	0.483		0.350	
Ec	0.595	x	0.672	x	0.396		0.452	
En	0.248		0.396		0.276		0.328	
G	1.984	xx	9.016	xx	0.368		0.318	
Gn	0.363		0.634	x	0.426		0.334	
Go	2.418	xx	3.314	xx	0.211		0.178	
Il	0.193		1.519	xx	0.167		0.177	
Im	0.237		1.171	xx	0.161		0.162	
Li	0.374		1.152	xx	0.386		0.272	
Lm	0.967	x	0.991	x	0.647	x	0.775	x
Ls	0.652	x	0.570		0.456		0.260	
N	1.082	xx	7.124	xx	0.220		0.168	
Sn	0.253		0.475		0.326		0.357	
Sto	0.272		0.328		0.280		0.199	
Zy	1.636	xx	5.155	xx	0.906	x	1.863	xx
Global	0.746	x	2.106	xx	0.372		0.403	

"xx" : above acceptable limits (> 1 mm); "x" : within the range of acceptability (0.575 and 1 mm); values without crosses have an ideal average dispersion (< 0.575 mm).

Figure Legends

FIG. 1—*Facial diagram representing the 16 landmarks used (left) and their nomenclature (right). Letter R corresponds to the right side and L to the left side.*

FIG. 2—*Example description for the Ectocanthion landmark taken from the facial photo-anthropometric (FPA) manual used in this work for the adapted positioning approach (AdMet) and provided in the Supplementary Information (SI).*

FIG. 3—*Comparison of the mean intra-landmark dispersion values (D_{MXY}) observed in the positioning of the 16 landmarks using the different experimental settings.*

FIG. 4—*Graphical comparison of the mean intra-landmark dispersion values (D_{MXY}) observed in the positioning of the 16 landmarks when different experimental settings were adopted (landmark-positioning approaches on left; examiners on right). The columns "Var." (variability) visually represent the overlap of the dispersions considering a 50-pixel scale. The columns "Sig." (significance), on the contrary, represent the statistical significance of the dispersion differences ($\alpha = 0.05$) using a color scale.*

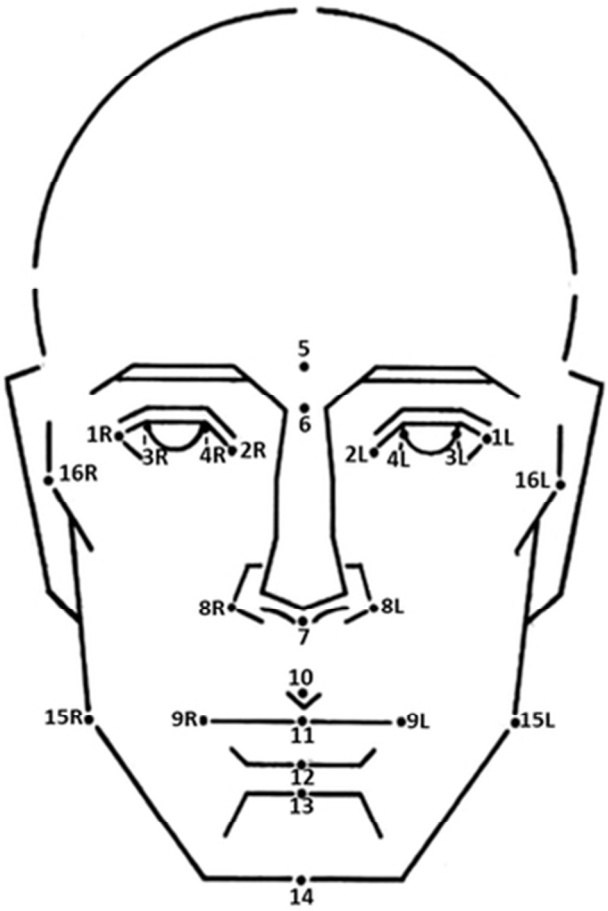

Num	Landmark
1	Ectocanthion (Ec)
2	Endocanthion (En)
3	Iridion Laterale (Il)
4	Iridion Mediale (Im)
5	Glabella (G)
6	Nasion (N)
7	Subnasale (Sn)
8	Alare (Al)
9	Chelion (Ch)
10	Labiale Superius (Ls)
11	Stomion (Sto)
12	Labiale Inferius (Li)
13	Labiomentale (Lm)
14	Gnathion (Gn)
15	Gonion (Go)
16	Zygion (Zy)

Facial diagram representing the 16 landmarks used (left) and their nomenclature (right). Letter R corresponds to the right side and L to the left side.

45x43mm (300 x 300 DPI)

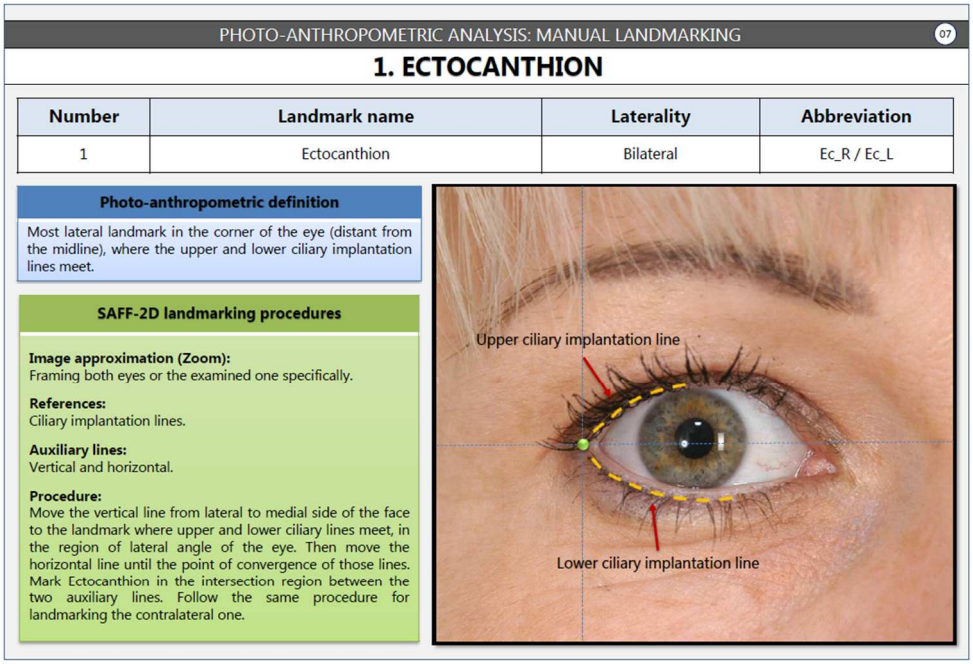

Example description for the Ectocanthion landmark taken from the facial photo-anthropometric (FPA) manual used in this work for the adapted positioning approach (AdMet) and provided in the Supplementary Information (SI).

93x64mm (300 x 300 DPI)

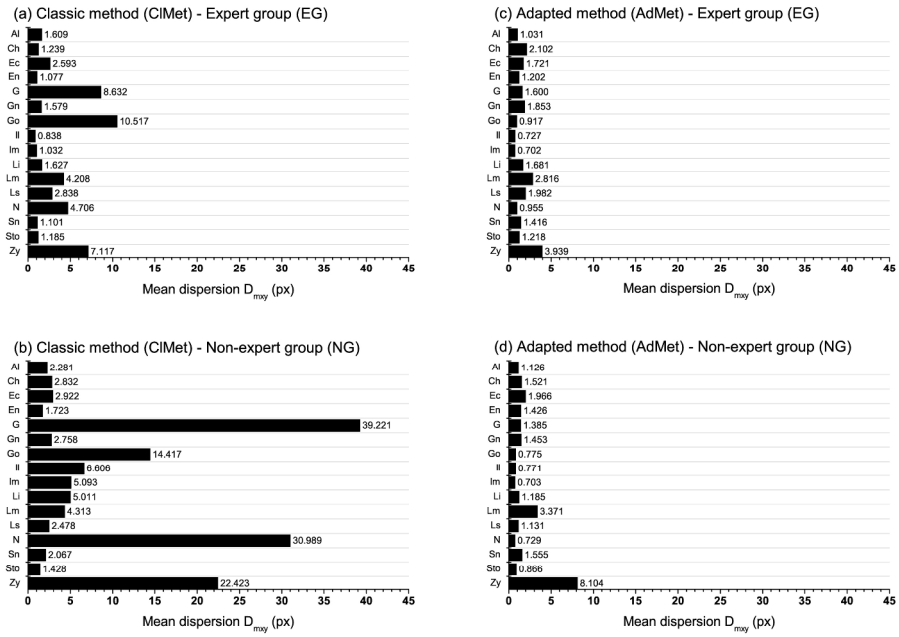

Comparison of the mean intra-landmark dispersion values (DMXY) observed in the positioning of the 16 landmarks using the different experimental settings.

254x176mm (300 x 300 DPI)

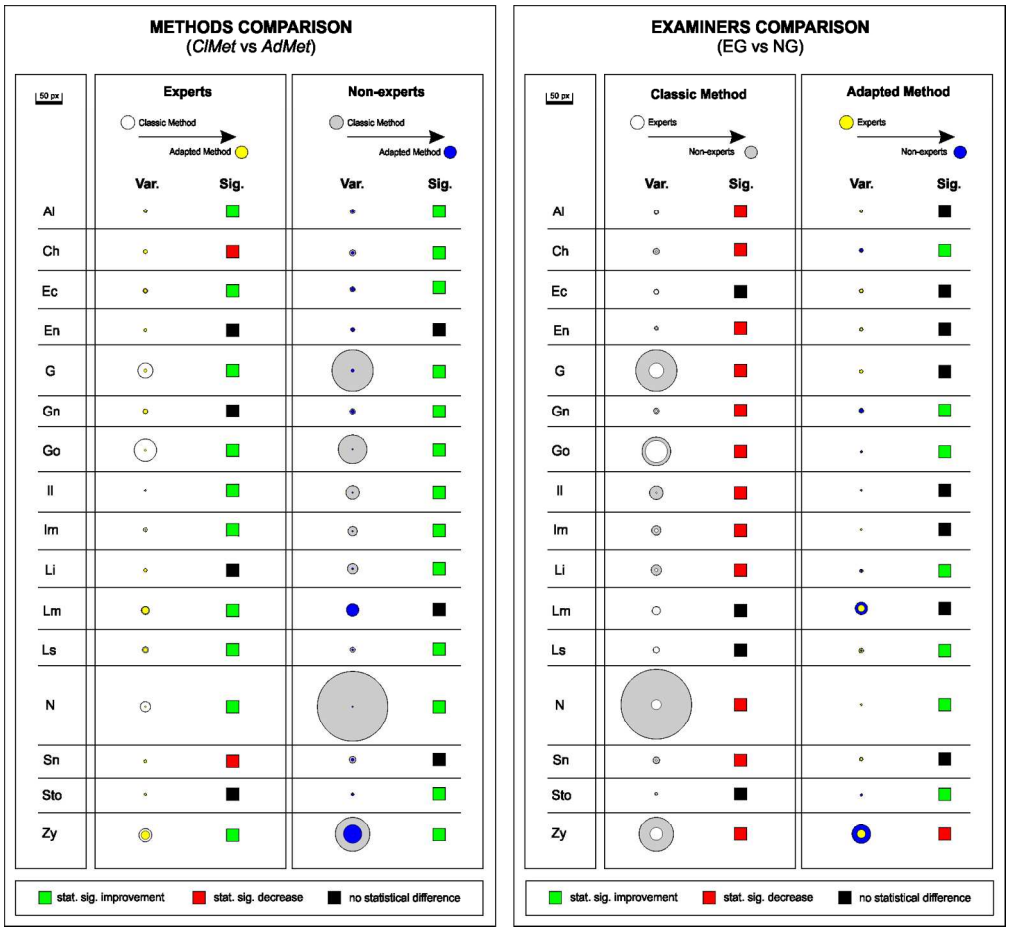

Graphical comparison of the mean intra-landmark dispersion values (DMXY) observed in the positioning of the 16 landmarks when different experimental settings were adopted (landmark-positioning approaches on left; examiners on right). The columns "Var." (variability) visually represent the overlap of the dispersions considering a 50-pixel scale. The columns "Sig." (significance), on the contrary, represent the statistical significance of the dispersion differences ($\alpha = 0.05$) using a color scale.

161x149mm (300 x 300 DPI)

MANUAL OF FACIAL PHOTO-ANTHROPOMETRY: VISUAL REFERENCES FOR LANDMARK POSITIONING IN FRONTAL VIEW IMAGES

AUTHORS
Marta Regina Pinheiro Flores
Carlos Eduardo Palhares Machado

COLABORATION
FACISGroup - Craniofacial Identification Scientific Group

SUPPORT
Edmar Antônio da Silva - SAFF-2D® Programming
Audiovisual and Electronic Skills Service of the National Institute of Criminalistics (SEPAEL/INC)

Produced within the Project nº 37 – Notice 25/2014 – Forensic Sciences Program (Pró-Forenses/CAPES)

FINANCING: INSTITUTIONS RESPONSIBLE FOR THE PROJECT:

PRESENTATION 02

This manual was designed to provide an objective and methodological approach for the analysis of frontal view facial images, through the establishment of anatomical points of reference (i.e. landmarks). In view of a current lack of standardization and objectivity in these analyses, the aim was to adapt the classic cephalometric descriptions presented in the literature by inserting visual references for its indirect application, thus favoring facial examination based exclusively on images (high demand from police and forensic examiners worldwide). The adapted descriptions were called photo-anthropometric.

The proposed standardization methodology is presented in a manual form and, for each landmark of analysis, contains: photo-anthropometric description through the use of visually identifiable references in frontal standard images; operational procedures for positioning each specific point with a detailed and stepwise explanation of the procedure; and illustrations referring to their location in facial topography. The analysis includes 32 facial landmarks (7 median and 25 bilateral) in which six of them had their landmarking procedures automatized. This means that despite being automatically settled, their landmarking remains dependent on the examiner by the previous positioning of correlated landmarks.

For greater objectivity of markings, commands and tools were included in the analysis to reduce the individual interpretation by different examiners of the adequate location of anatomical structures. Horizontal and vertical mobile reference lines have been included to facilitate the visualization of the landmark itself (through the intersection of both) and of the structure ends (through the landmark of tangency). Other fixed reference structures were created by the determination of specific points such as orbital midline, pupil centers and orbital circumferences, which will be described later (Appendix).

Although this manual has been developed by using SAFF-2D® software (2D Forensic Facial Analysis System - a non-commercial software developed by the Brazilian Federal Police for two-dimensional facial analysis), the methodological understanding acquired through it does not exclude the use of other software to carry out the proposed facial analyses.

INDEX

PHOTO-ANTHROPOMETRIC LANDMARKS

04

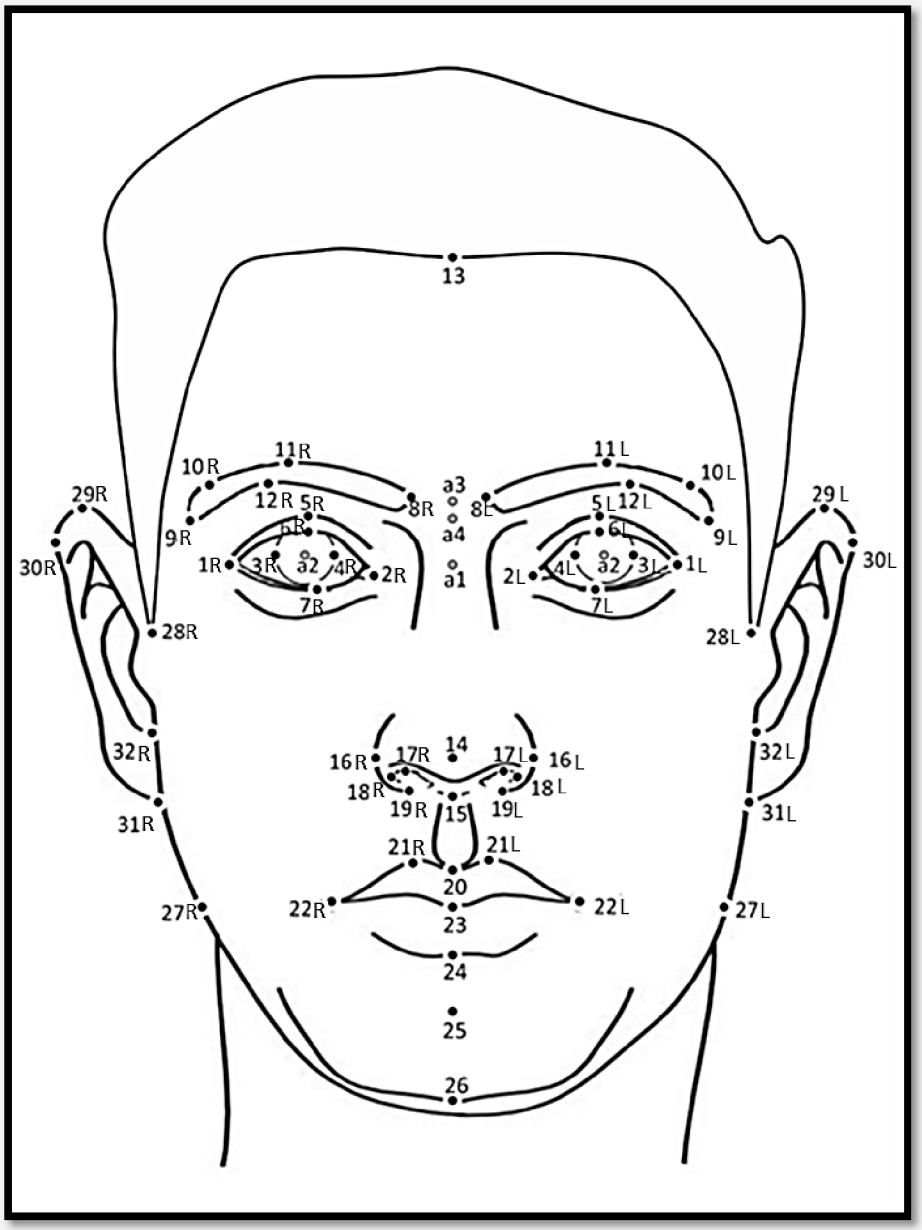

Photo-anthropometric landmarking order			
Manual landmarking			
Number	**Landmark**	**Laterality**	**Abbreviation**
1	Ectocanthion	Bilateral	Ec_R / Ec_L
2	Endocanthion	Bilateral	En_R / En_L
3	Iridion Laterale	Bilateral	Il_R / Il_L
4	Iridion Mediale	Bilateral	Im_R / Im_L
5	Palpebrale Superius Groove	Bilateral	Psg_R / Psg_L
6	Palpebrale Superius	Bilateral	Ps_R / Ps_L
7	Palpebrale Inferius	Bilateral	Pi_R / Pi_L
8	Mediale Eyebrow	Bilateral	Me_R / Me_L
9	Laterale Eyebrow	Bilateral	Le_R / Le_L
10	Frontotemporale	Bilateral	Ft_R / Ft_L
11	Superius Eyebrow	Bilateral	Se_R / Se_L
12	Inferius Eyebrow	Bilateral	Ie_R / Ie_L
13	Trichion	Median	Tr
14	Pronasale	Median	Prn
15	Subnasale	Median	Sn
16	Alare	Bilateral	Al_R / Al_L
17	Superius Nostril	Bilateral	Spn_R / Spn_L
18	Laterale Nostril	Bilateral	Ln_R / Ln_L
19	Subalare	Bilateral	Sbal_R / Sbal_L
20	Labiale Superius	Median	Ls
21	Crista Philtre	Bilateral	Cph_R / Cph_L
22	Chelion	Bilateral	Ch_R / Ch_L
23	Stomion	Median	Sto
24	Labiale Inferius	Median	Li
25	Labiomentale	Median	Lm
26	Gnathion	Median	Gn
27	Gonion	Bilateral	Go_R / Go_L
28	Zygion	Bilateral	Zy_R / Zy_L
29	Superaurale	Bilateral	Sa_R / Sa_L
30	Postaurale	Bilateral	Pa_R / Pa_L
31	Subaurale	Bilateral	Sba_R / Sba_L
32	Supralobulare	Bilateral	Slb_R / Slb_L

Automated landmarking			
Number	**Landmark**	**Laterality**	**Abbreviation**
a1	Midnasale	Median	Mid
a2	Pupil	Bilateral	Pu_R / Pu_L
a3	Glabella	Median	G
a4	Nasion	Median	N

FACIAL REGIONS – ADOPTED ORDER BY SAFF-2D

05

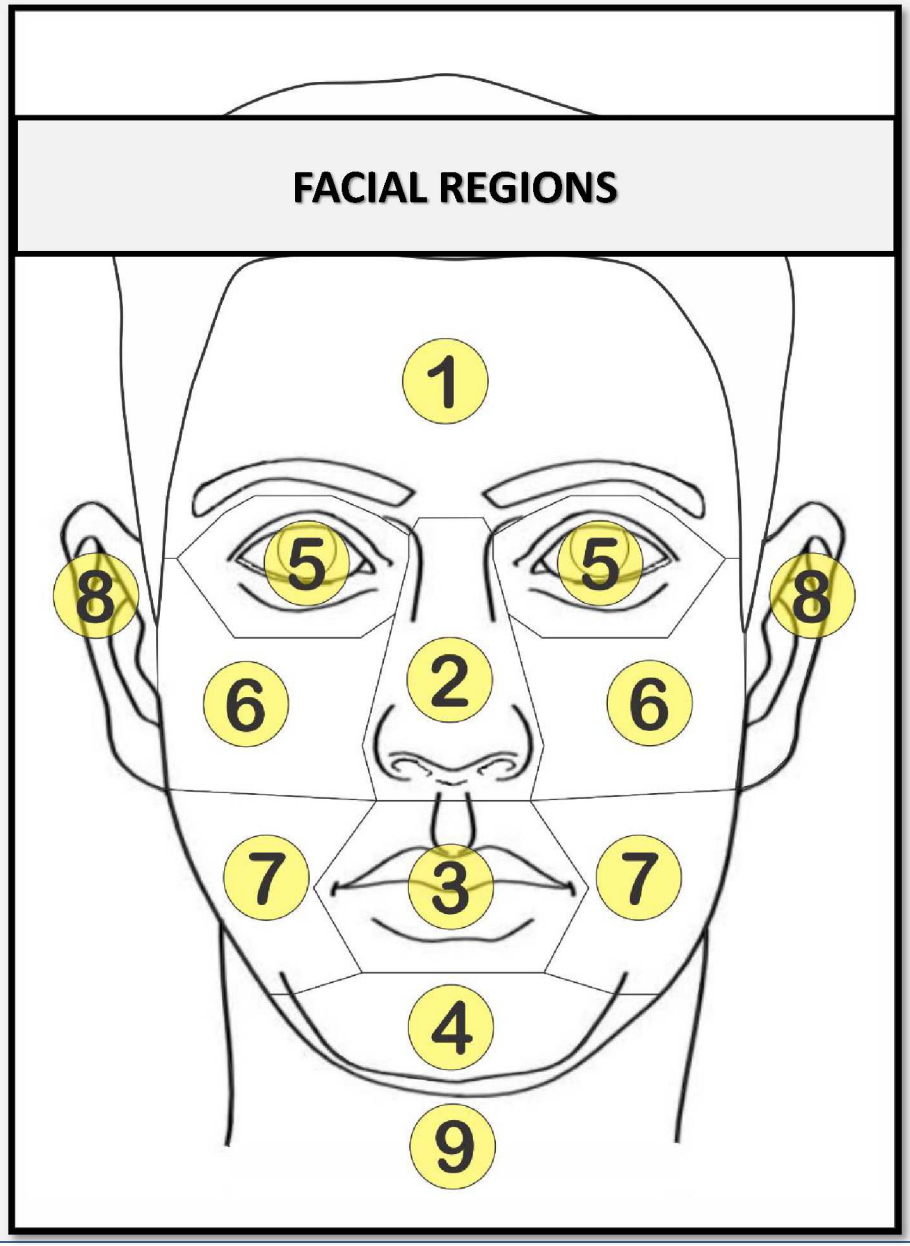

FACIAL REGIONS			
Number	**Region**	**Laterality**	**Code**
1	Frontal	Median	R1
2	Nasal	Median	R2
3	Labial	Median	R3
4	Menton	Median	R4
5	Orbital	Right	R5R
		Left	R5L
6	Zygomaxillary	Right	R6R
		Left	R6L
7	Buccomandibular	Right	R7R
		Left	R7L
8	Auricular	Right	R8R
		Left	R8L
9	Cervical	Median	R9

PHOTO-ANTHROPOMETRIC LANDMARKING ANALYSIS 06

REFERENCE SLIDE

Number	Landmark name	Laterality	Abbreviation
Number of references on the facial diagram	Nomenclature	Median or Bilateral	Reference acronym adopted

Photo-anthropometric definition

Definition based exclusively on image analysis. Descriptive adaptation of the anthropometric physical definition. Some landmarks do not differ much from their classic definition. Others, however, have a description solely developed for this purpose, denoted 'photo-anthropometric' (PT).

SAFF-2D landmarking procedures

Herein, procedures to be followed during landmarking are presented. For non-calibrated examiners, the careful adoption of all procedures is suggested. Over time, auxiliary tools can become unnecessary.

Image approximation (Zoom):
Suggested image framing.

References:
Resources and tools needed to determine the landmark in question.

Auxiliary lines:
Lines recommended for easy landmarking. As described above, they are not mandatory. In this field, the use of the Laplace edge detection filter is included, mostly suggested to confirm landmark positioning on linear structures. This tool should be used only as an aid. The original image must be considered as the primary source of analysis.

Procedure:
Suggested guidance for photo-anthropometric landmarking.

Illustration

PHOTO-ANTHROPOMETRIC ANALYSIS: MANUAL LANDMARKING 07

1. ECTOCANTHION

Number	Landmark name	Laterality	Abbreviation
1	Ectocanthion	Bilateral	Ec_R / Ec_L

Photo-anthropometric definition

The most lateral landmark in the corner of the eye (distant from the midline), where the upper and lower ciliary implantation lines meet.

SAFF-2D landmarking procedures

Image approximation (Zoom):
Framing both eyes or the examined one specifically.

References:
Ciliary implantation lines.

Auxiliary lines:
Vertical and horizontal.

Procedure:
Move the vertical line from lateral to medial side of the face to the landmark where upper and lower ciliary lines meet, in the region of lateral angle of the eye. Then move the horizontal line until the point of convergence of those lines. Mark *Ectocanthion* in the intersection region between the two auxiliary lines. Follow the same procedure for landmarking the contralateral one.

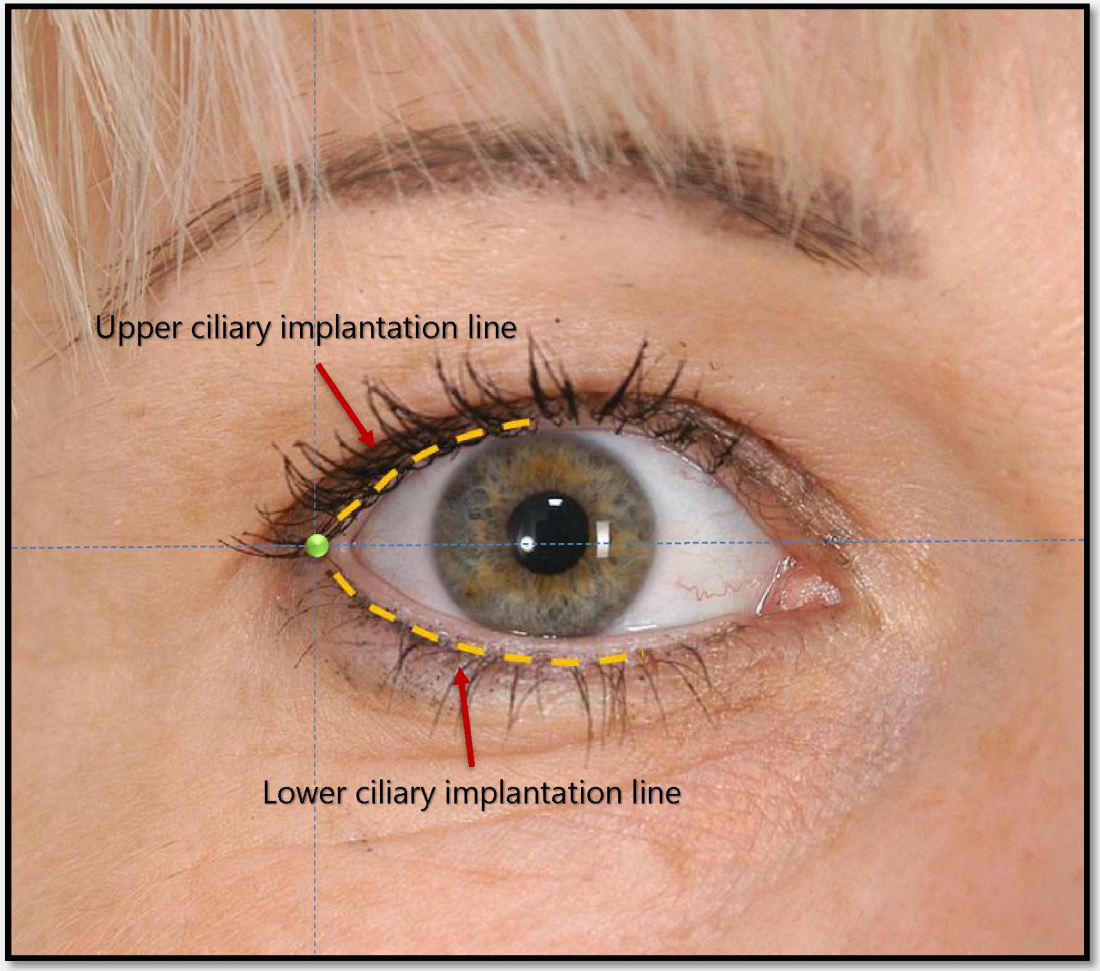

ECTOCANTHION: Observation 1

08

Consider as reference the region of encounter between the lines of implantation of superior and inferior cilia and not the region of internal angle, near the white part of the eye (sclera).

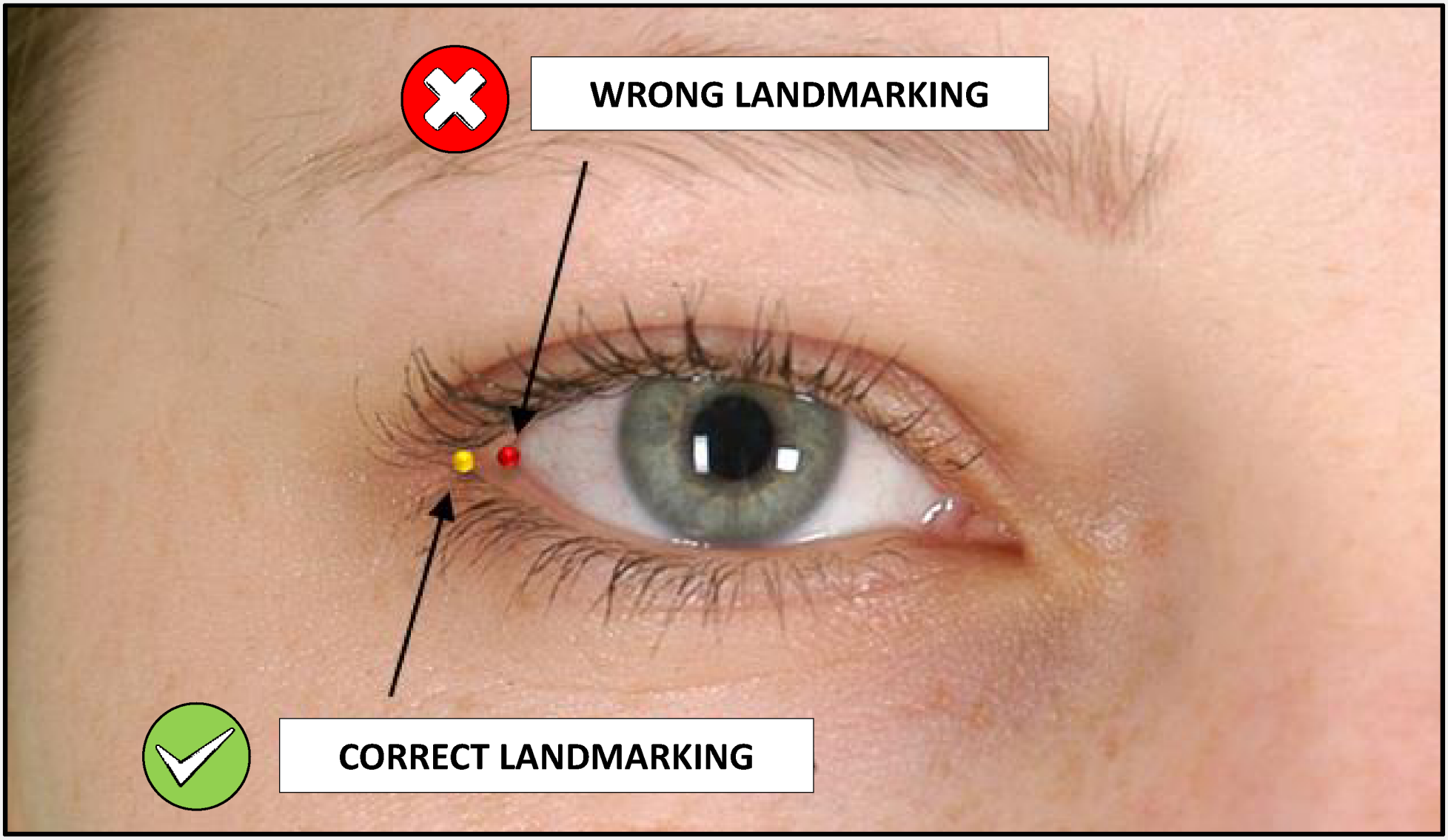

ECTOCANTHION: Observation 2

09

In cases where eyelashes are covering the region, an estimated region should be considered by taking as reference the projection of imaginary lines that pass over cilia implantation lines.

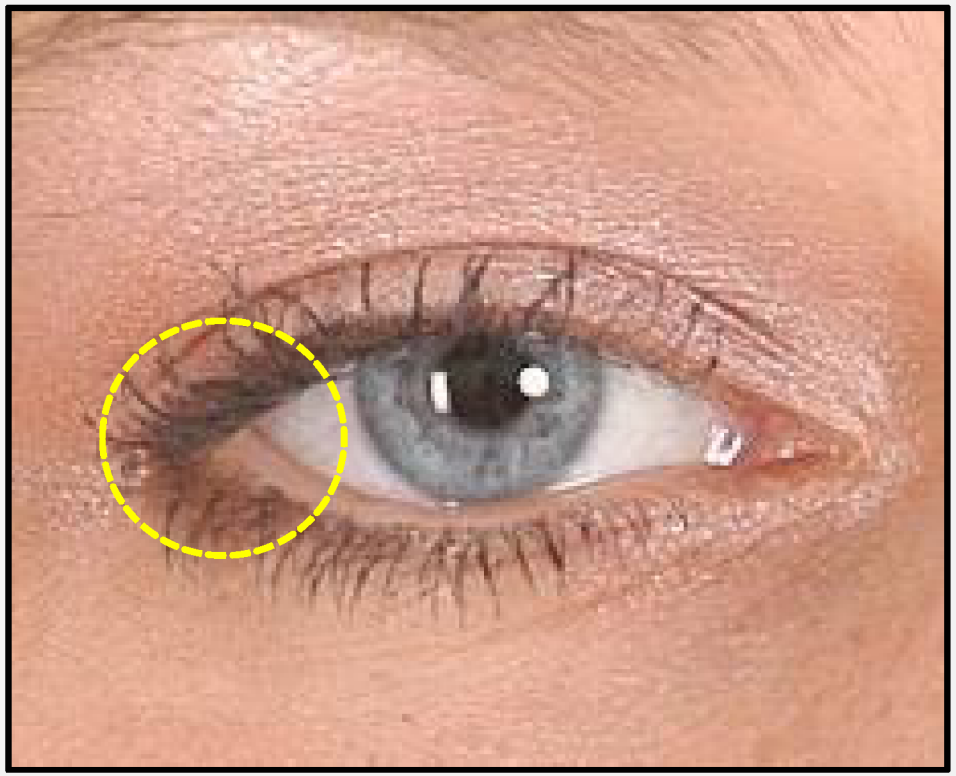

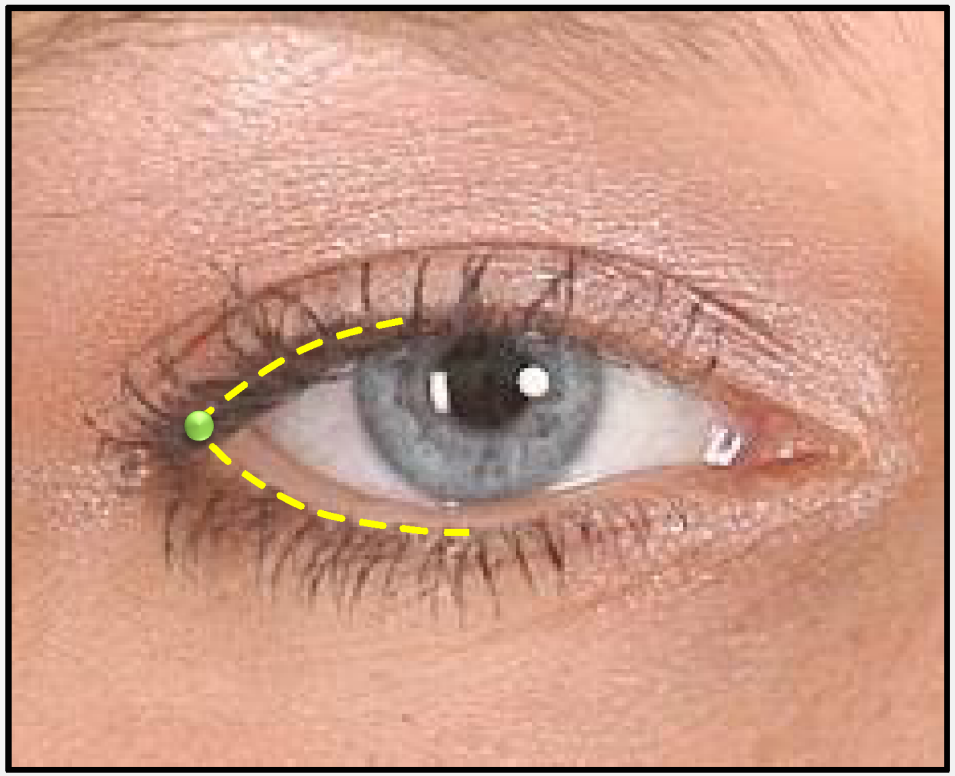

Number	Landmark name	Laterality	Abbreviation
1	Ectocanthion	Bilateral	Ec_R / Ec_L

PHOTO-ANTHROPOMETRIC ANALYSIS: MANUAL LANDMARKING 10

2. ENDOCANTHION

Number	Landmark name	Laterality	Abbreviation
2	Endocanthion	Bilateral	En_R / En_L

Photo-anthropometric definition

The most medial landmark in the corner of the eye (near midline), where the upper and lower eyelids meet.

SAFF-2D landmarking procedures

Image approximation (Zoom):
Framing both eyes or the examined one specifically.

References:
Free margin of upper and lower eyelid.

Auxiliary lines:
Vertical and horizontal.

Procedure:
Move the vertical line from the medial to lateral side of the face, to the region where upper and lower eyelids meet, in the "inner" corner of the eye. Then move the horizontal line until it is positioned at the point of ciliary lines convergence. Mark the *Endocanthion* in the intersection region between the two auxiliary lines. Follow the same procedure for marking the contralateral point.

ENDOCANTHION: Observation

11

Consider as reference the most medial landmark of the eye contour and not the region of the internal angle, next to lacrimal caruncle.

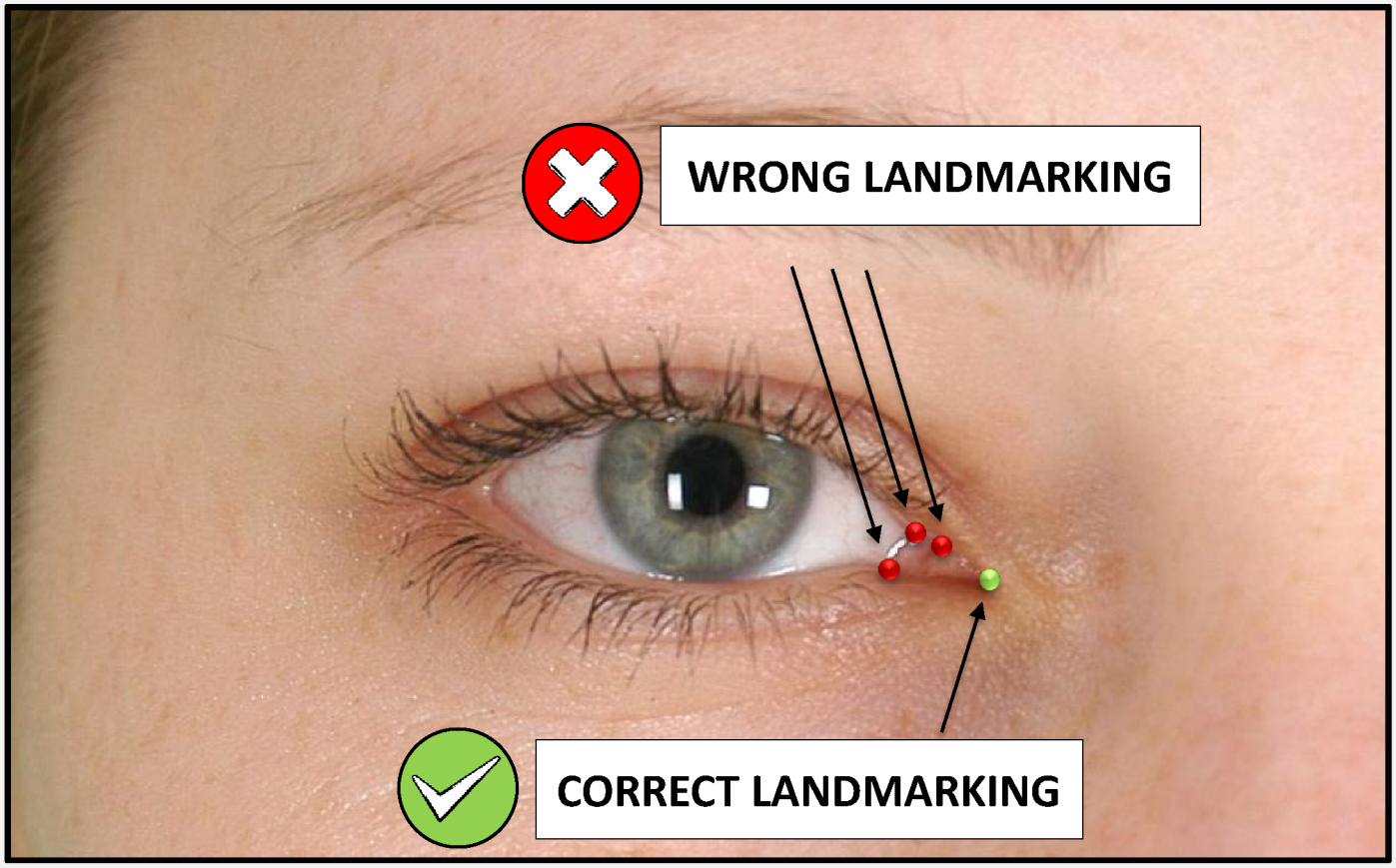

Number	Landmark name	Laterality	Abbreviation
2	Endocanthion	Bilateral	En_R / En_L

PHOTO-ANTHROPOMETRIC ANALYSIS 12

ORBITAL MIDLINE

After determining the corner points of the eyes, a midline (orbital midline) will appear in a lighter shade than that of the vertical and horizontal reference lines.

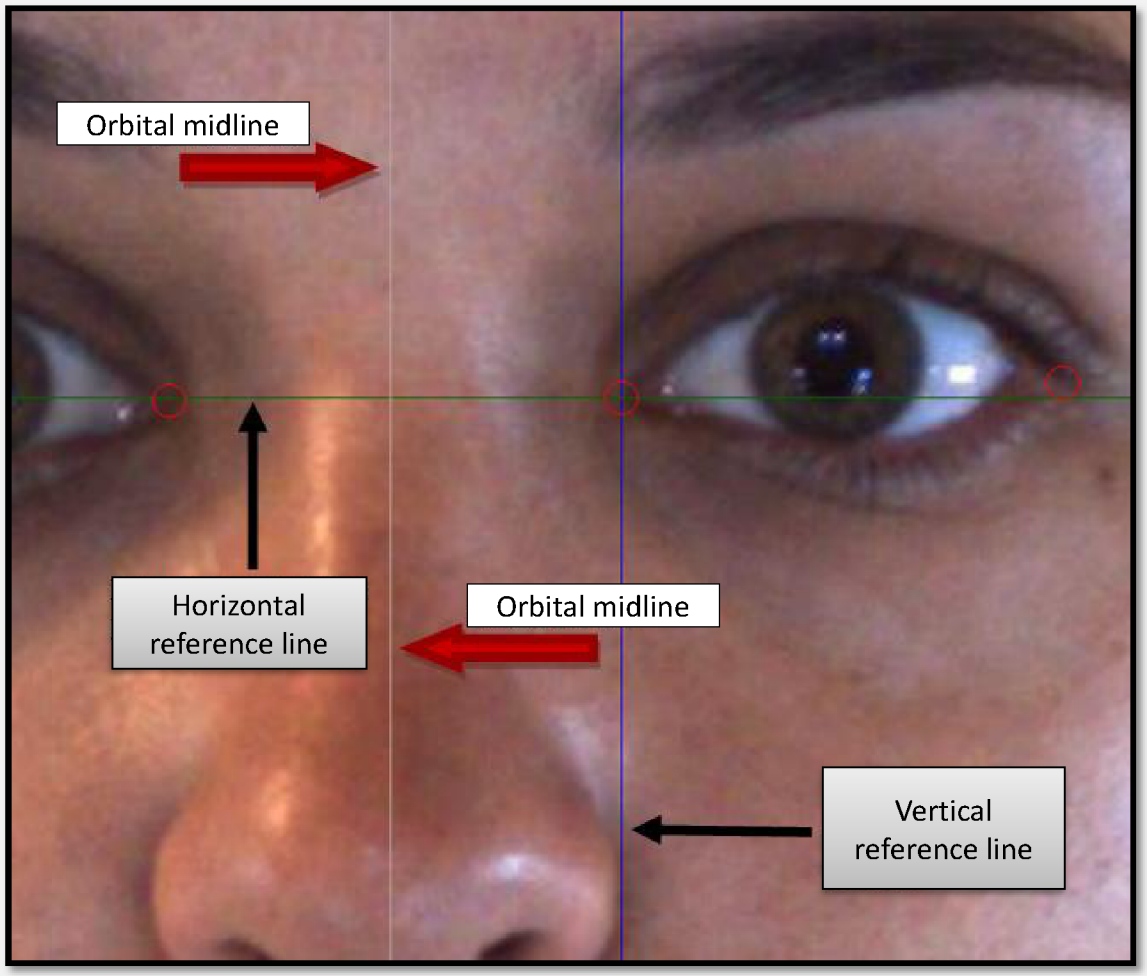

PHOTO-ANTHROPOMETRIC ANALYSIS: MANUAL LANDMARKING 13

3. IRIDION LATERALE

Number	Landmark name	Laterality	Abbreviation
3	Iridion Laterale	Bilateral	Il_R / Il_L

Photo-anthropometric definition

The most lateral landmark of the contour of the iridian circumference.

SAFF-2D landmarking procedures

Image approximation (Zoom):
Examined eye framing.

References:
Greater horizontal iris diameter.

Auxiliary lines:
Vertical and horizontal.

Procedure:
Position horizontal auxiliary line at the height of the largest iris diameter. Move the vertical auxiliary line from lateral to medial, until it is tangential with the iris. Landmark is the intersection of auxiliary lines.

Observation:
The same positioning of the horizontal line must be considered for landmarking the *Iridion Mediale* ipsilateral (from the same facial side).

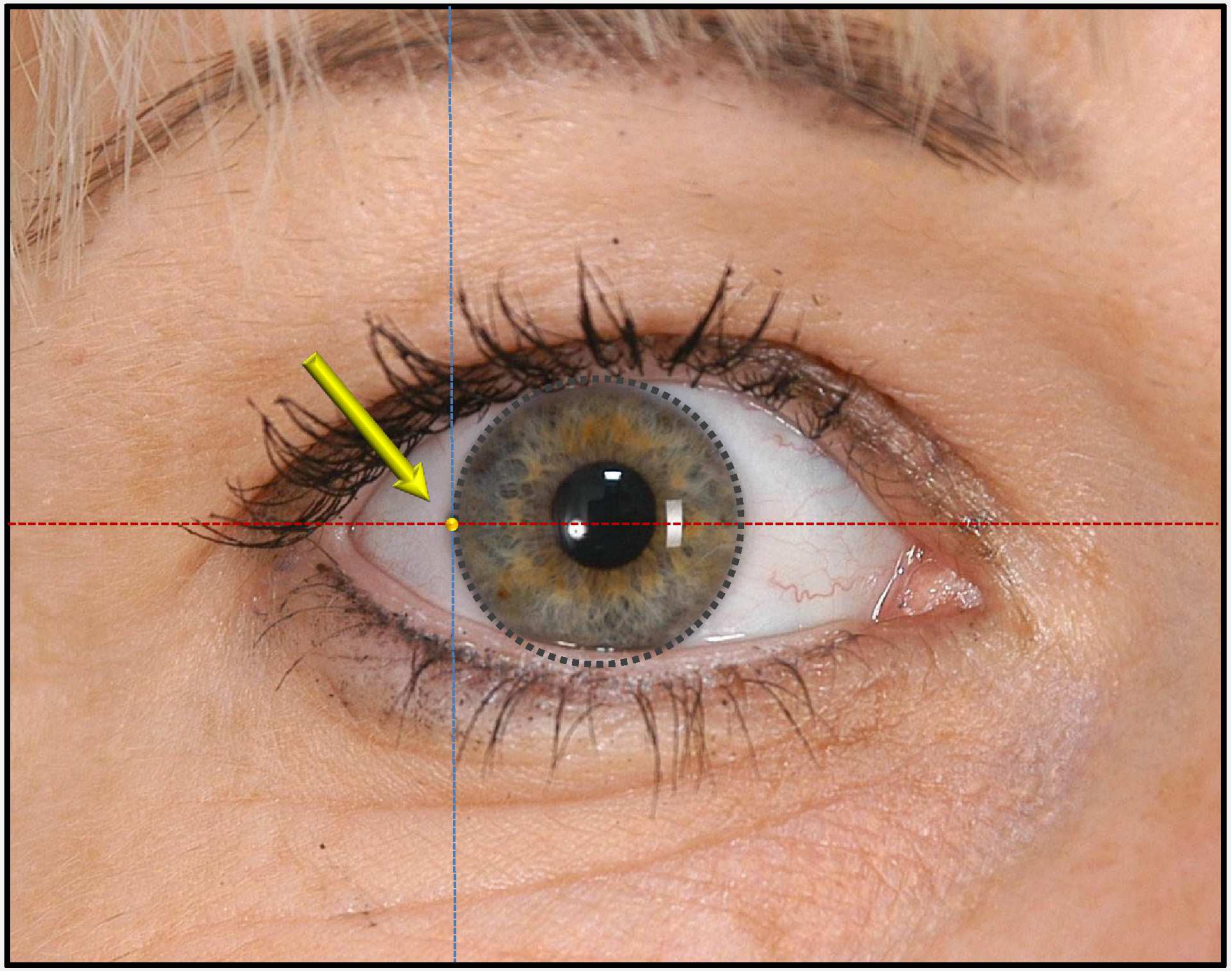

PHOTO-ANTHROPOMETRIC ANALYSIS: MANUAL LANDMARKING 14

4. IRIDION MEDIALE

Number	Landmark name	Laterality	Abbreviation
4	Iridion Mediale	Bilateral	Im_R / Im_L

Photo-anthropometric definition

The most medial landmark of the contour of the iridian circumference.

SAFF-2D landmarking procedures

Image approximation (Zoom):
Examined eye framing.

References:
Greater horizontal iris diameter.

Auxiliary lines:
Vertical and horizontal.

Procedure:
Position horizontal auxiliary line over the *Iridion Laterale* landmark. Move vertical auxiliary line from medial to lateral, until it is once again tangential with the iris. Landmark is the intersection of auxiliary lines.

Observation:
The same positioning of horizontal line must be considered for landmarking *Iridion Laterale* and *Iridion Mediale* ipsilateral points.

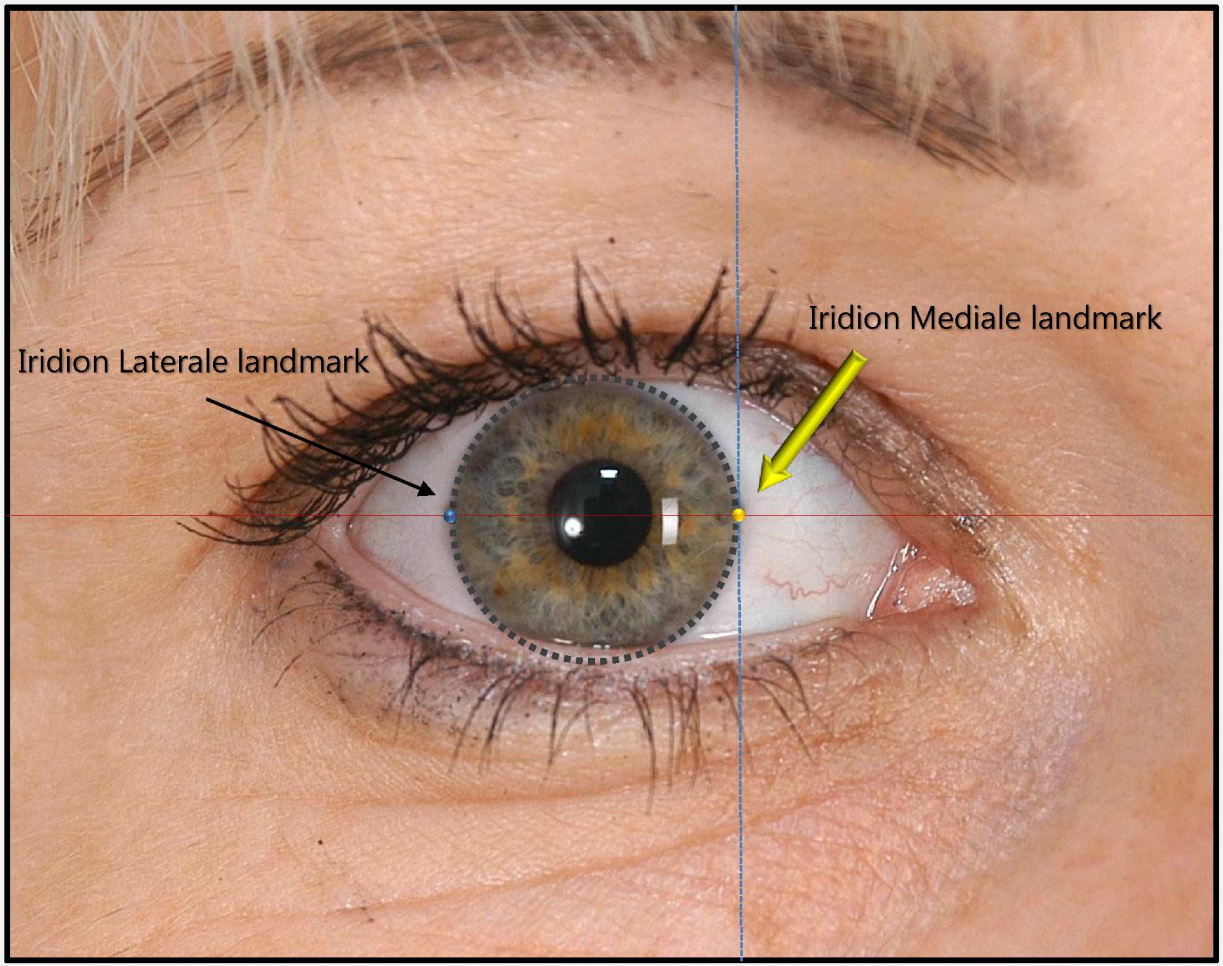

IRIDION LATERALE AND MEDIALE: Observation

15

The right and left iridion landmarks are not always at the same facial height. However, the same horizontal reference must be used for landmarking Iridions Laterale and Mediale of the same eye (ipsilateral).

Number	Landmark name	Laterality	Abbreviation
3	Iridion Laterale	Bilateral	Il_R / Il^{P}_L

Number	Landmark name	Laterality	Abbreviation
4	Iridion Mediale	Bilateral	Im_R / Im_L

PHOTO-ANTHROPOMETRIC ANALYSIS: MANUAL LANDMARKING 16

5. PALPEBRALE SUPERIUS GROOVE

Number	Landmark name	Laterality	Abbreviation
5	Palpebrale Superius Groove	Bilateral	Psg_R / Psg_L

Photo-anthropometric definition

The uppermost landmark of upper palpebral groove.

SAFF-2D landmarking procedures

Image approximation (Zoom):
Examined eye framing.

Reference:
Upper palpebral crease.

Auxiliary lines:
Vertical and horizontal lines.
Edge detection filter (Laplace).

Procedure:
Position the vertical auxiliary line to pass through the most visible and highest point of the upper palpebral groove (move it from side to side until it passes through the curvature region). Move the horizontal auxiliary line until it is tangential with the upper palpebral groove. The point of intersection is the position of the landmark. Same procedure for the contralateral point.

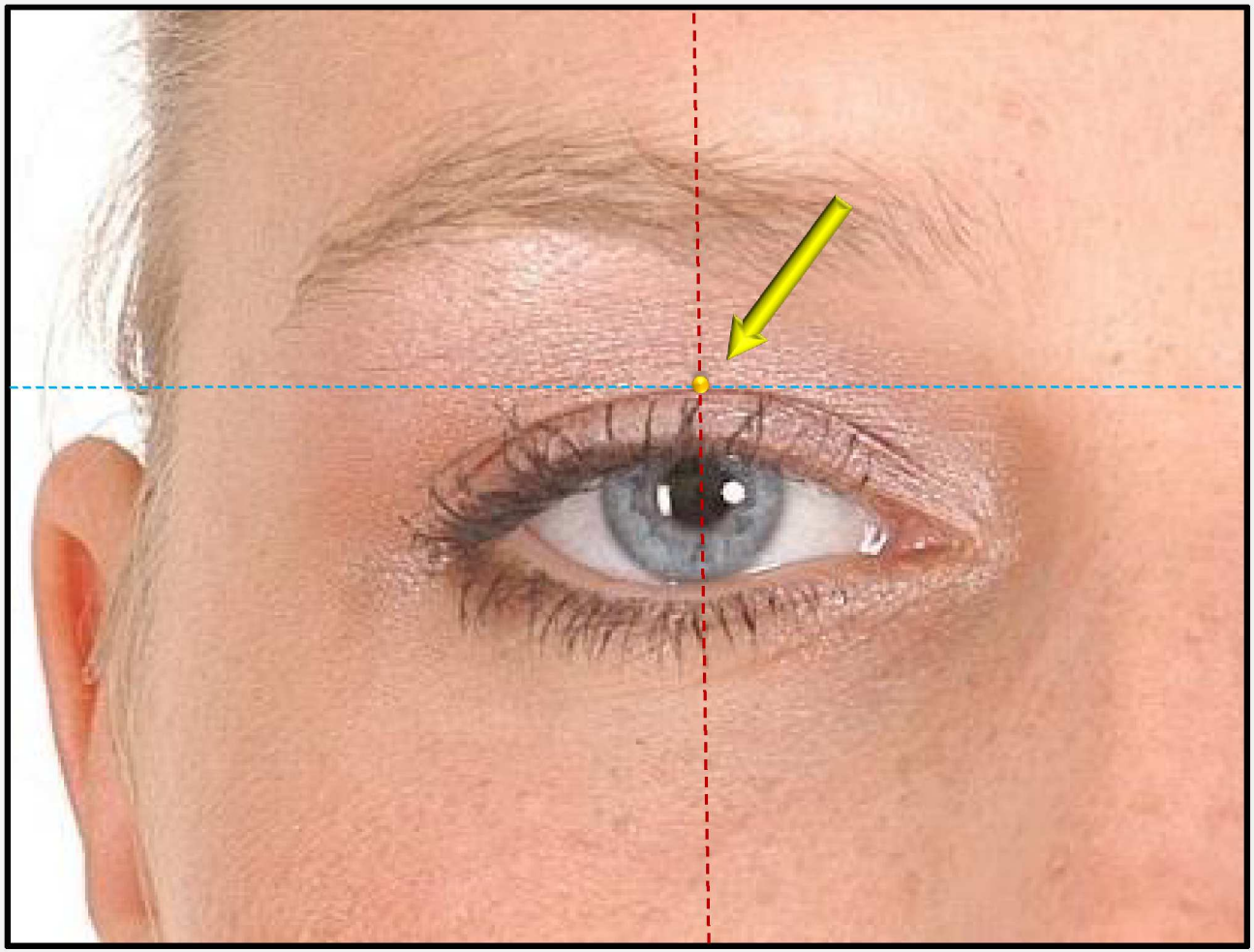

PALPEBRALE SUPERIUS GROOVE: Observation

17

When the *Palpebrale Superius Groove* is not completely visible due to masking by the upper palpebral tissue (palpebral ptosis), **do not landmark it** and include an observation in the specific field of SAFF-2D.

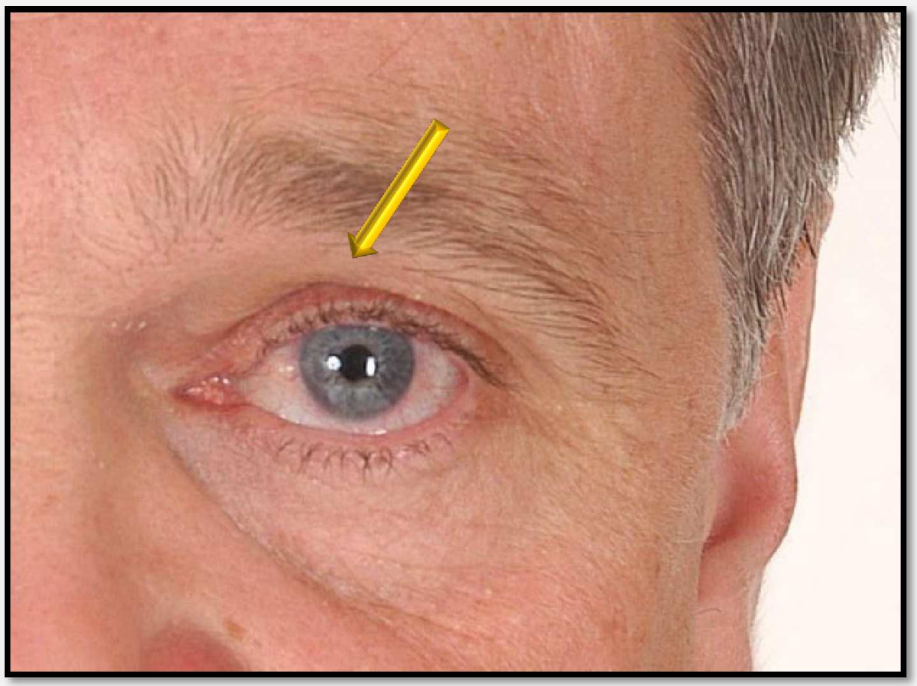

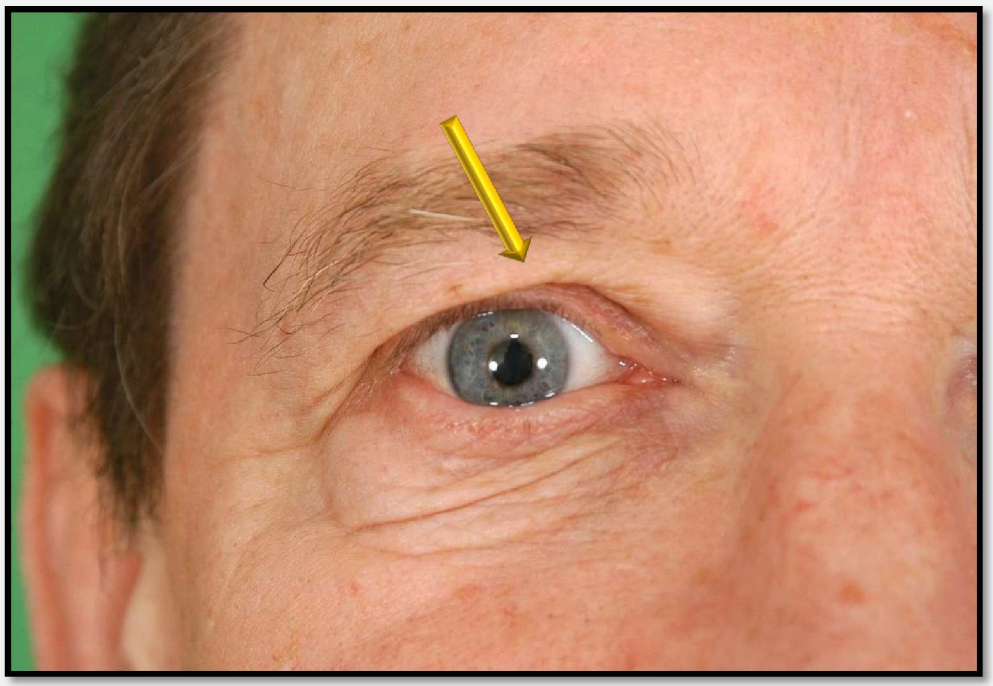

Number	Landmark name	Laterality	Abbreviation
5	Palpebrale Superius Groove	Bilateral	Psg_R / Psg_L

PHOTO-ANTHROPOMETRIC ANALYSIS: MANUAL LANDMARKING 18

6. PALPEBRALE SUPERIUS

Number	Landmark name	Laterality	Abbreviation
6	Palpebrale Superius	Bilateral	Ps_R / Ps_L

Photo-anthropometric definition

The uppermost landmark of the upper, eyelid-free margin, above the line of the eyelashes.

SAFF-2D landmarking procedures

Image approximation (Zoom):
Examined eye framing.

Reference:
Upper eyelid-free margin.
(Ciliary implantation line)

Auxiliary lines:
Vertical and horizontal.

Procedure:
Position vertical auxiliary line to pass through the most visible and highest point of the ciliary implantation line of the upper eyelid. Move the horizontal auxiliary line from top to bottom until it is tangential with the upper eyelid. Landmark at the intersection of auxiliary lines. Same procedure for the contralateral point.

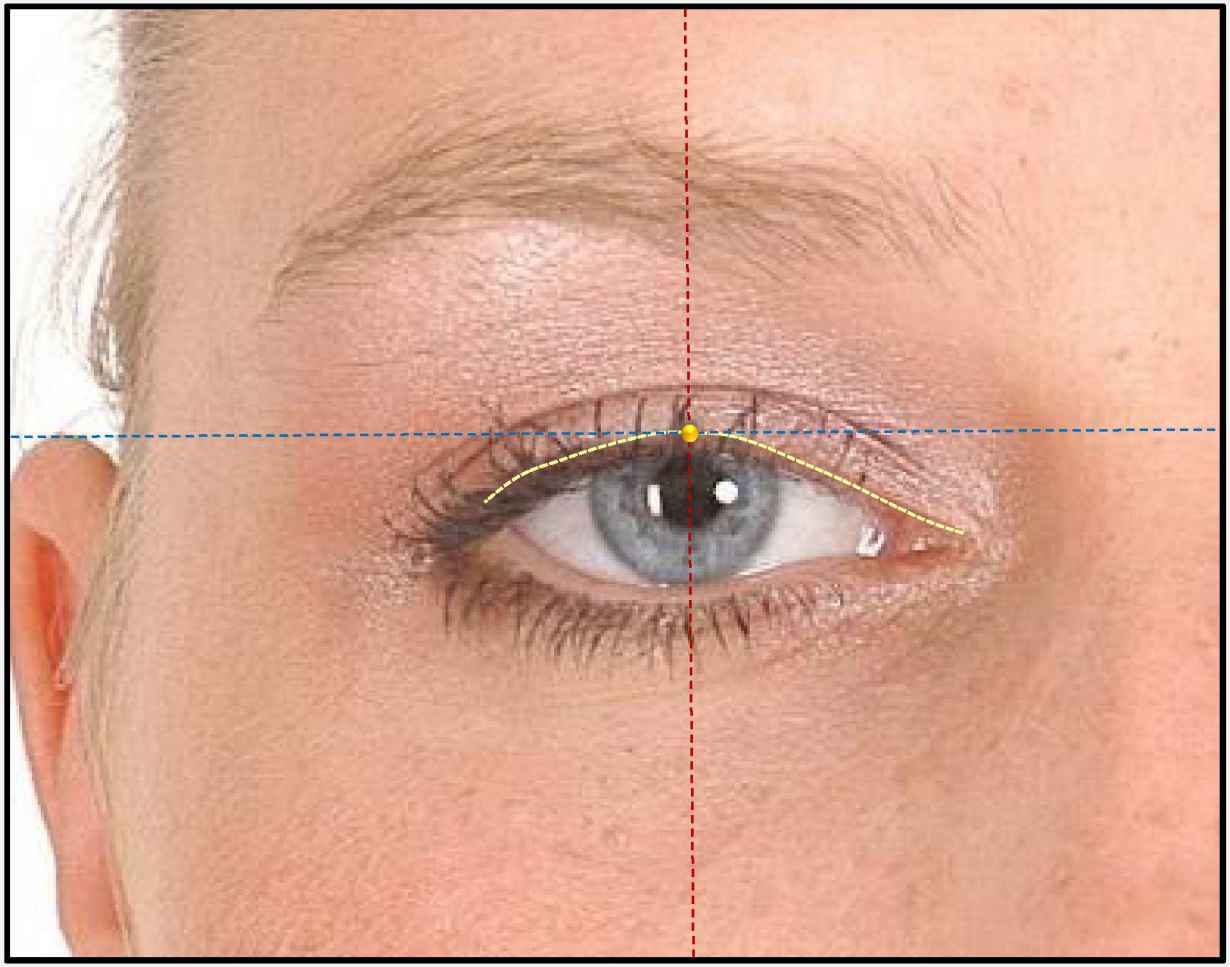

PALPEBRALE SUPERIUS GROOVE AND PALPEBRALE SUPERIUS: Observation

19

Palpebrale Superius Groove and *Palpebrale Superius* landmarks are not always vertically aligned. The landmarking reference for both must be **assessed individually** and located at the highest region of each feature.

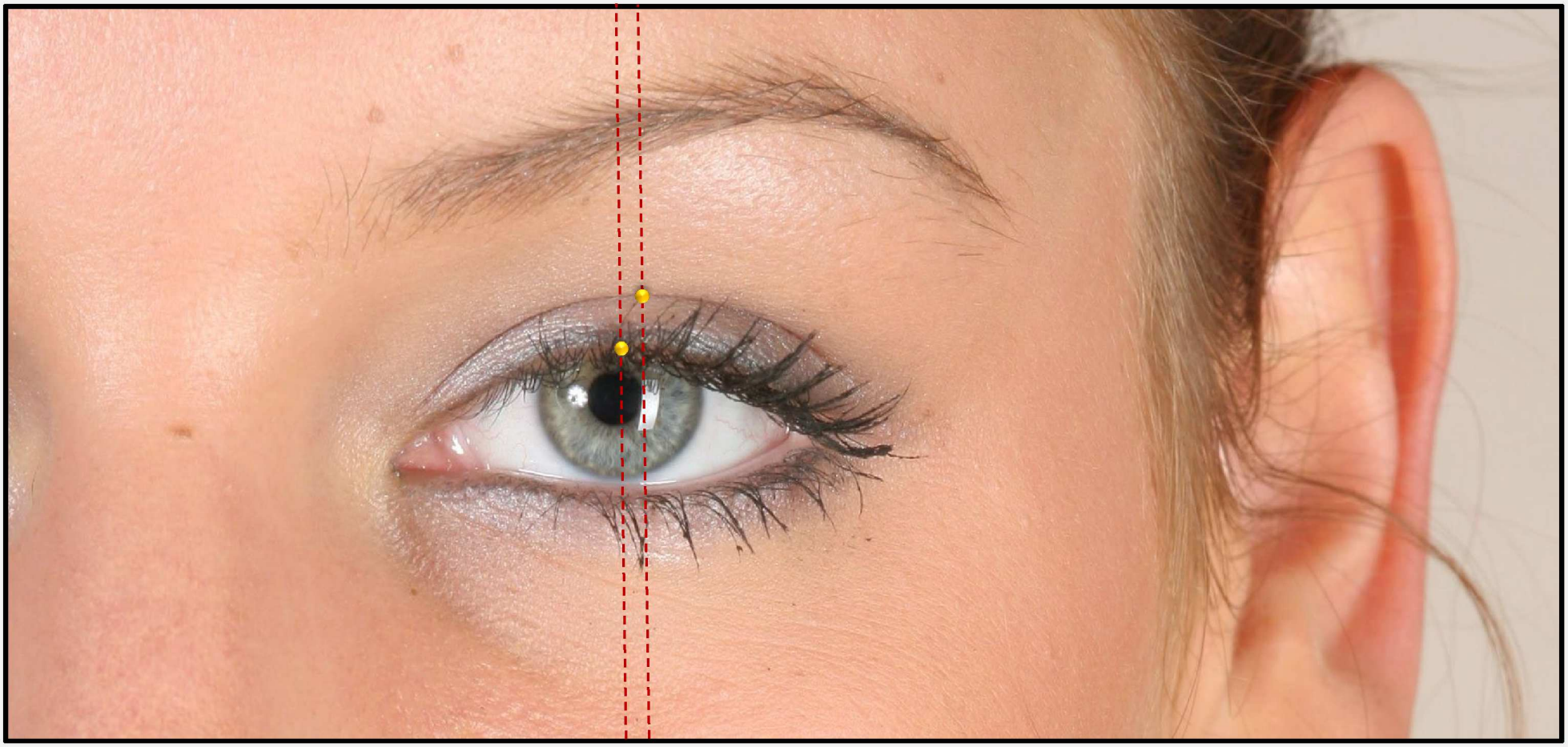

7. PALPEBRALE INFERIUS

Number	Landmark name	Laterality	Abbreviation
7	Palpebrale Inferius	Bilateral	Pi_R / Pi_L

Photo-anthropometric definition

The lower landmark of the lower, eyelid-free margin, above the line of the eyelashes.

SAFF-2D landmarking procedures

Image approximation (Zoom):
Examined eye framing.

Reference:
Lower eyelid-free margin.
(Ciliary implantation line)

Auxiliary lines:
Vertical and horizontal.

Procedure:
Position vertical auxiliary line to pass through the lowest point of the lower eyelid ciliary implantation line. Move horizontal auxiliary line from bottom to top until it is tangential with the lower eyelid. Mark this landmark at the intersection of auxiliary lines. Same procedure for the contralateral point.

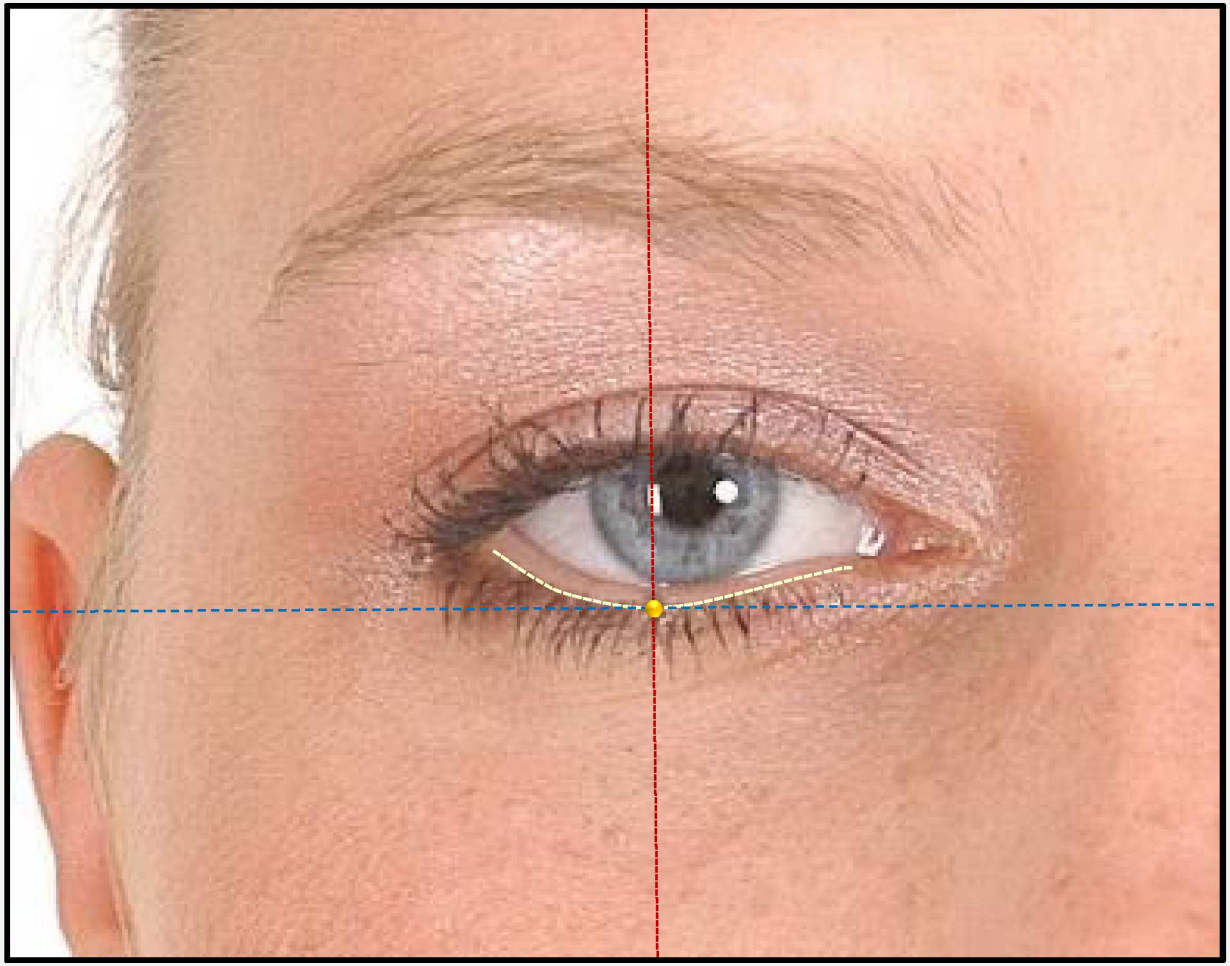

PHOTO-ANTHROPOMETRIC ANALYSIS: MANUAL LANDMARKING 21

8. MEDIALE EYEBROW

Number	Landmark name	Laterality	Abbreviation
8	Mediale Eyebrow	Bilateral	Me_R / Me_L

Photo-anthropometric definition

The most medial landmark of the eyebrow.

SAFF-2D landmarking procedures

Image approximation (Zoom):
Frontal, orbital and nasal framing.

Reference:
Eyebrow design.

Auxiliary lines:
Vertical and horizontal.

Procedure:
Move the vertical auxiliary line from the medial to lateral side of the face until it touches the most medial portion of the eyebrow design. Then, use the horizontal line to locate the apex of the convex feature. Follow the same procedure to locate the contralateral landmark, which will not necessarily be at the same facial height.

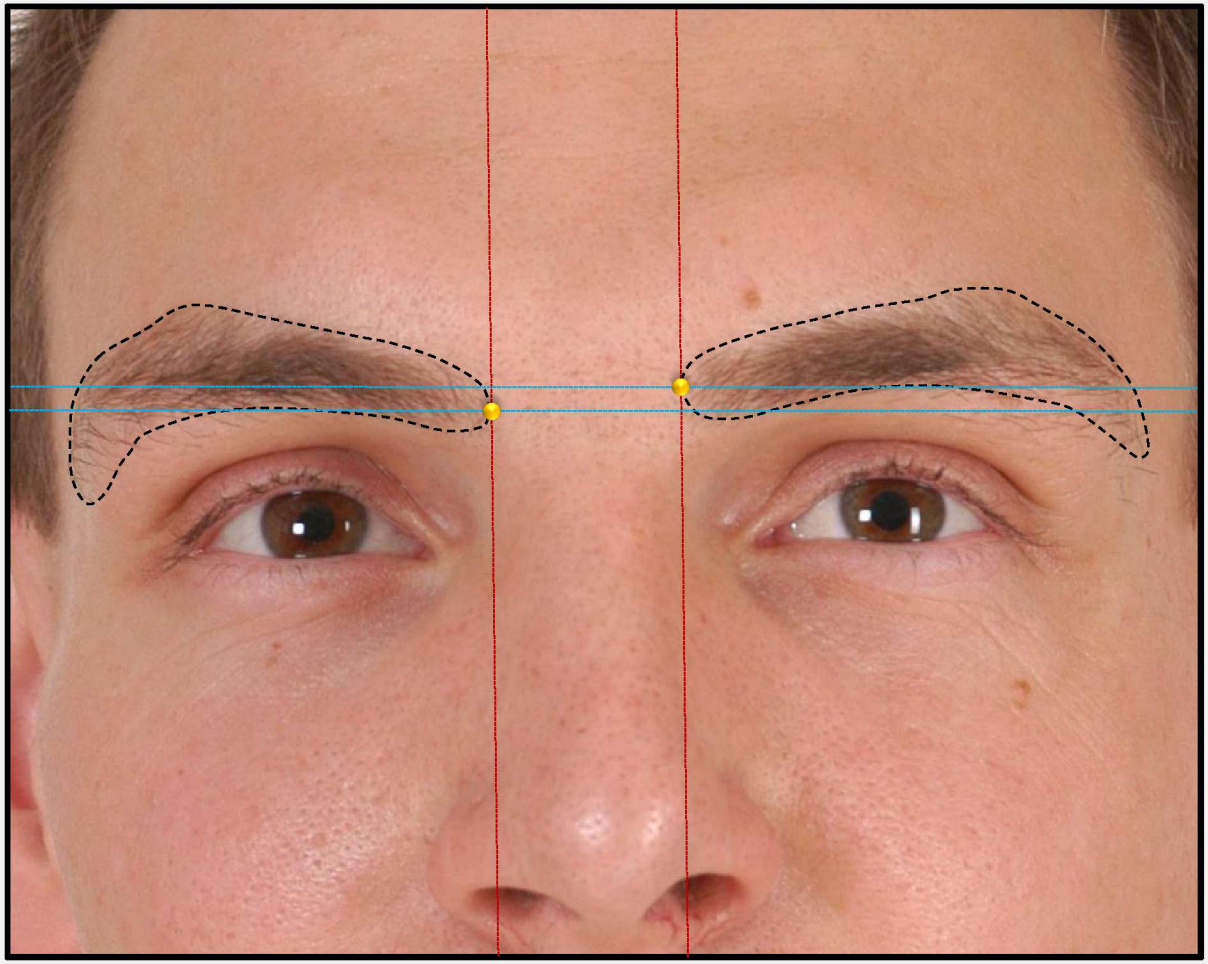

PHOTO-ANTHROPOMETRIC ANALYSIS: MANUAL LANDMARKING 22

9. LATERALE EYEBROW

Number	Landmark name	Laterality	Abbreviation
9	Laterale Eyebrow	Bilateral	Le_R / Le_L

Photo-anthropometric definition

The most lateral landmark of the eyebrow.

SAFF-2D landmarking procedures

Image approximation (Zoom):
Frontal, orbital and nasal framing.

Reference:
Eyebrow design.

Auxiliary lines:
Vertical and horizontal.

Procedure:
Move the vertical auxiliary line from the lateral to medial facial region until it touches the most lateral portion of the eyebrow design. Then, use horizontal line to locate the most lateral region of its contour. Follow the same procedure to mark the contralateral point, which will not necessarily be at the same facial height.

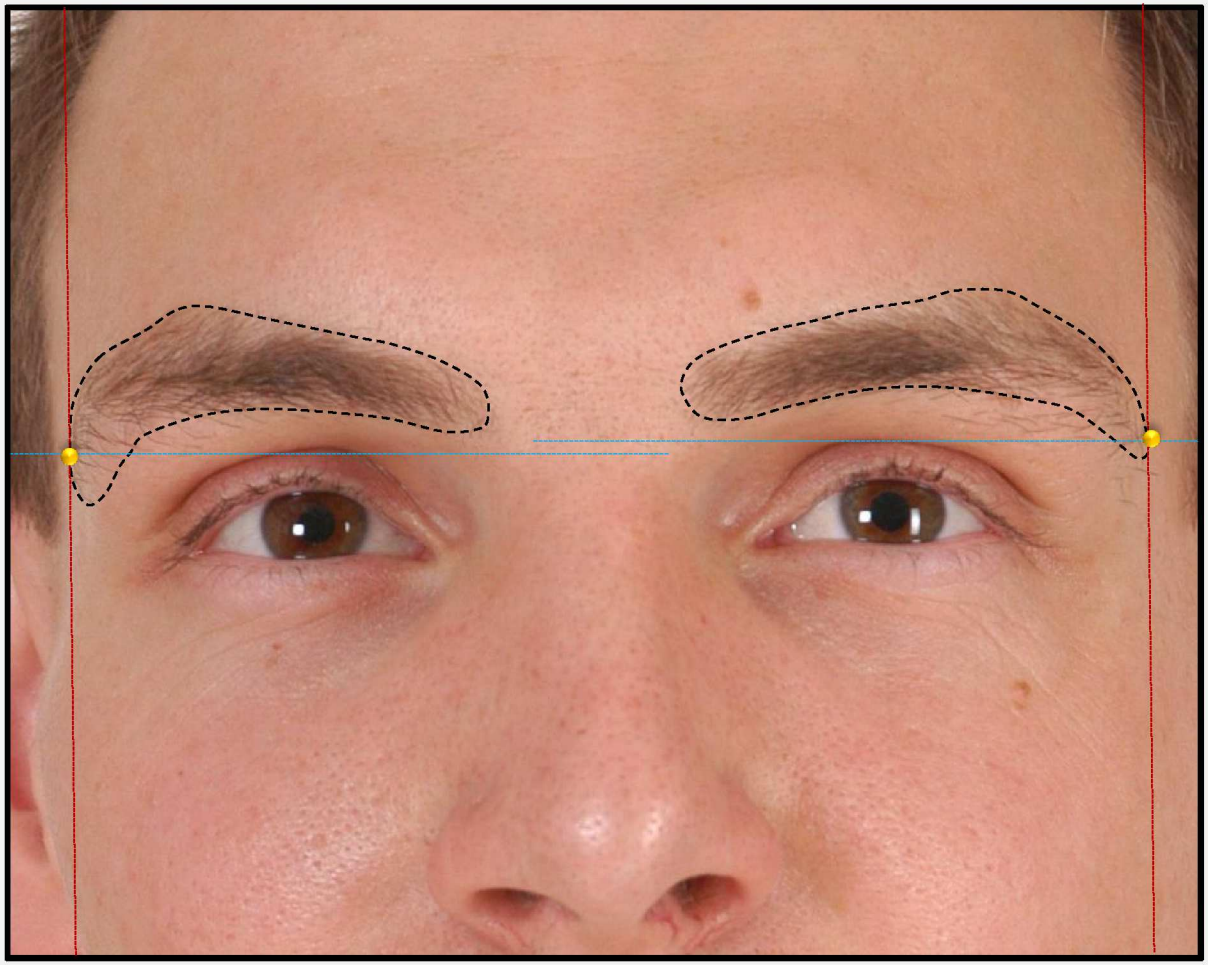

10. FRONTOTEMPORALE

Number	Landmark name	Laterality	Abbreviation
10	Frontotemporale	Bilateral	Ft_R / Ft_L

Photo-anthropometric definition

The uppermost landmark of the eyebrow above the Frontotemporale line (determined by the horizontal mean of *Ectocanthion* and the ipsilateral *Lateral Eyebrow* landmarks).

SAFF-2D landmarking procedures

Image approximation (Zoom):
Frontal, orbital and nasal framing.

Reference:
Eyebrow design.
Frontotemporale line (automated).

Auxiliary lines:
Horizontal line.

Procedure:
Move horizontal line from top to bottom until the uppermost portion of the eyebrow design, where it meets the Frontotemporale vertical line, is found. Landmark at the intersection of the two auxiliary lines. Follow the same procedure to locate contralateral point, which will not necessarily be at the same facial height.

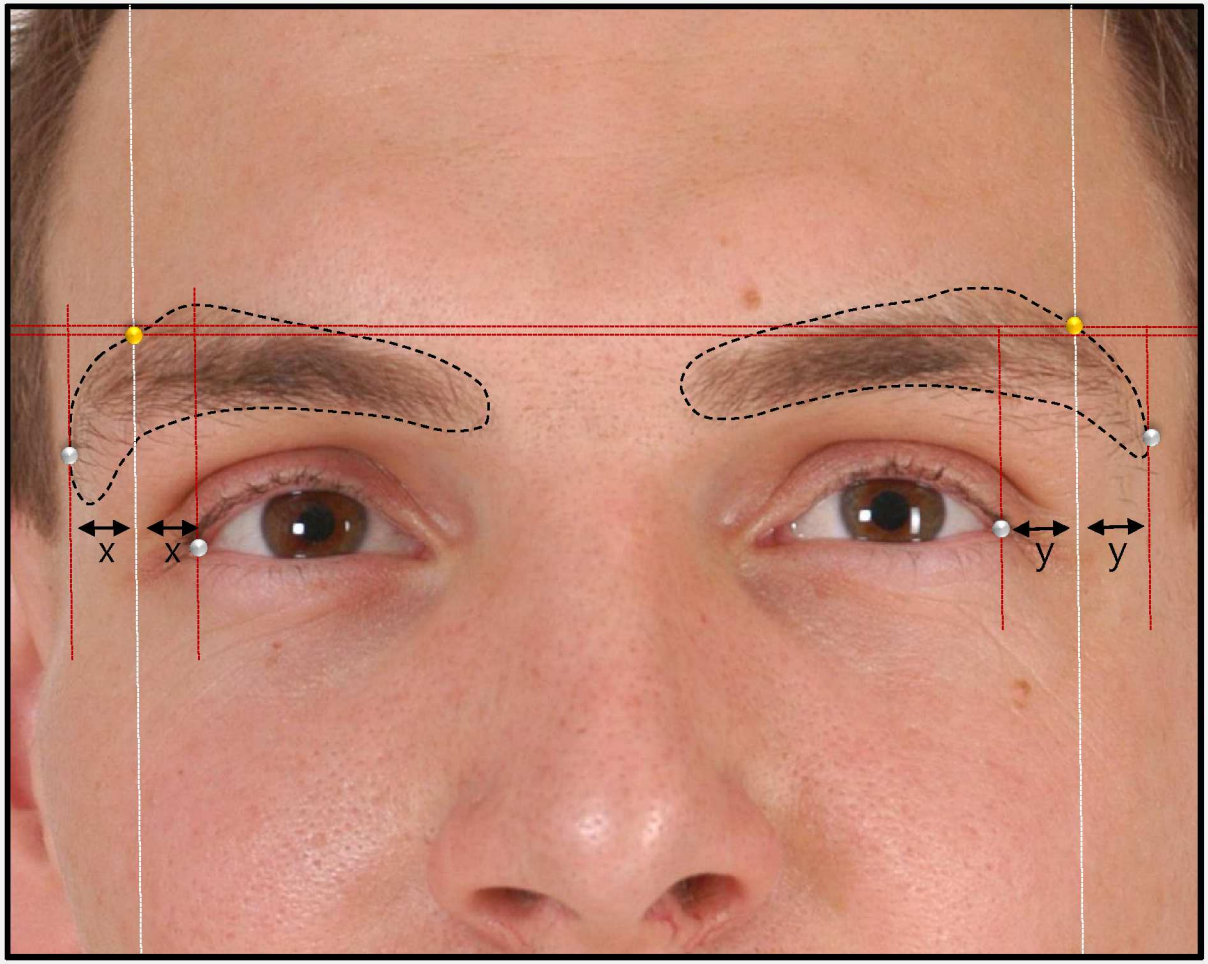

PHOTO-ANTHROPOMETRIC ANALYSIS: MANUAL LANDMARKING 24

11. SUPERIUS EYEBROW

Number	Landmark name	Laterality	Abbreviation
11	Superius Eyebrow	Bilateral	Se_R / Se_L

Photo-anthropometric definition

The uppermost landmark of the eyebrow.

SAFF-2D landmarking procedures

Image approximation (Zoom):
Frontal, orbital and nasal framing.

Reference:
Eyebrow design.

Auxiliary lines:
Vertical and horizontal.

Procedure:
Move the horizontal auxiliary line from the top to bottom of the face until the uppermost portion of eyebrow design is crossed. Then, use the vertical line to pass through the same point. The point of intersection of the auxiliary lines is the position of the landmark. Follow the same procedure for the location of the contralateral point, which will not necessarily be at the same facial height.

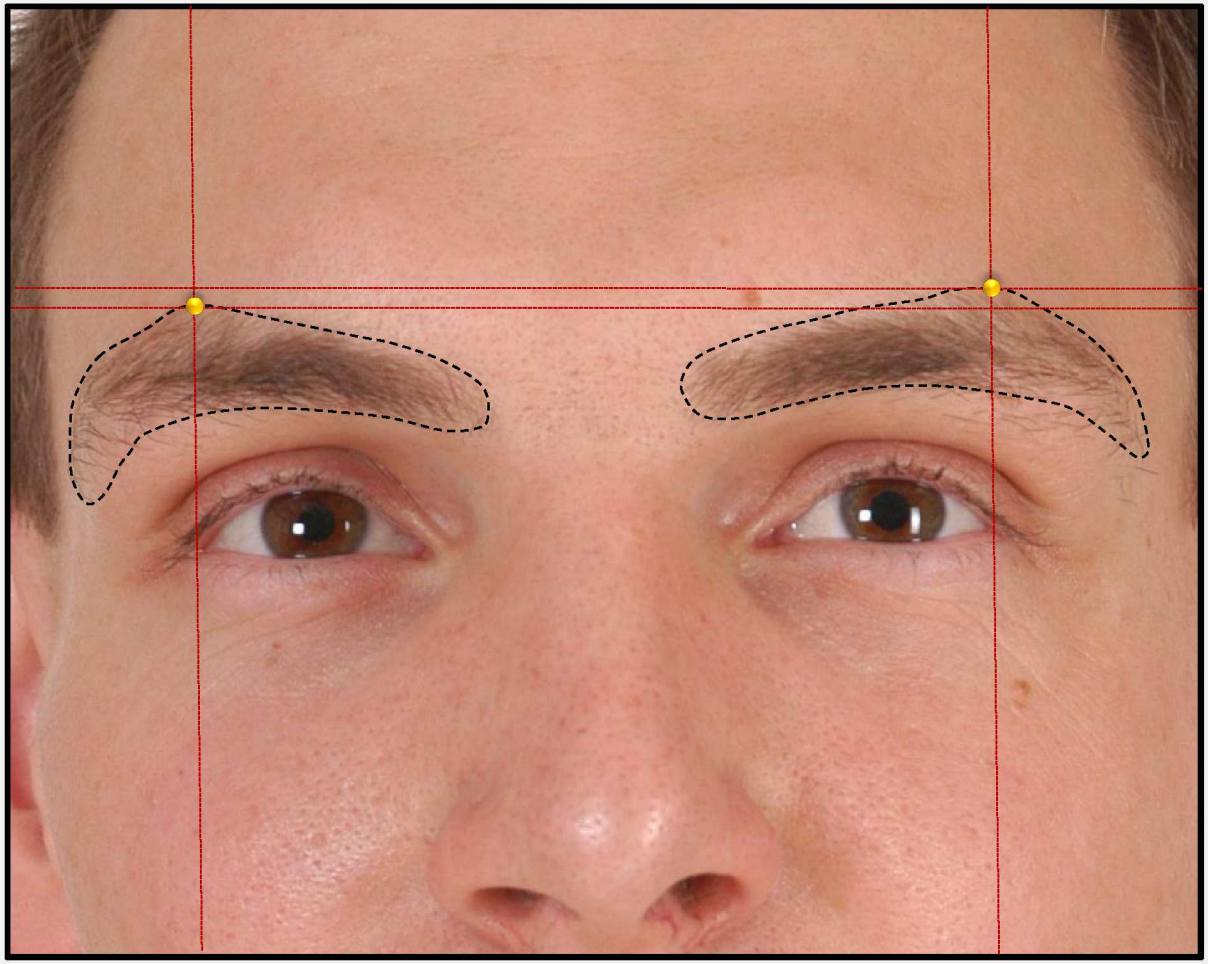

12. INFERIUS EYEBROW

Number	Landmark name	Laterality	Abbreviation
12	Inferius Eyebrow	Bilateral	Ie_R / Ie_L

Photo-anthropometric definition

The lower eyebrow point.

SAFF-2D landmarking procedures

Image approximation (Zoom):
Frontal, orbital and nasal framing.

Reference:
Eyebrow design.
Eyebrow midline (automated).

Auxiliary lines:
Horizontal.

Procedure:
The point on the eyebrow midline (aut.) that is tangential with the lower portion of the eyebrow design is the position of this landmark. Follow the same procedure for the location of the contralateral point, which will not necessarily be at the same facial height.

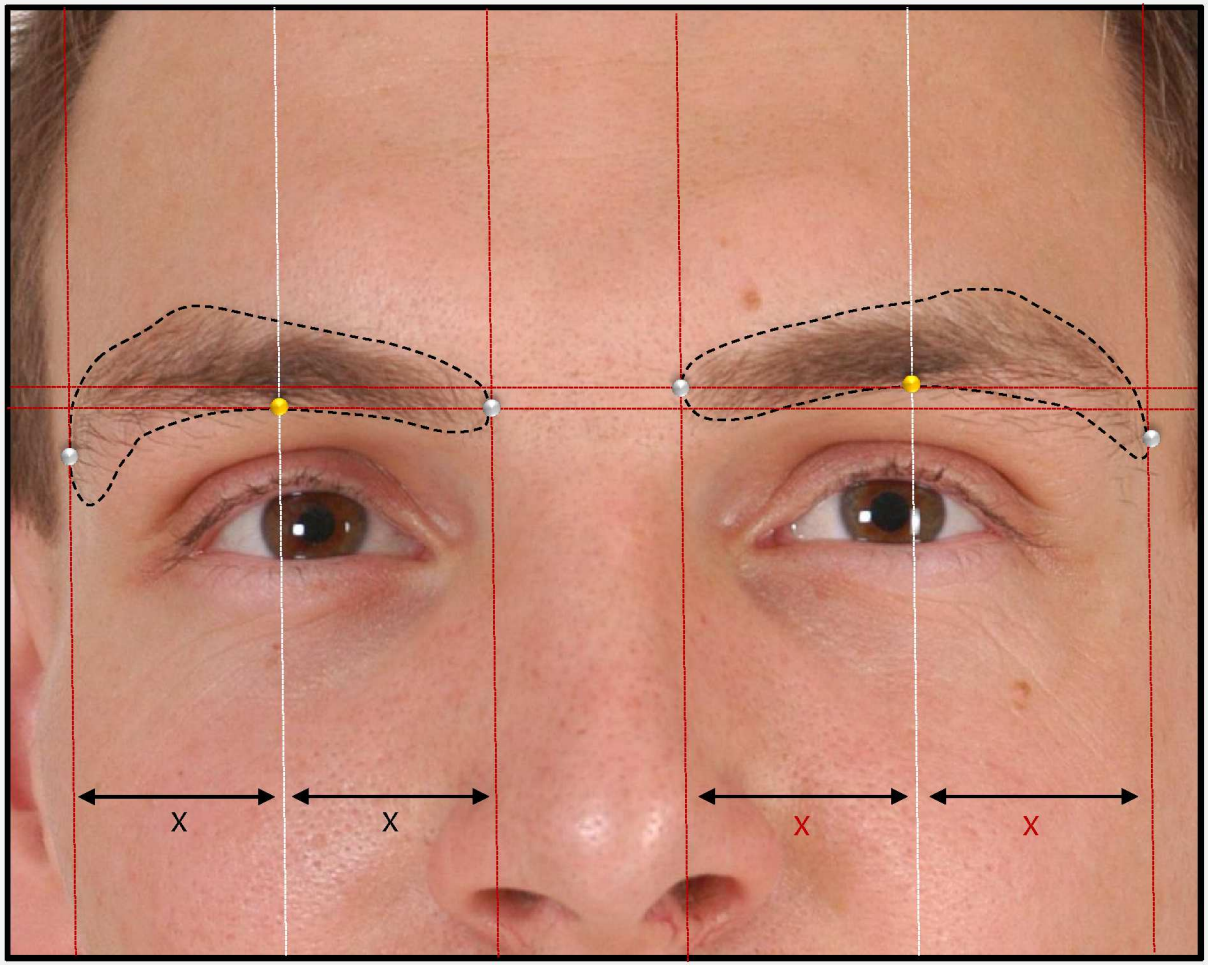

Eyebrow design: Observation 1

26

For landmarking **points 8 to 12 (eyebrow points)**, it is necessary to encompass all regions with a high density of hairs when encircling the eyebrow. Very sparse (those outside the area of higher density hairs) and/or misaligned hairs must not be considered for landmarking purposes.

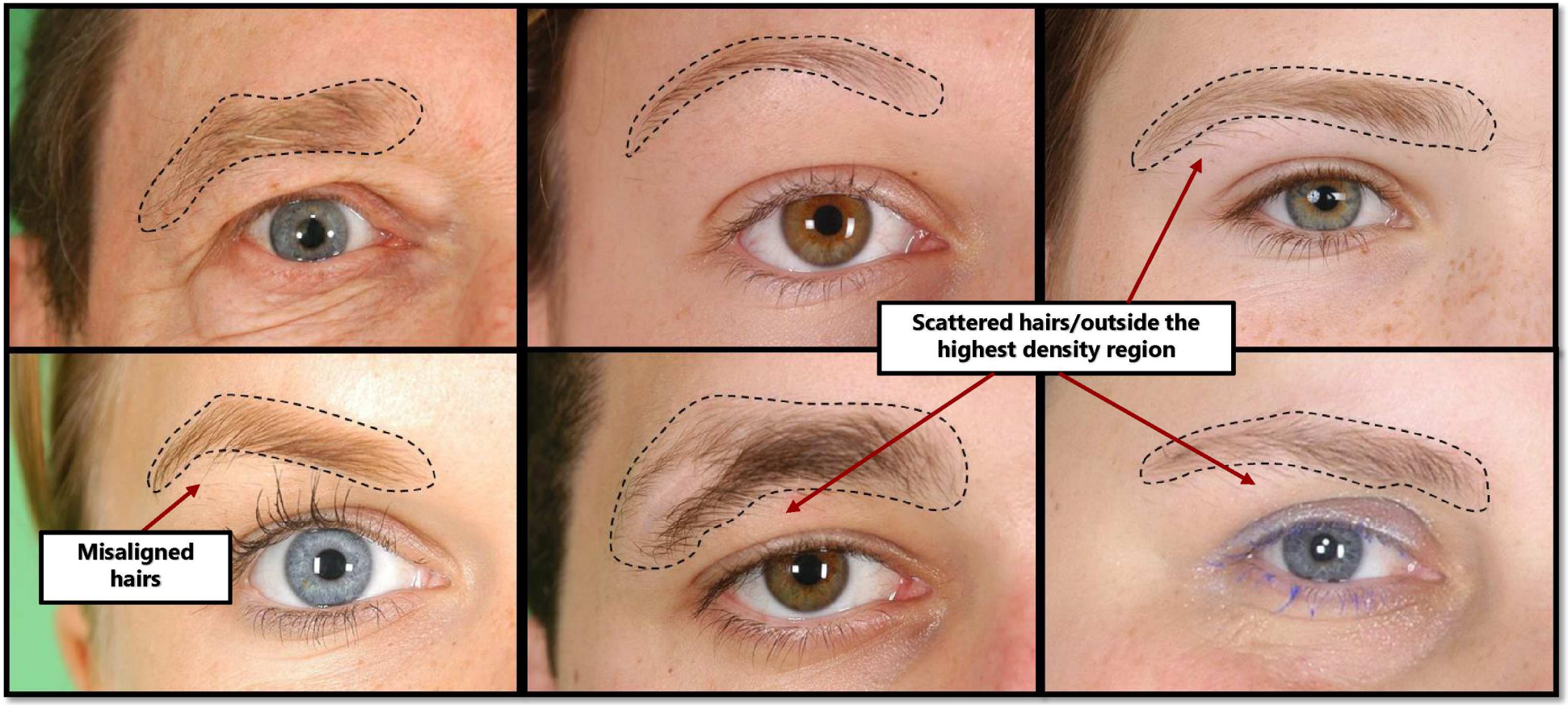

Eyebrow design: Observation 2

27

When exogenous pigmentation (cosmetic tattoos) are present, **mark the points from 8 to 12 (eyebrow points)** and include an observation in the specific field of SAFF-2D.

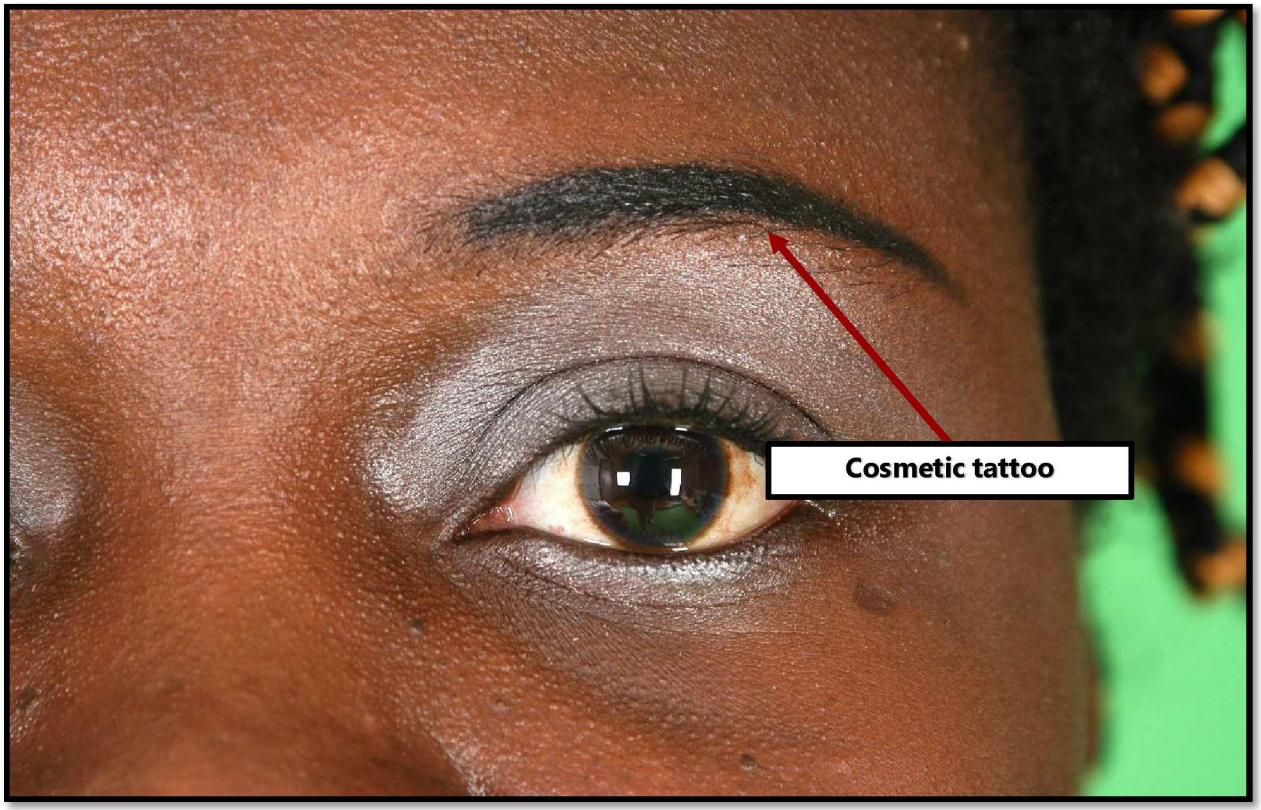

Eyebrow design: Observation 3

28

When visibly **altered and/or unnatural contours** are present, **mark the eyebrow points (from 8 to 12)** and include an observation in the specific field of SAFF-2D.

Eyebrow design: Unibrow

29

When hairs with similar or the same density are present between eyebrows in a way that would characterize them as a single one (unibrow), **do not mark the points referring to the eyebrows (from 8 to 12)** and include an observation in the specific field of SAFF-2D.

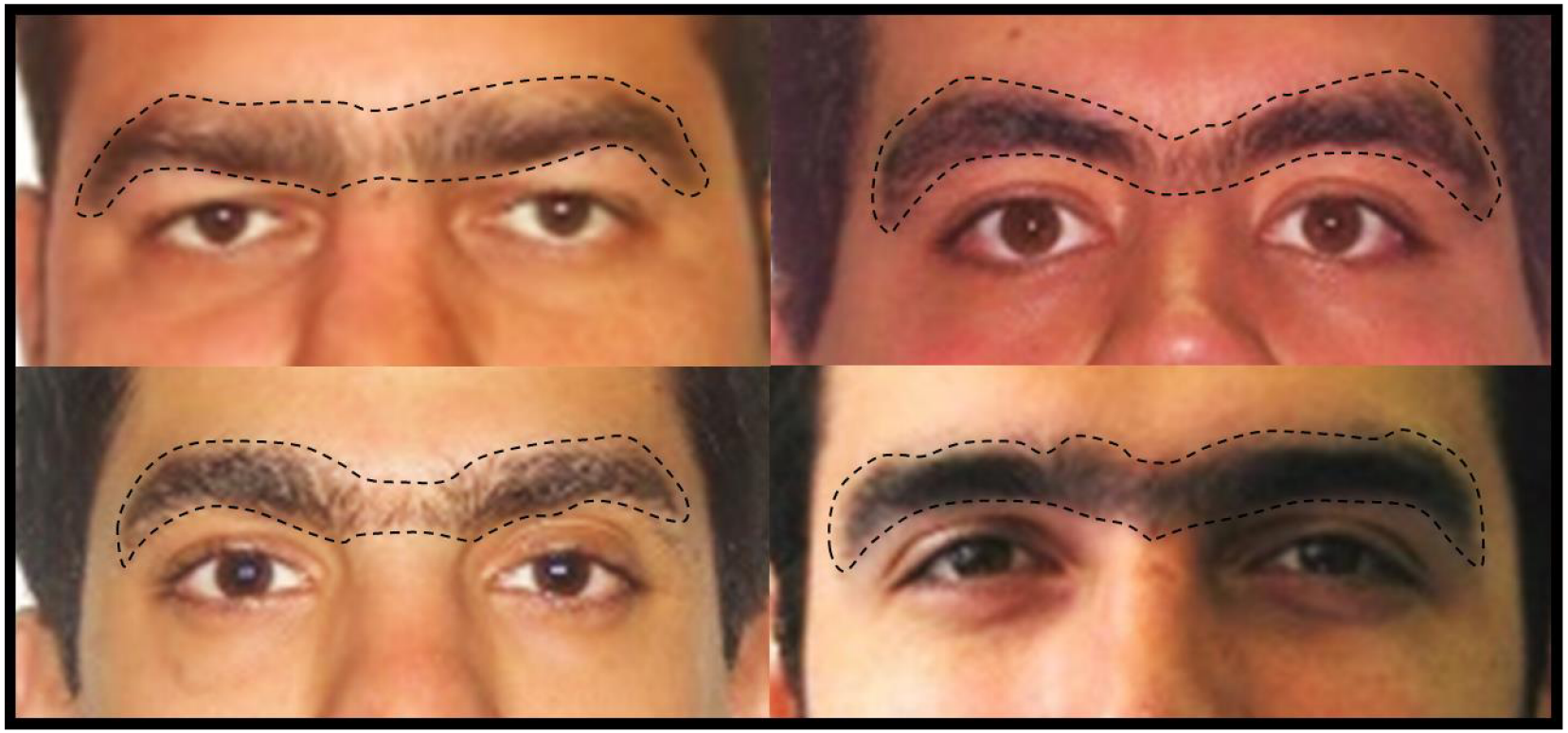

PHOTO-ANTHROPOMETRIC ANALYSIS: MANUAL LANDMARKING 30

13. TRICHION

Number	Landmark name	Laterality	Abbreviation
13	Trichion	Median	Tr

Photo-anthropometric definition

Meeting landmark of the orbital midline with the lowermost region of the hairline.

SAFF-2D landmarking procedures

Image approximation (Zoom):
Framing of middle and upper face portion or complete face.

Reference:
Capillary implantation line.
Orbital midline (automated).

Auxiliary lines:
Horizontal line.

Procedure:
Move the horizontal line from bottom to top until the lowest point of the capillary implantation is met. Locate this landmark on the hair implant line. If necessary, use the vertical reference line.

Observation:
In case where this is not visible, do not landmark it and include an observation in the specific field of SAFF-2D.

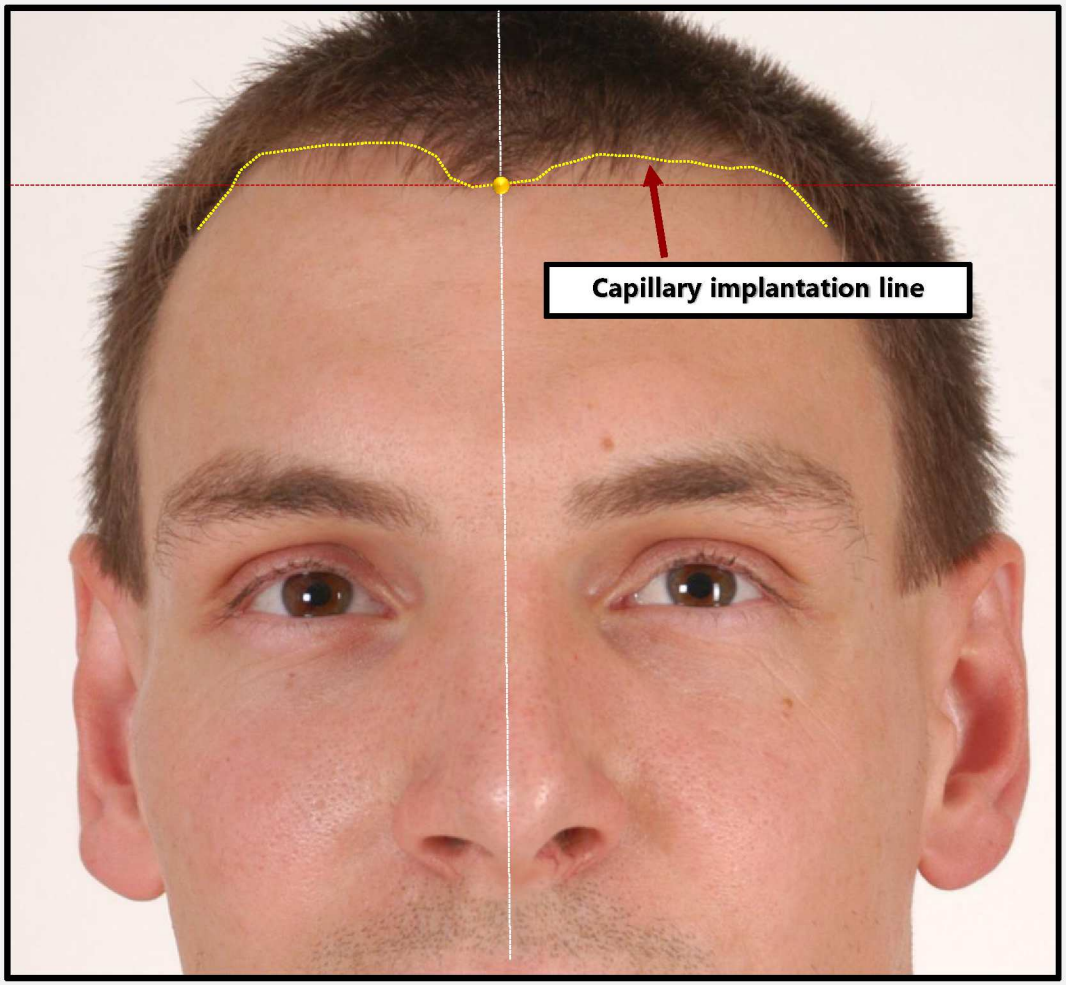

Capillary implantation line: Observation

31

Similarly to the eyebrow design, it is important to note that very sparse hairs on the capillary implantation line (those out of the higher density area) and/or misaligned hairs must not be included when constructing the line. Consider the hair implantation line as that between the hair on the scalp and the facial skin.

PHOTO-ANTHROPOMETRIC ANALYSIS: MANUAL LANDMARKING 32

14. PRONASALE

Number	Landmark name	Laterality	Abbreviation
14	Pronasale	Median	Prn

Photo-anthropometric definition

The most anterior landmark of the cartilaginous portion of the nose (nose tip).

SAFF-2D landmarking procedures

Image approximation (Zoom):
Framing of middle portion of, or complete, face.

Reference:
Region of greatest light reflection on the nose tip.

Auxiliary lines:
Not required.

Procedure:
Position the landmark on the cartilaginous portion of the nose at the point of greatest light reflection (visual perception of the most anterior portion of nose, i.e. the tip).

Observation:
When viewing an *area*, instead of a *point*, mark in its most central portion.

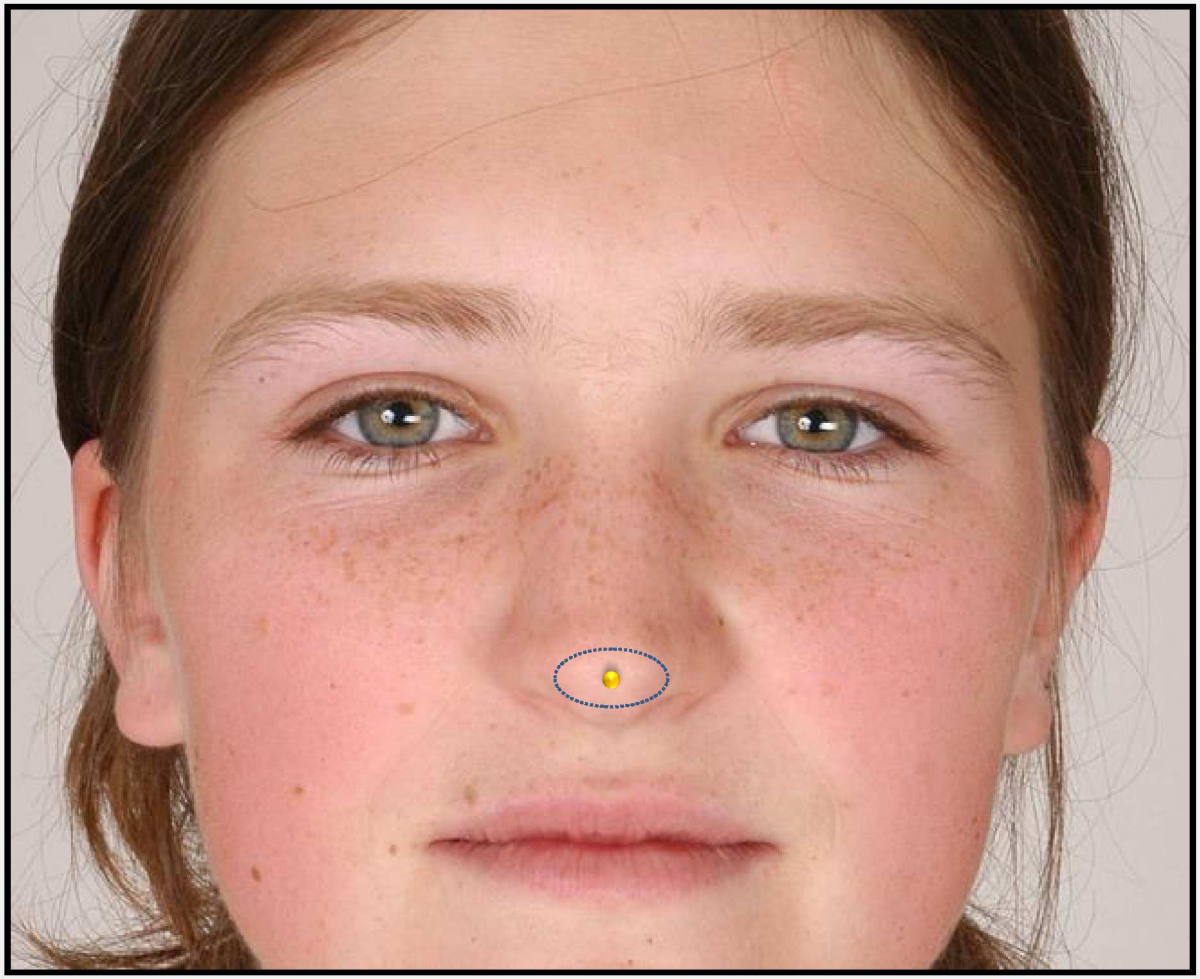

PHOTO-ANTHROPOMETRIC ANALYSIS: MANUAL LANDMARKING 33

15. SUBNASALE

Number	Landmark name	Laterality	Abbreviation
15	Subnasale	Median	Sn

Photo-anthropometric definition

The lowermost landmark of the nose (base of columella).

SAFF-2D landmarking procedures

Image approximation (Zoom):
Framing of middle portion of, or complete, face.

Reference:
Columella basis.

Auxiliary lines:
Vertical and horizontal lines.
Edge detection filter (Laplace).

Procedure:
Position the vertical auxiliary line in the lowermost region of the columella (move it from side to side until it passes through the region of greatest curvature). Then move the horizontal auxiliary line from bottom to top until it passes through the same region. The intersection of the auxiliary lines is the point to landmark.

Observation:
Do not take into account the orbital and labial midlines (automated) for this specific landmark.

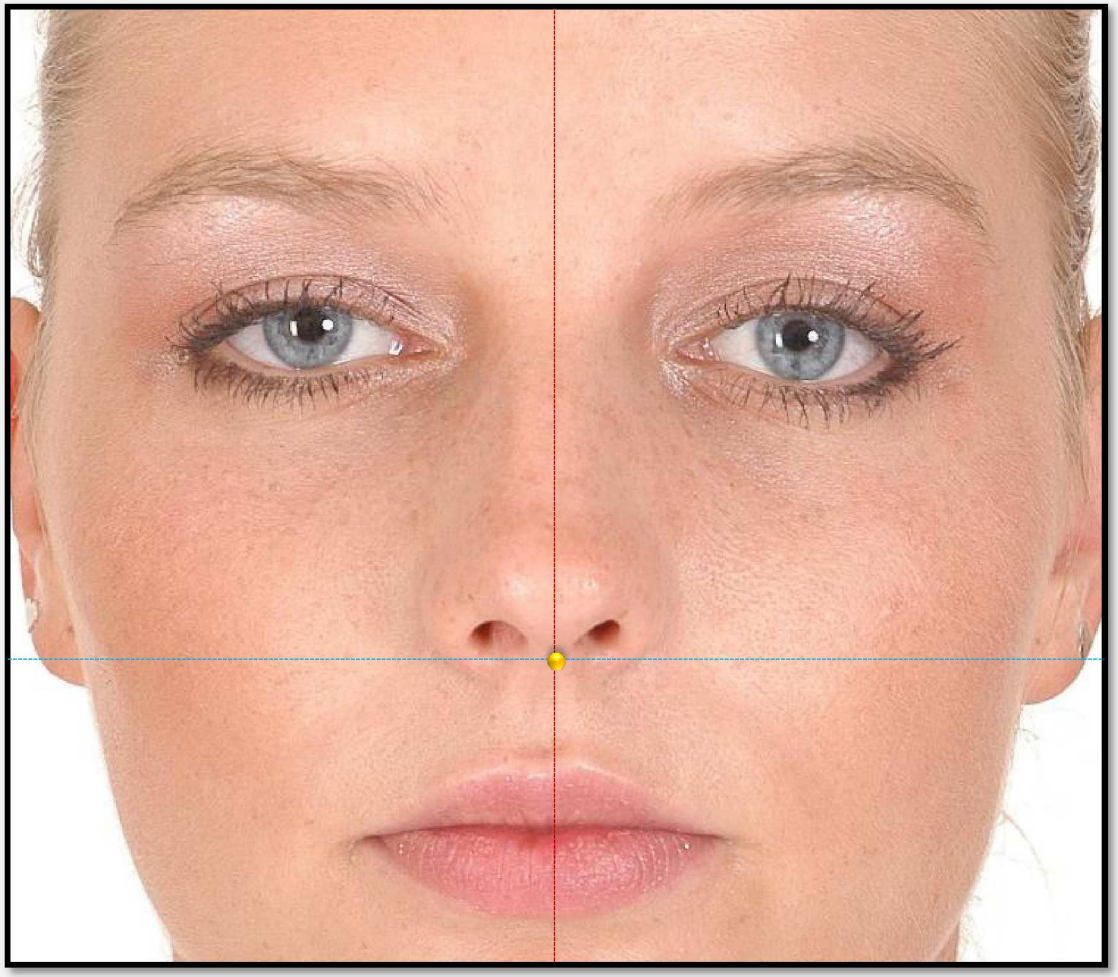

Columella basis: Observation

34

When the columella basis is not visible, or it is covered by the nose tip, mark the lowest contour of nasal projection.

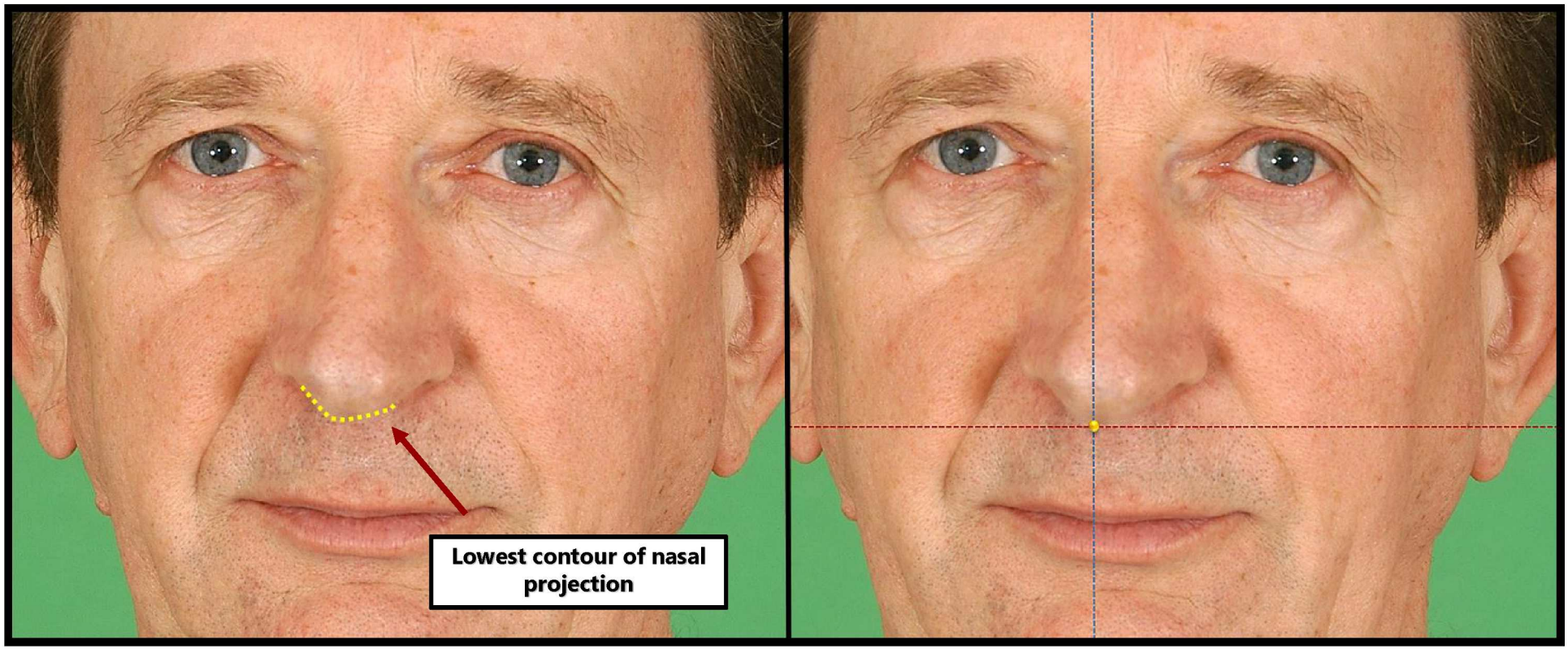

PHOTO-ANTHROPOMETRIC ANALYSIS: MANUAL LANDMARKING 35

16. ALARE

Number	Landmark name	Laterality	Abbreviation
16	Alare	Bilateral	Al_R / Al_L

Photo-anthropometric definition

The most lateral landmark of the nose wing.

SAFF-2D landmarking procedures

Image approximation (Zoom):
Framing of middle portion of, or complete, face.

Reference:
Lateral region of nose wing.

Auxiliary lines:
Vertical and horizontal lines.
Edge detection filter (Laplace).

Procedure:
Move the vertical auxiliary line from the lateral to medial side of the nose and the horizontal line from bottom to top, until they cross at the outermost point of the nose flap. *Alare* should be marked in the region of intersection between the two reference lines. Follow the same procedure for marking the contralateral point, which will not necessarily be at the same facial height.

Alare: Observation

36

The right and left *Alare* landmarks are not always at the same facial height.

Number	Landmark name	Laterality	Abbreviation
16	Alare	Bilateral	Al_R / Al_L

17. SUPERIUS NOSTRIL

Number	Landmark name	Laterality	Abbreviation
17	Superius Nostril	Bilateral	Spn_R / Spn_L

Photo-anthropometric definition

The uppermost landmark of nasal orifice (nostril).

SAFF-2D landmarking procedures

Image approximation (Zoom):
Framing of middle portion of, or complete, face.

Reference:
Upper region of nasal orifice.

Auxiliary lines:
Vertical and horizontal lines.
Edge detection filter (Laplace).

Procedure:
Move the horizontal auxiliary line from top to bottom until it is tangential with the uppermost portion of the nasal orifice. Align the vertical auxiliary line to also pass through the highest position. Landmark the point of intersection of the two lines. Follow the same procedure for marking the contralateral point, which will not necessarily be at the same facial height.

PHOTO-ANTHROPOMETRIC ANALYSIS: MANUAL LANDMARKING 38

18. LATERALE NOSTRIL

Number	Landmark name	Laterality	Abbreviation
18	Laterale Nostril	Bilateral	Ln_R / Ln_L

Photo-anthropometric definition

The most lateral landmark of nasal orifice (nostril).

SAFF-2D landmarking procedures

Image approximation (Zoom):
Framing of middle portion of, or complete, face.

Reference:
Lateral region of nasal orifice.

Auxiliary lines:
Vertical line.
Edge detection filter (Laplace).

Procedure:
Move the vertical auxiliary line, from lateral to medial, until the region of greatest lateral curvature of the nasal orifice is found. Follow the same procedure for marking the contralateral point, which will not necessarily be at the same facial height.

19. SUBALARE

Number	Landmark name	Laterality	Abbreviation
19	Subalare	Bilateral	Sbal_R / Sbal_L

Photo-anthropometric definition

Landmark below the nostril where alare sulcus disappears.

SAFF-2D landmarking procedures

Image approximation (Zoom):
Framing of middle portion of, or complete, face.

Reference:
Lower nose region.

Auxiliary lines:
Edge detection filter (Laplace).

Procedure:
Position this landmark in the region where the lateral contour of the lower nose (region of *Alares*) disappears. Follow the same procedure for marking the contralateral point, which will not necessarily be at the same facial height.

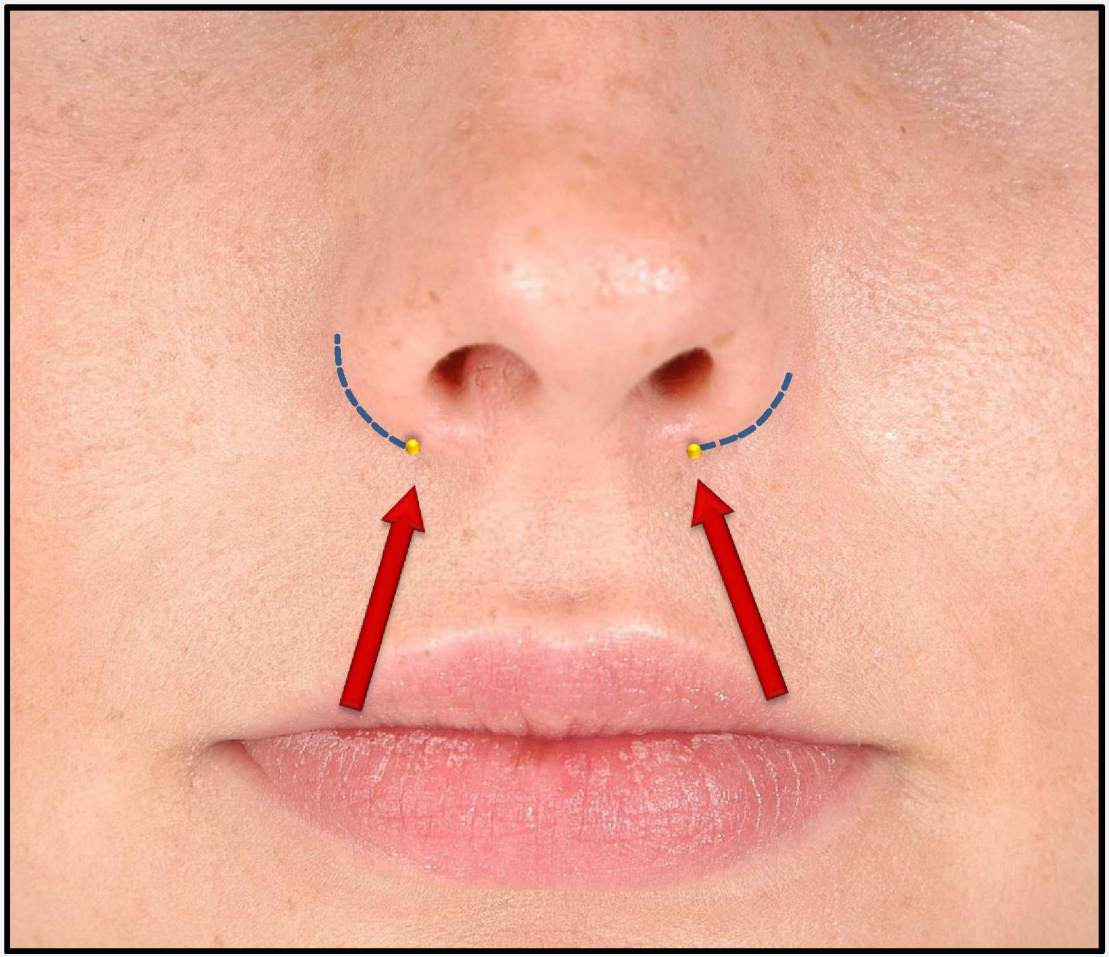

PHOTO-ANTHROPOMETRIC ANALYSIS: MANUAL LANDMARKING 40

20. LABIALE SUPERIUS

Number	Landmark name	Laterality	Abbreviation
20	Labiale Superius	Median	Ls

Photo-anthropometric definition

Mid-landmark of the vermilion border of the upper lip. Lowermost landmark of cupid's bow (when present).

SAFF-2D landmarking procedures

Image approximation (Zoom):
Lower facial region.

References:
Cupid's bow region.
Vermilion border.

Auxiliary lines:
Edge detection filter (Laplace).

Procedure:
Position this landmark over the vermilion border (transition line from the vermilion of the mouth to surrounding skin), at the lowest point of the apex of the "V" of the cupid's bow (medial region of upper lip).

Observation:
When cupid's bow is absent (primary reference), use labial midline as reference (in this case, the *Labiale Superius* must be marked after *Chelions*, for helpline appearance).

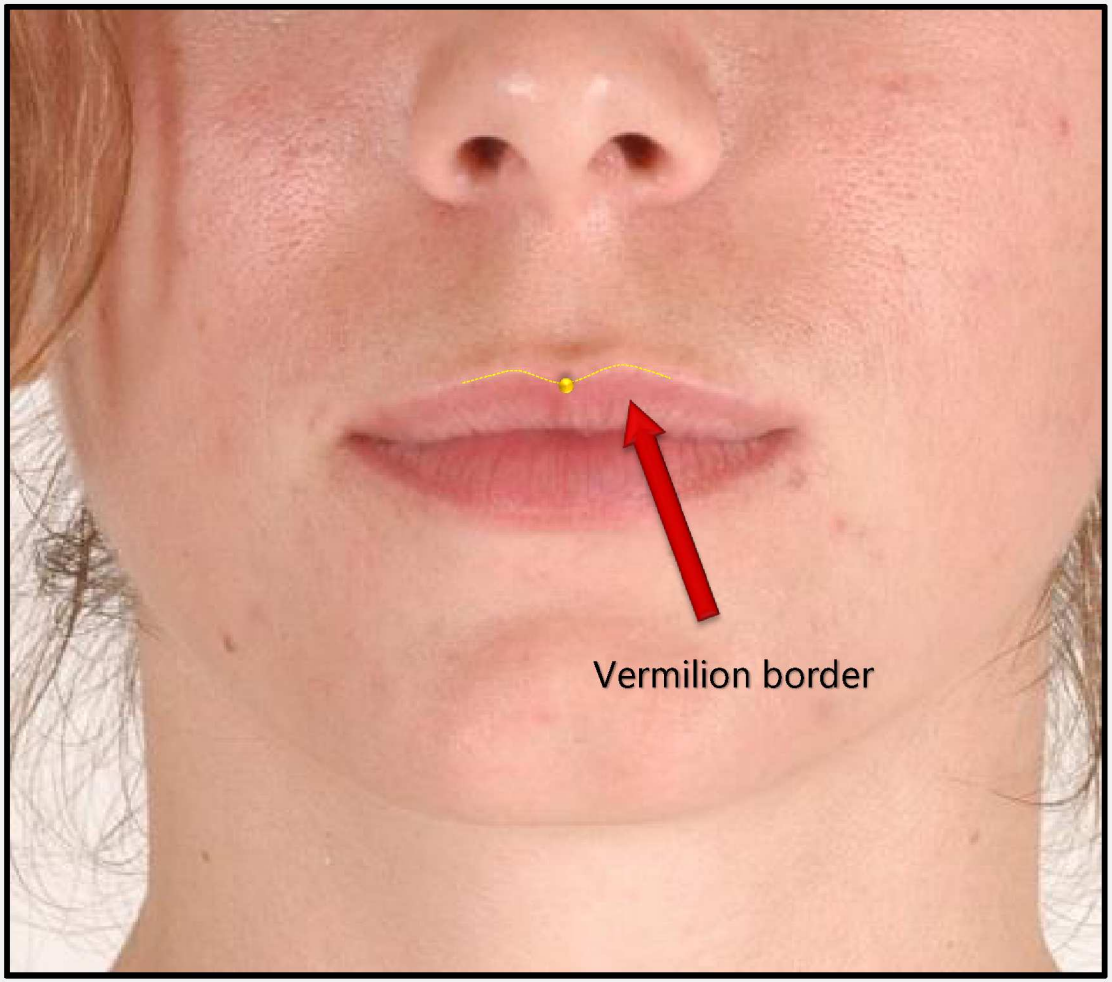

21. CRISTA PHILTRE

Number	Landmark name	Laterality	Abbreviation
21	Crista Philtre	Bilateral	Cph_R / Cph_L

Photo-anthropometric definition

The uppermost landmark of cupid's bow crest, where philtrum columns meet the vermilion border.

SAFF-2D landmarking procedures

Image approximation (Zoom):
Lower facial region.
References:
Cupid's bow region.
Vermilion border.
Auxiliary lines:
Vertical and horizontal.
Procedure:
Move the horizontal auxiliary line from top to bottom, and then the vertical line, from lateral to medial, until they both pass through the uppermost landmark of the "V" of the cupid's bow. The *Crista Philtre* must be landmarked over the vermilion transition line between the mouth and surrounding skin (vermilion border).

Observation:
When the cupid's bow is not present, do not mark these points and include an observation in the SAFF-2D specific field. Contralateral points will not necessarily be at the same facial height.

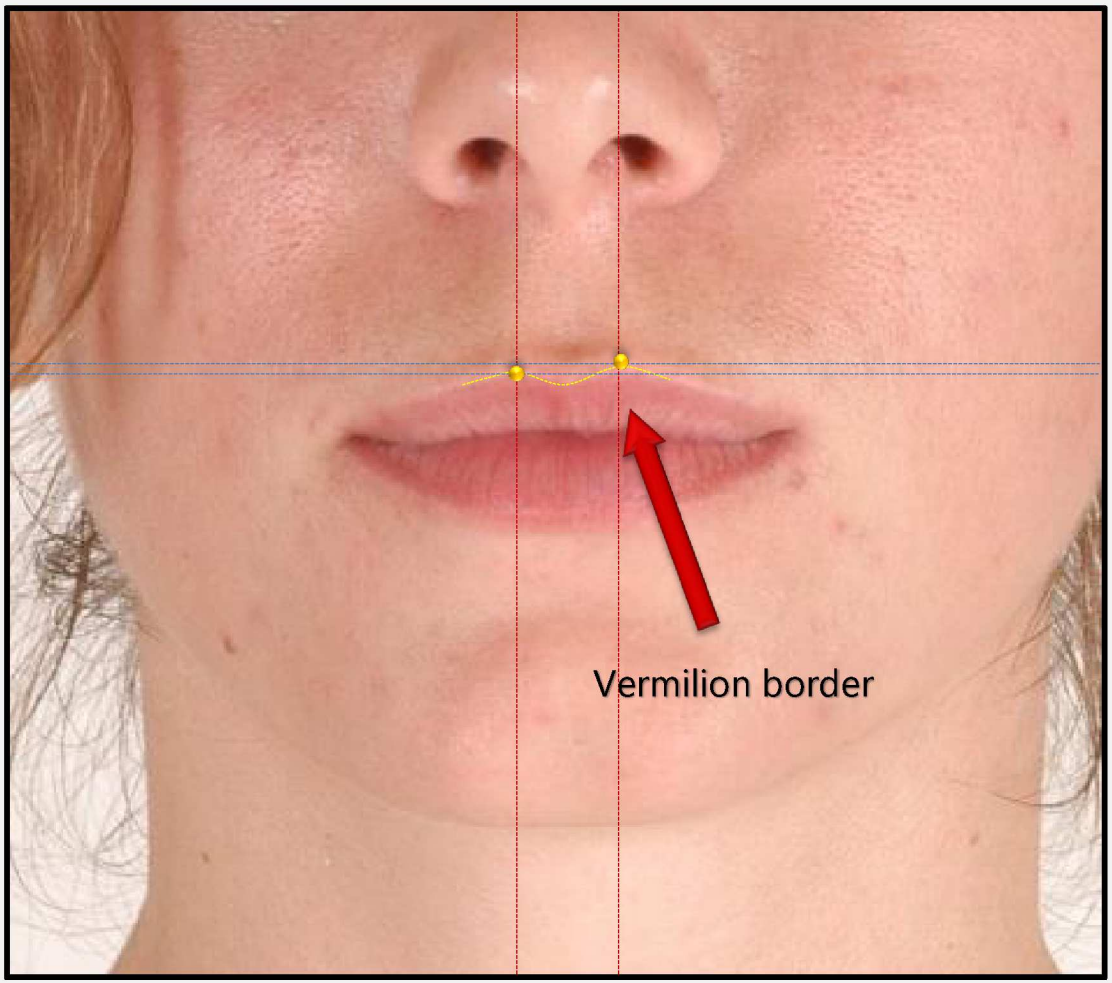

PHOTO-ANTHROPOMETRIC ANALYSIS: MANUAL LANDMARKING 42

22. CHELION

Number	Landmark name	Laterality	Abbreviation
22	Chelion	Bilateral	Ch_R / Ch_L

Photo-anthropometric definition

Intersection landmark of vermilion borders (transition line between labial mucosa and epidermis) of upper and lower lips in the labial commissure.

SAFF-2D landmarking procedures

Image approximation (Zoom):
Lower facial region.

References:
Labial commissure region.
Vermilion border.

Auxiliary lines:
Vertical and horizontal.

Procedure:
Move the vertical line from the lateral to medial side of the mouth and then the horizontal line from the bottom to the top, until they cross at the intersection of the vermilion borders over rima oris (dark line formed by lower and upper lips union). The *Chelion* should be marked in the region of intersection between the two reference lines. Follow the same procedure for marking the contralateral point, which will not necessarily be at the same height.

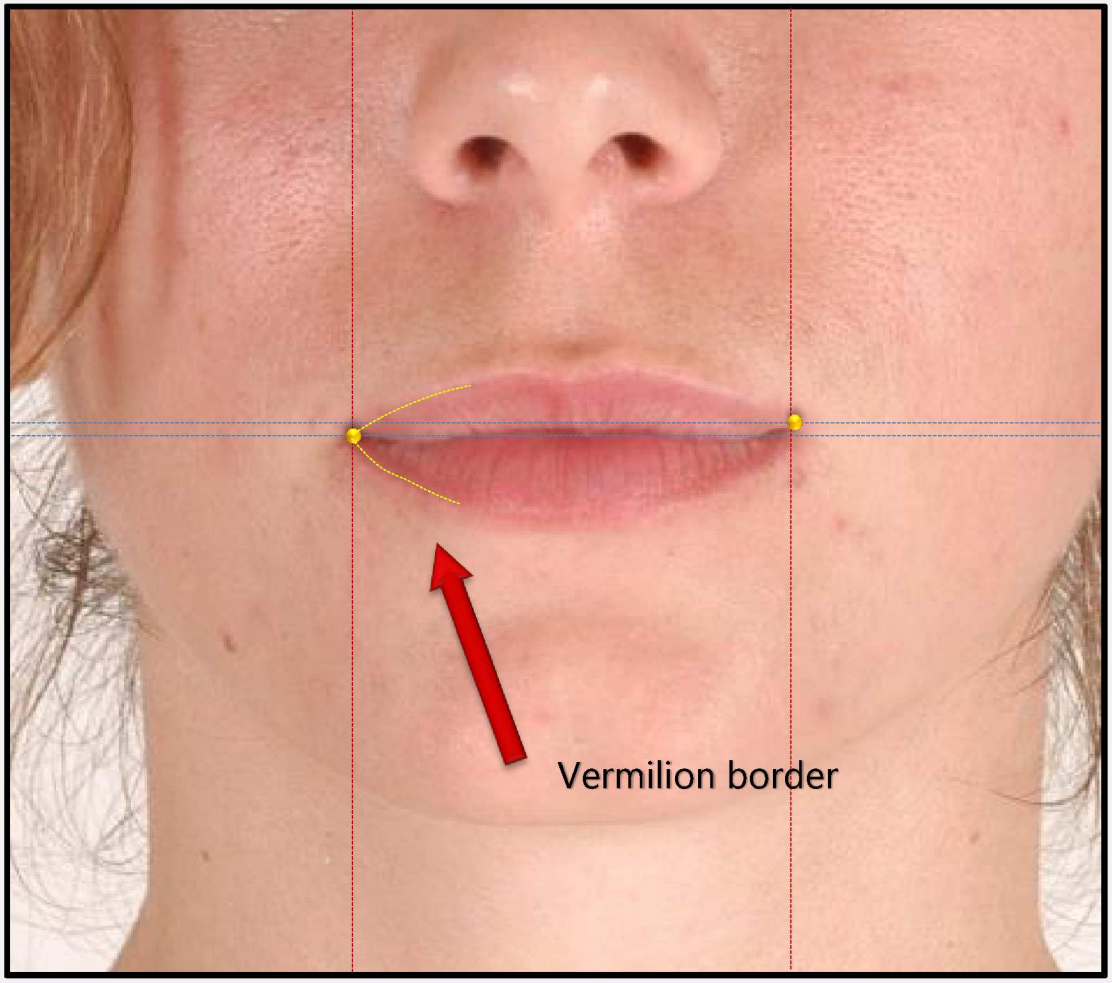

CHELION: Observation 1

43

When the upper and lower vermilion border meet in different regions of the rima oris, landmark where rima oris meets the **most lateral** border.

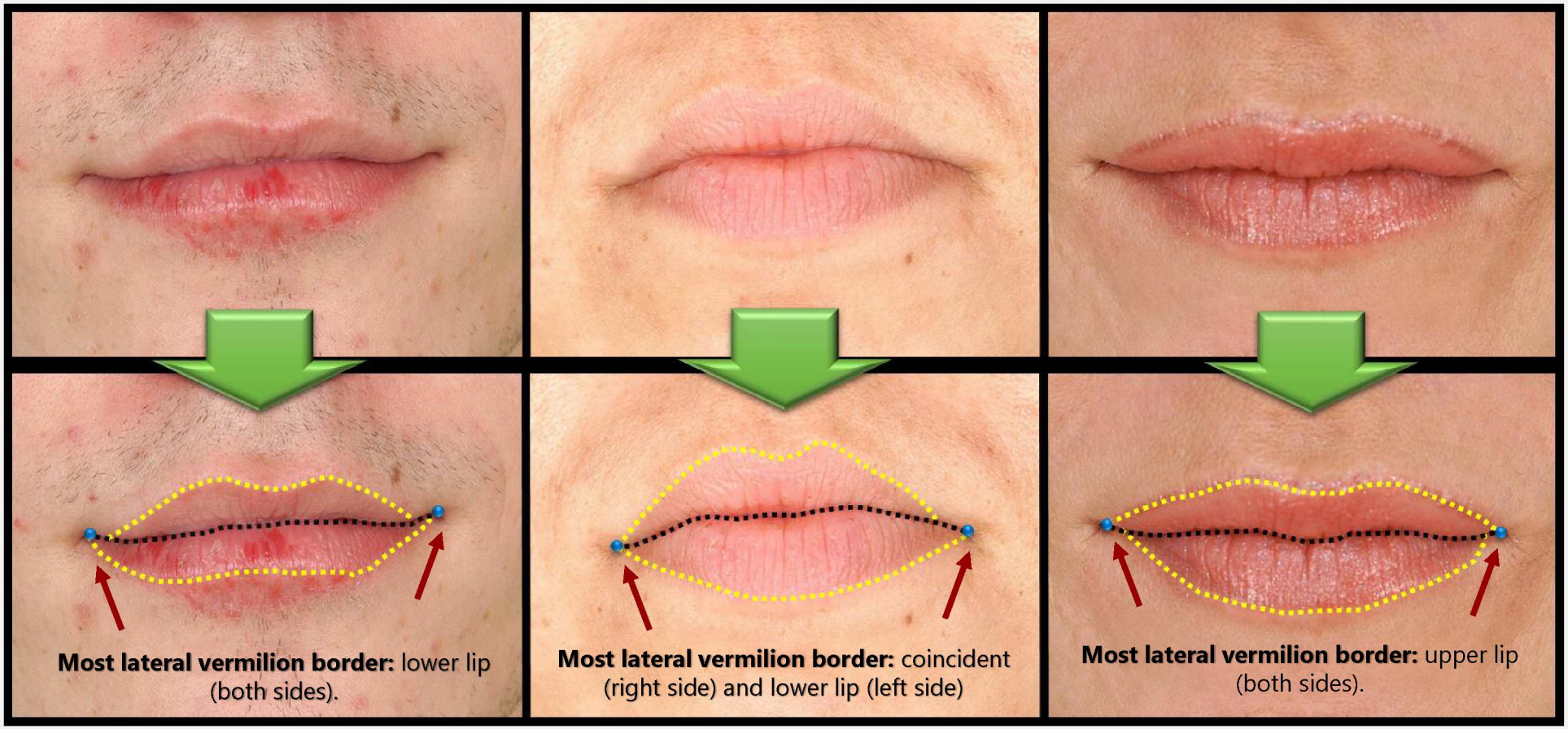

Number	Landmark name	Laterality	Abbreviation
22	Chelion	Bilateral	Ch_R / Ch_L

CHELION: Observation 2

44

Note that this landmark should be marked on the rima oris and not on the oromental wrinkles, when present.

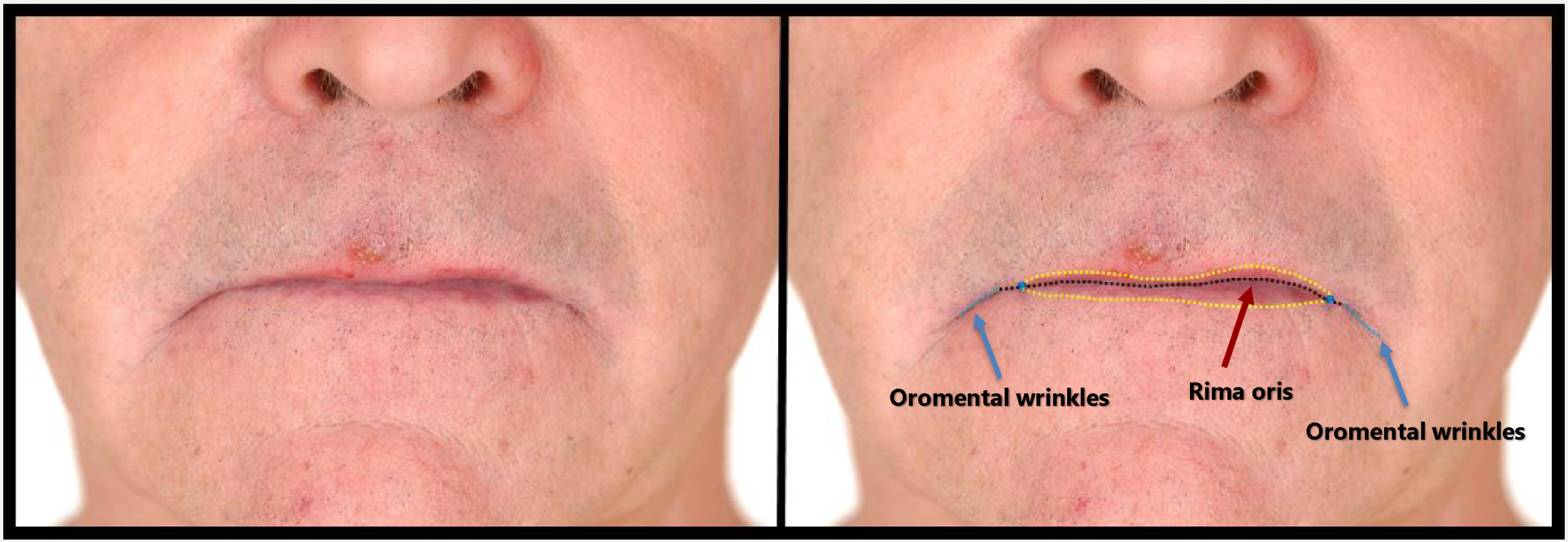

Number	Landmark name	Laterality	Abbreviation
22	Chelion	bilateral	Ch_R / Ch_L

LABIAL MIDLINE

The determination of *Chelions* will reveal the labial midline, which will aid the determination of the *Stomion*, *Labiale Inferius*, *Labiomentale* and *Gnathion* points.

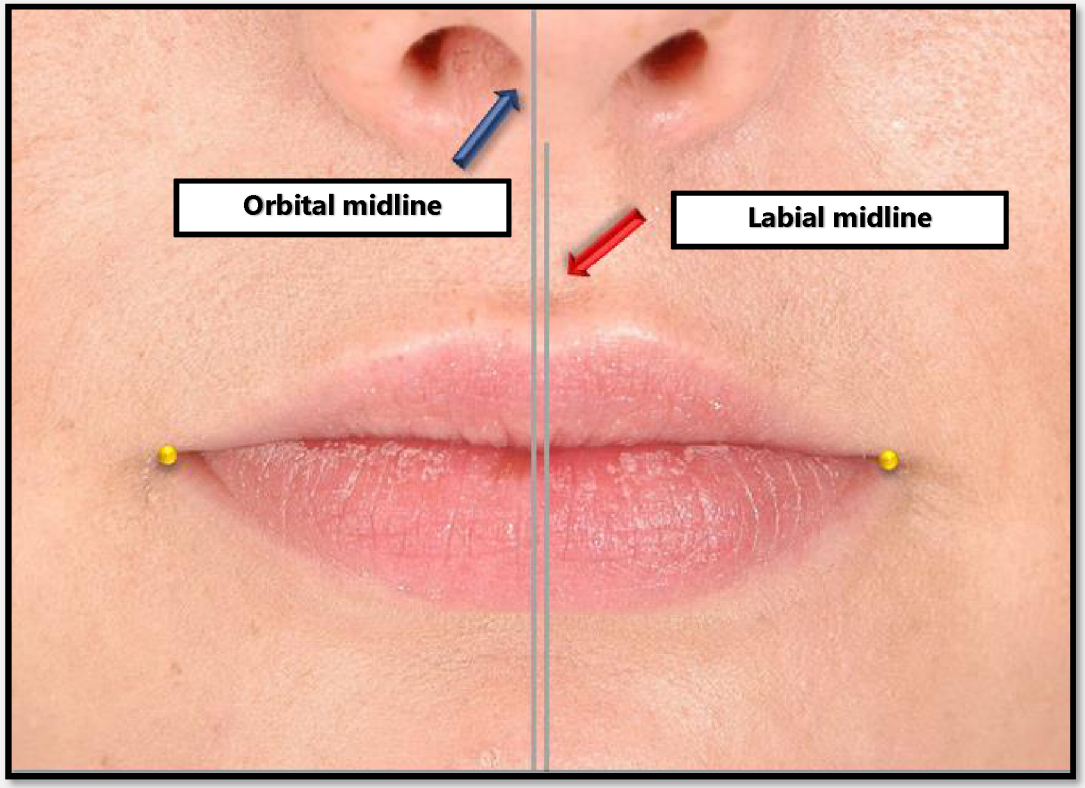

This line is different from the orbital midline. In the example, the two middle lines practically coincide but this is not always the case.

PHOTO-ANTHROPOMETRIC ANALYSIS: MANUAL LANDMARKING 46

23. STOMION

Number	Landmark name	Laterality	Abbreviation
23	Stomion	Median	Sto

Photo-anthropometric definition

Mid-landmark of rima oris (dark line formed when upper and lower lips meet), marked on labial midline (average between the right and left *Chelions*).

SAFF-2D landmarking procedures

Image approximation (Zoom):
Lower facial region.

References:
Rima oris region.
Labial midline (automated).

Auxiliary lines:
Edge detection filter (Laplace).

Procedure:
Position the landmark on the rima oris (dark line formed by the union of the upper and lower lips) where it meets the labial midline and the upper lip.

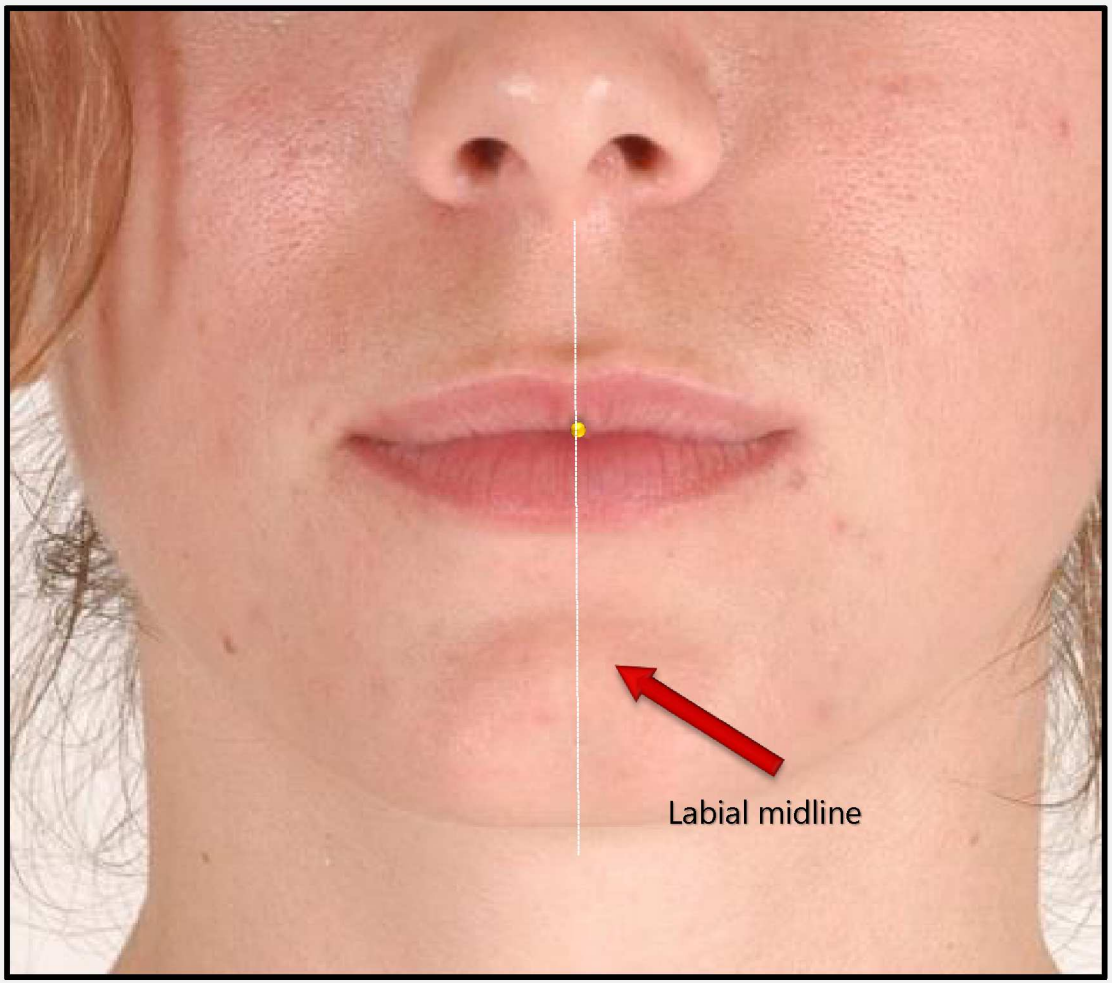

24. LABIALE INFERIUS

Number	Landmark name	Laterality	Abbreviation
24	Labiale Inferius	Median	Li

Photo-anthropometric definition

Meeting point of labial midline with the lowest landmark of the vermilion border of the lower lip.

SAFF-2D landmarking procedures

Image approximation (Zoom):
Lower facial region.

References:
Inferior region of the lower lip.
Labial midline (automated).

Auxiliary line:
Horizontal.

Procedure:
Landmark the point of the lower lip where the vermilion transition line from mouth to surrounding skin (vermilion border) intersects the labial midline.

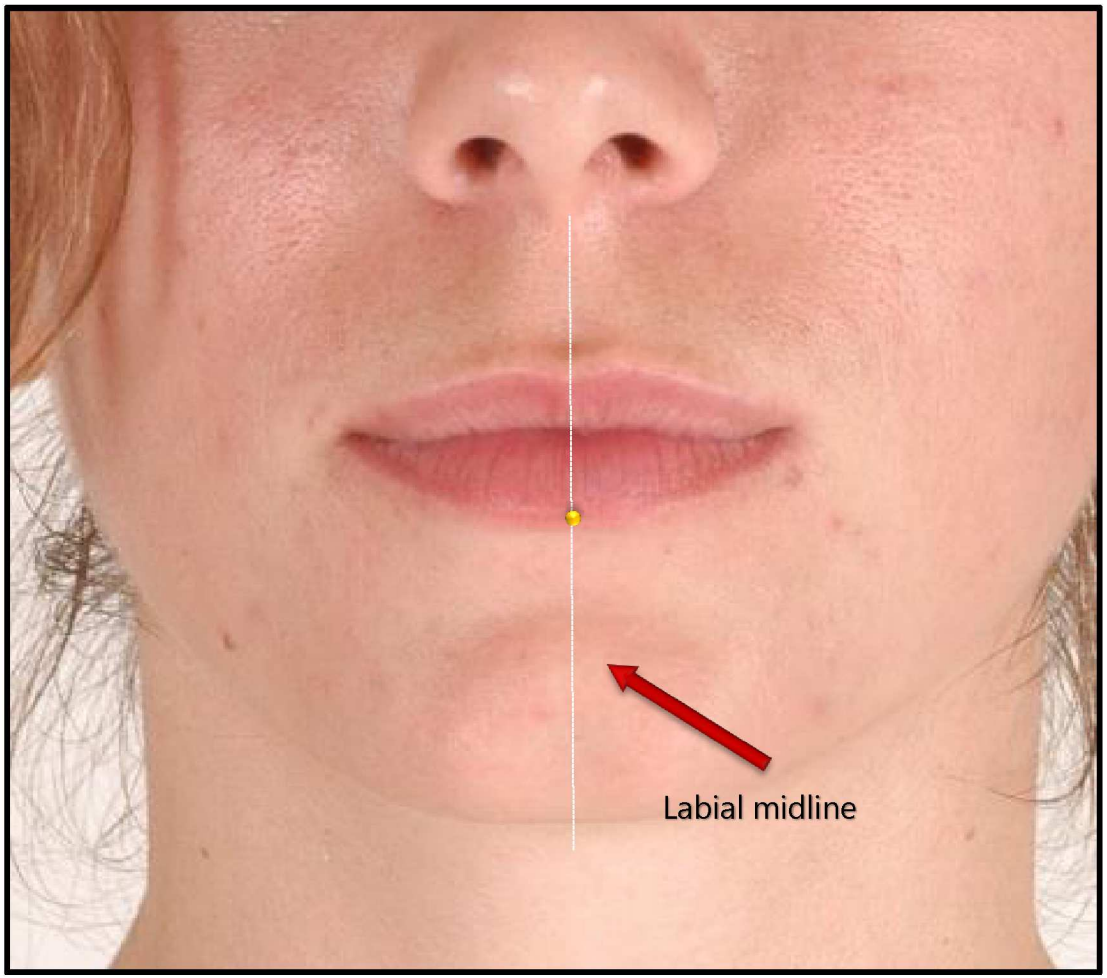

PHOTO-ANTHROPOMETRIC ANALYSIS: MANUAL LANDMARKING 48

25. LABIOMENTALE

Number	Landmark name	Laterality	Abbreviation
25	Labiomentale	Median	Lm

Photo-anthropometric definition

Median landmark of labiomental sulcus (semilunar line of greatest depression between the lower lip and mental protuberance).

SAFF-2D landmarking procedures

Image approximation (Zoom):
Lower facial region.

References:
Labiomental sulcus region.
Labial midline (automated).

Auxiliary line:
Horizontal.

Procedure:
Landmark the point between the lower lip and the chin, at which the transition between shade (labiomental sulcus - in the example, represented by the yellow dotted line) and light (projection of the chin) is seen. Mark over the shadow region.

Observation:
In case of non-visualization, do not landmark it and include an observation in the specific field of SAFF-2D.

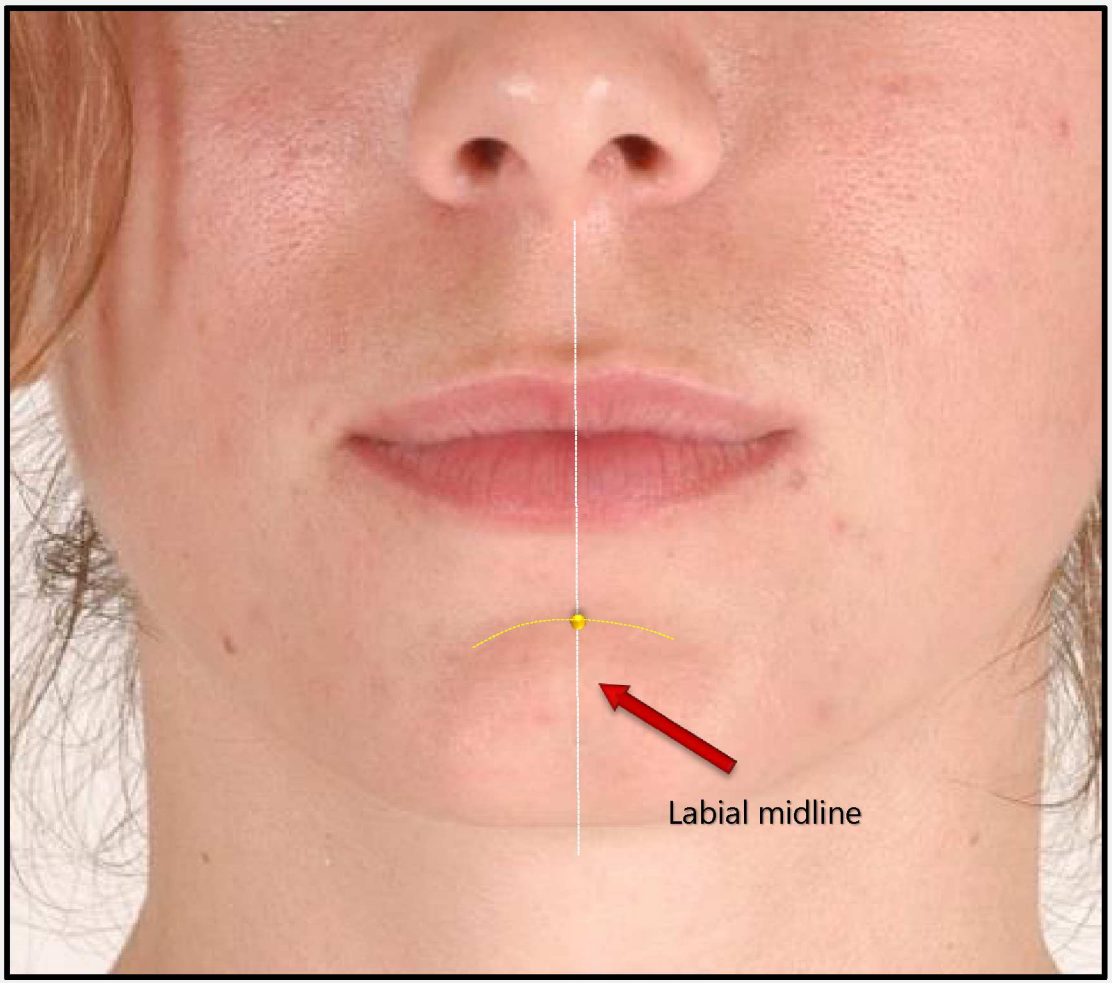

26. GNATHION

Number	Landmark name	Laterality	Abbreviation
26	Gnathion	Median	Gn

Photo-anthropometric definition

Landmark on the labial midline that meets the lowest point of mental protuberance.

SAFF-2D landmarking procedures

Image approximation (Zoom):
Lower facial region.

References:
Bottom contour of the mental protuberance.
Labial midline (automated).

Auxiliary line:
Horizontal.

Procedure:
Landmark the labial midline at the point where it meets the lowest region of the chin.

Observation:
Do not consider the region of double-chin, when present.

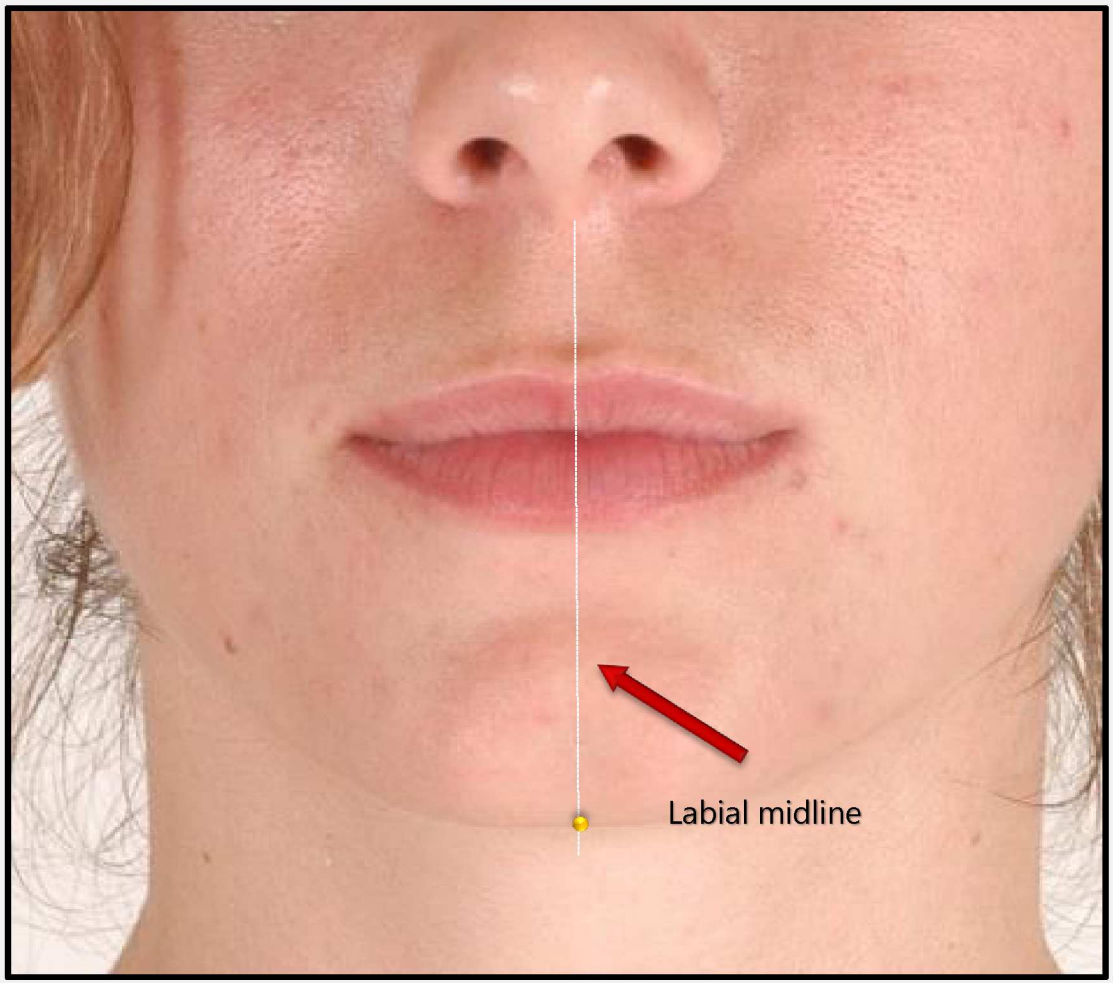

PHOTO-ANTHROPOMETRIC ANALYSIS: MANUAL LANDMARKING 50

27. GONION

Number	Landmark name	Laterality	Abbreviation
27	Gonion	Bilateral	Go_R / Go_L

Photo-anthropometric definition

The most lateral landmark where the horizontal line of reference passes through *Stomion* landmark and crosses the contour line of the face.

SAFF-2D landmarking procedures

Image approximation (Zoom):
Lower facial region.

Reference:
Facial lateral contour.

Auxiliary line:
Horizontal.

Procedure:
Position the horizontal auxiliary line over the *Stomion* point. Mark *Gonions* landmarks where this line meets the lateral contour of the face. Follow the same procedure for marking the contralateral point.

Observation:
The contralateral *Gonion* landmark will have the same position relative to the vertical axis (determined by the horizontal auxiliary line).

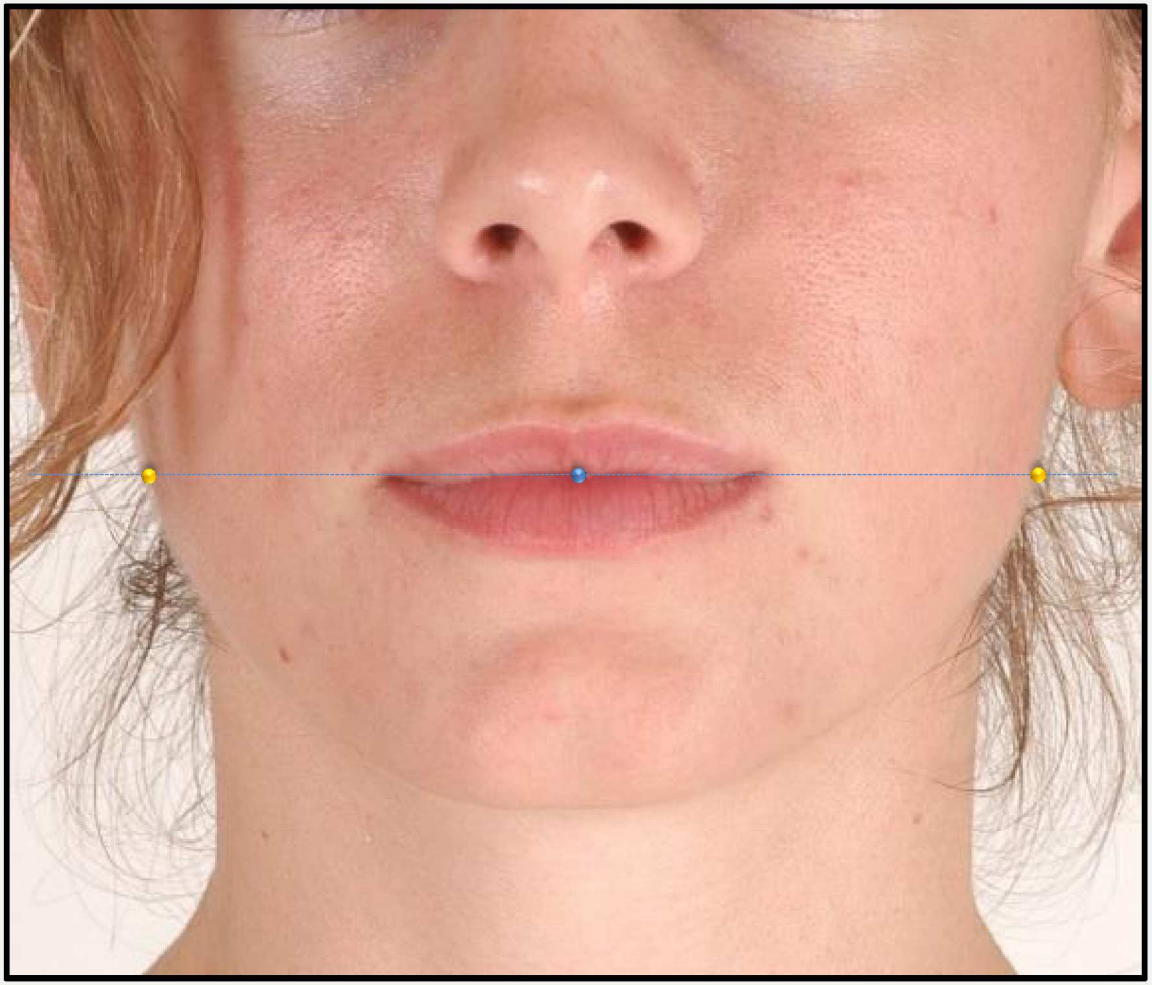

GONION: Observation

51

When images of overweight people are analyzed and adipose tissue is present in the landmarking region, the examiner must landmark the *Gonion* where the *Stomion* horizontal line of reference crosses the most external contour line present and include an observation in the SAFF-2D.

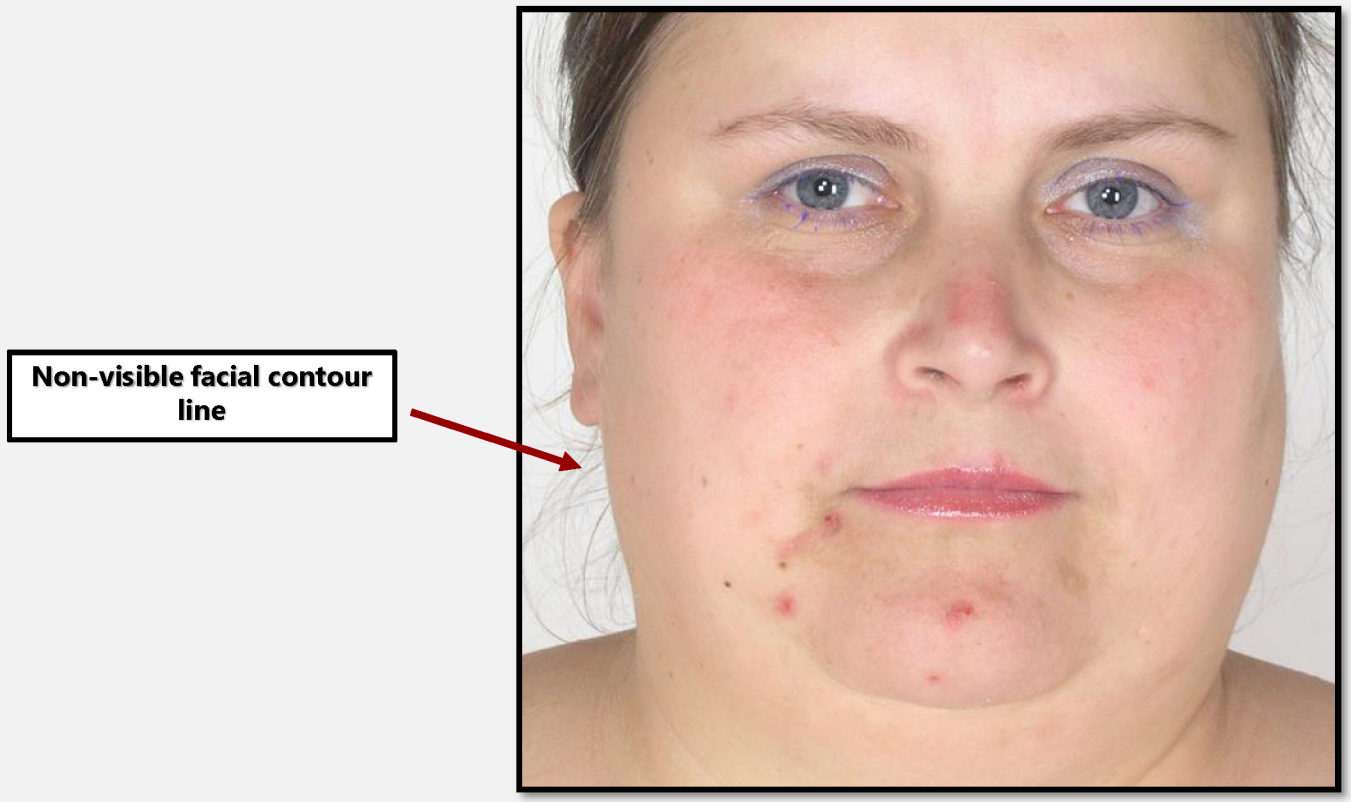

Number	Landmark name	Laterality	Abbreviation
27	Gonion	Bilateral	Go_R / Go_L

PHOTO-ANTHROPOMETRIC ANALYSIS: MANUAL LANDMARKING 52

28. ZYGION

Number	Landmark name	Laterality	Abbreviation
28	Zygion	Bilateral	Zy_R / Zy_L

Photo-anthropometric definition

The most lateral landmark of the face (greatest width) with respect to the zygomatic bone, in the apple region of the face.

SAFF-2D landmarking procedures

Image approximation (Zoom):
Framing of middle portion of, or complete, face.

References:
Lateral facial contour.
Ear (tragus and insertion of helix).

Auxiliary lines:
Horizontal and Vertical.

Procedure:
Move the horizontal line from bottom to top until it is positioned in the region of largest facial width, referring to the insertion of the helix (top) and tragus (bottom). The *Zygion* should be marked in the region of intersection between the lines. Follow the same procedure for landmarking the contralateral point.

Observation:
This landmarking is independent of the contralateral point.

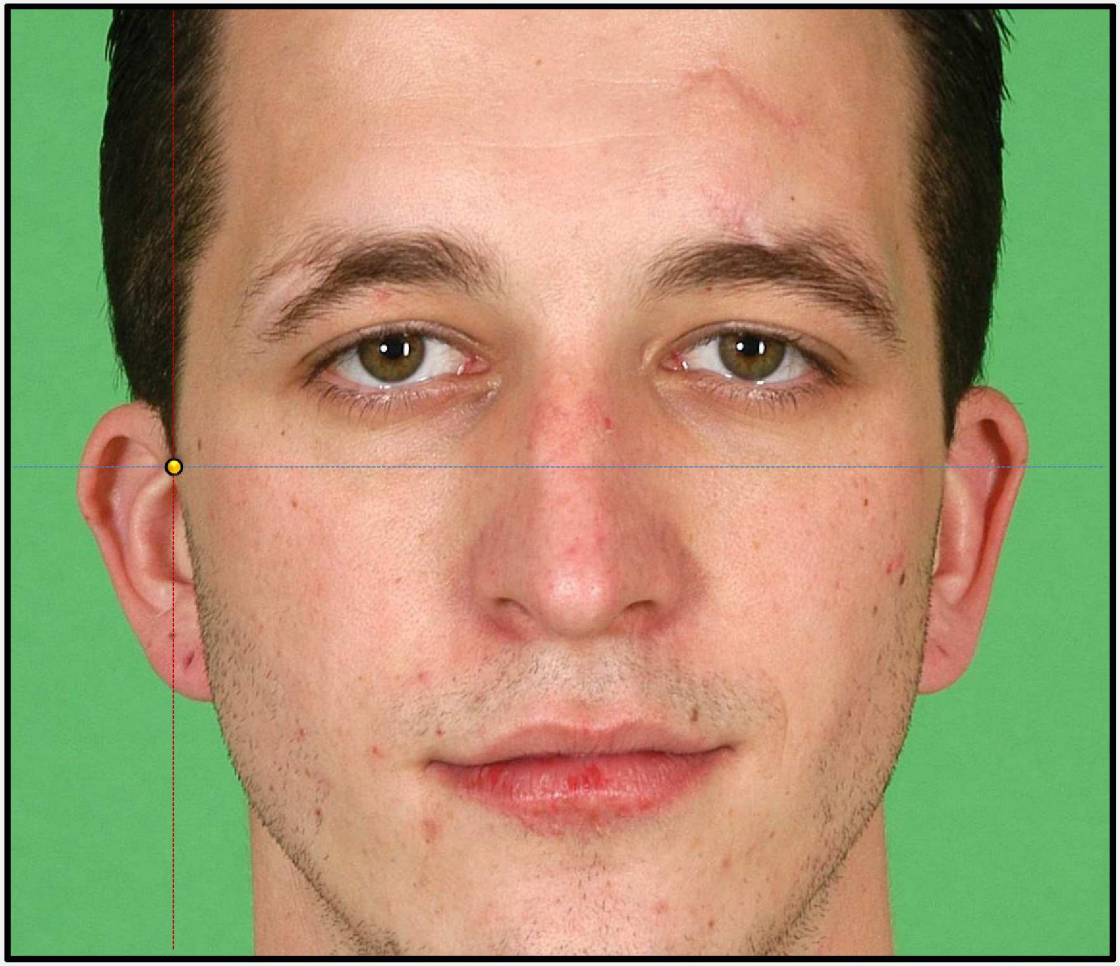

ZYGION: Observation 1

53

Since images have eyes aligned with the upper portion of the ears, the *Zygion* must have as a vertical height limit the region of the helix insertion and, as lower limit, the intermediate height of the tragus (corresponding in skin to the temporal process of the zygomatic bone, positioned above the external acoustic meatus).

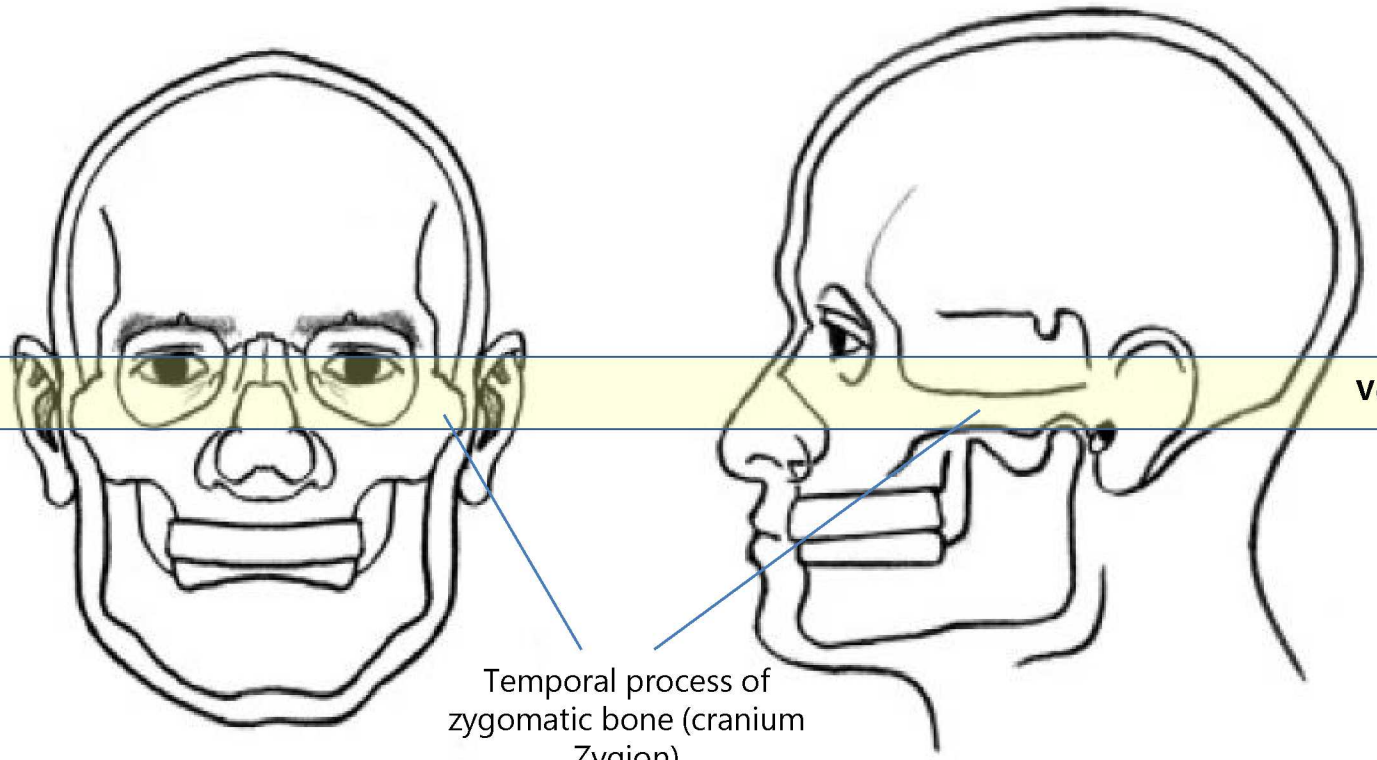

Number	Landmark name	Laterality	Abbreviation
28	Zygion	Bilateral	Zy_R / Zy_L

ZYGION: Observation 2

54

Since images have eyes aligned with the upper portion of the ears, the *Zygion* must have as a vertical height limit the region of the helix insertion and, as lower limit, the intermediate height of the tragus (corresponding in skin to the temporal process of the zygomatic bone, positioned above the external acoustic meatus).

Helix insertion

Vertical landmarking limit

Medium height of Tragus

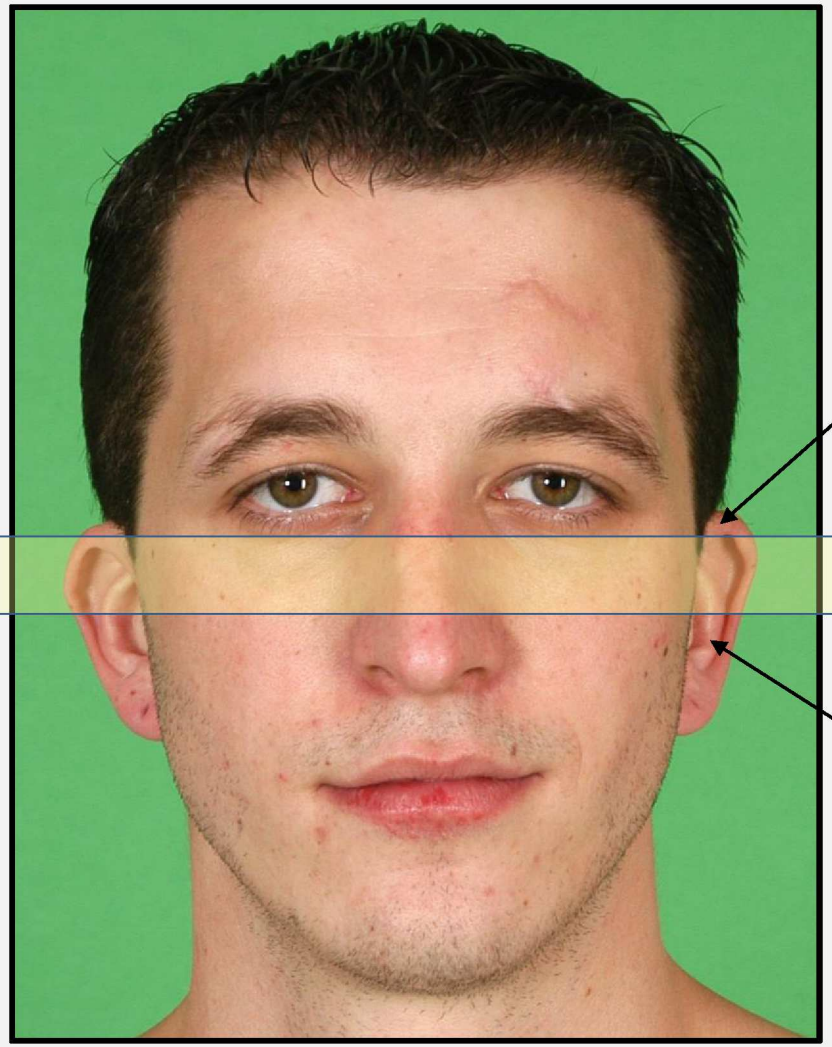

ZYGION: Observation 3

55

This landmark must be marked in front of the capillary region, i.e., on the cutaneous tissue of the face. It is recommended that the upper and lower vertical boundaries be marked with auxiliary lines prior to marking this point.

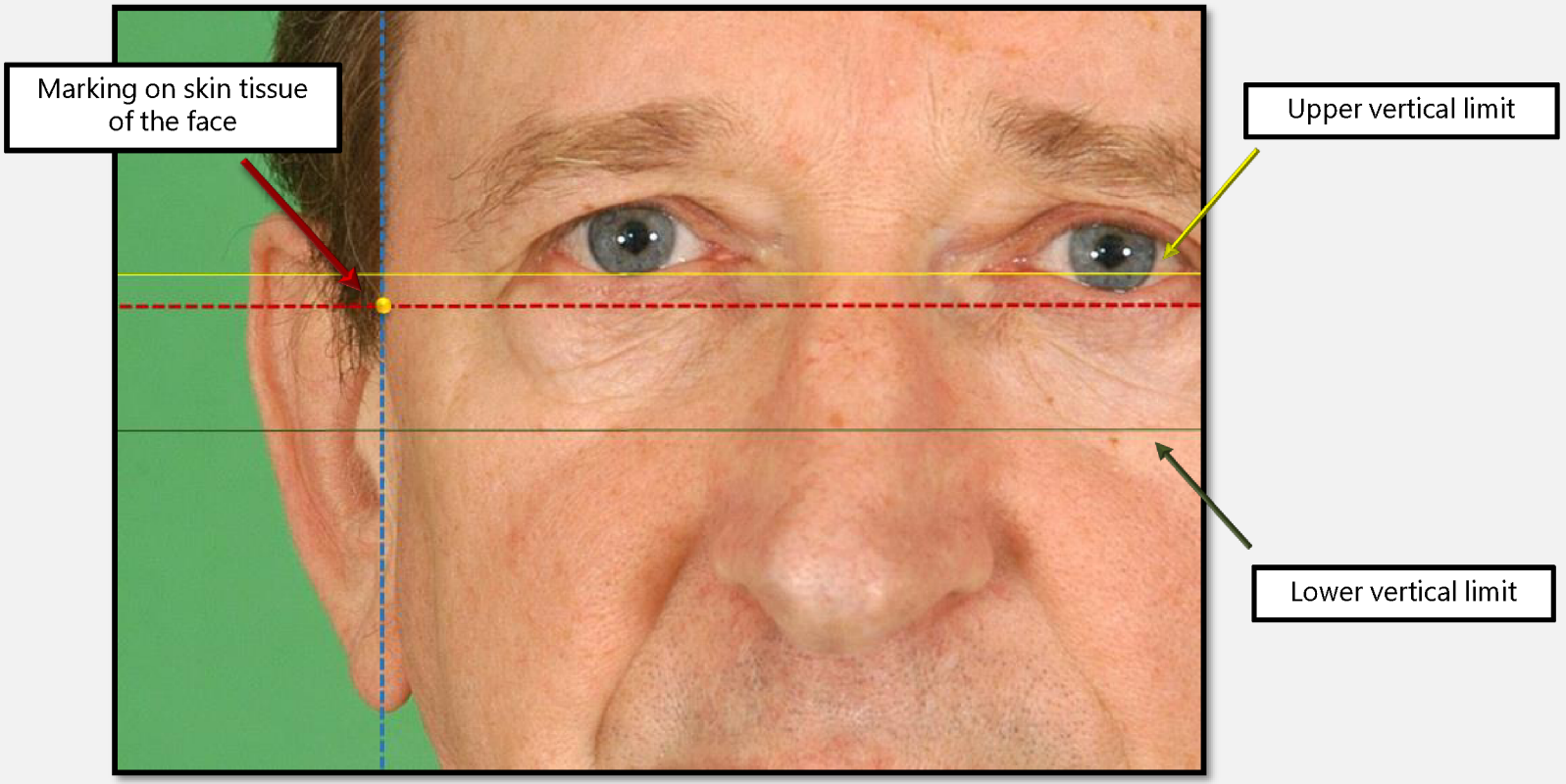

Number	Landmark name	Laterality	Abbreviation
28	Zygion	Bilateral	Zy_R / Zy_L

29. SUPERAURALE

Number	Landmark name	Laterality	Abbreviation
29	Superaurale	Bilateral	Sa_R / Sa_L

Photo-anthropometric definition

The uppermost landmark of pinna (external ear).

SAFF-2D landmarking procedures

Image approximation (Zoom):
External ear region.

Reference:
Pinna (external ear).

Auxiliary lines:
Horizontal and Vertical.

Procedure:
Move the horizontal line from top to bottom until the line touches the uppermost landmark of the external ear. Subsequently, the vertical line should be moved from the lateral to medial side to also cross through this uppermost point. The *Superaurale* should be marked at the point of intersection of the two reference lines. Follow the same procedure for landmarking the contralateral point.

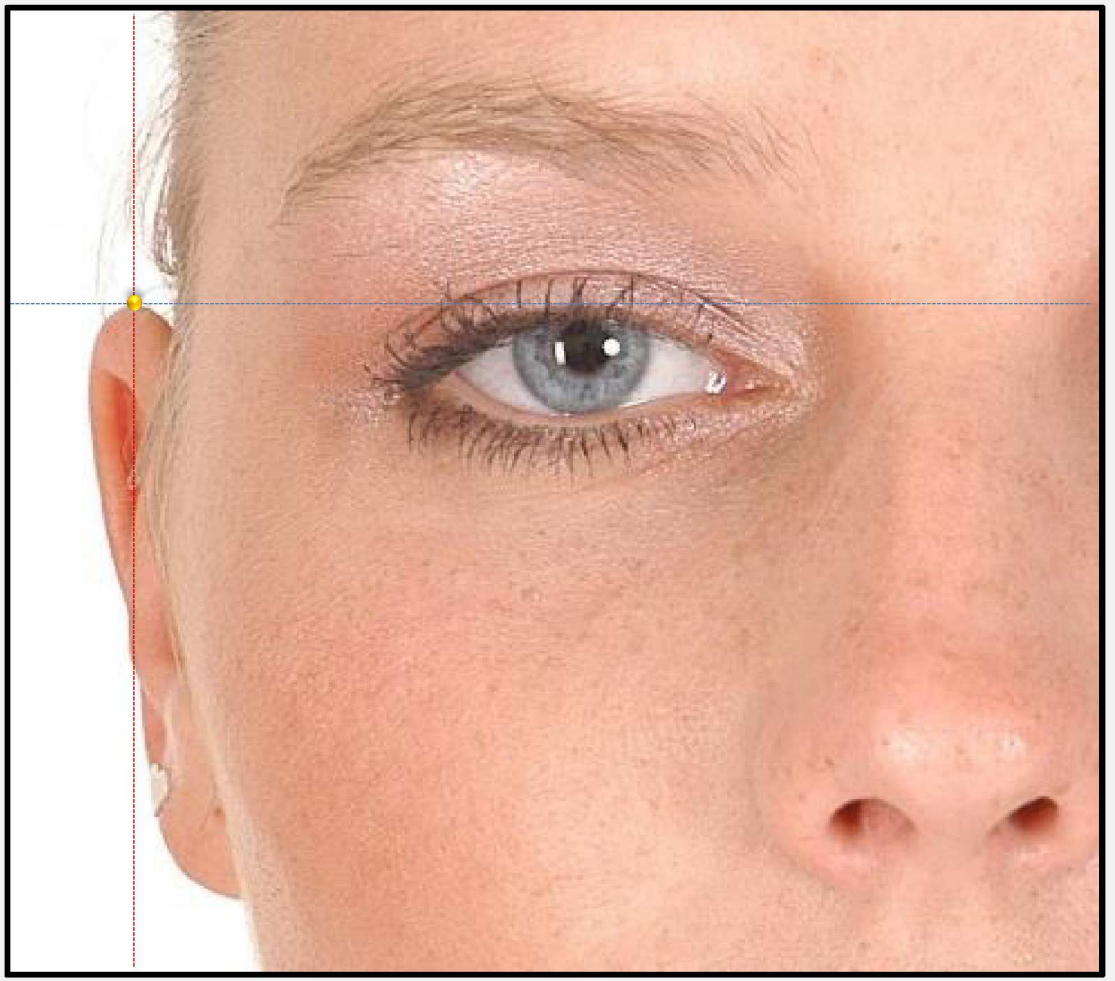

30. POSTAURALE

Number	Landmark name	Laterality	Abbreviation
30	Postaurale	Bilateral	Pa_R / Pa_L

Photo-anthropometric definition

The most lateral landmark of pinna (external ear).

SAFF-2D landmarking procedures

Image approximation (Zoom):
External ear region.

Reference:
Pinna (external ear).

Auxiliary lines:
Horizontal and Vertical.

Procedure:
Move the vertical line, from lateral to medial, until the line is tangential to the most lateral point of the external ear. Move the horizontal line from bottom to top to also cross through the most lateral point. The landmark should be marked at the point of intersection between the two reference lines. Follow the same procedure for landmarking the contralateral point.

Observation:
When moving the vertical line, find *an area* rather than *a point*, mark the central point of this tangential area.

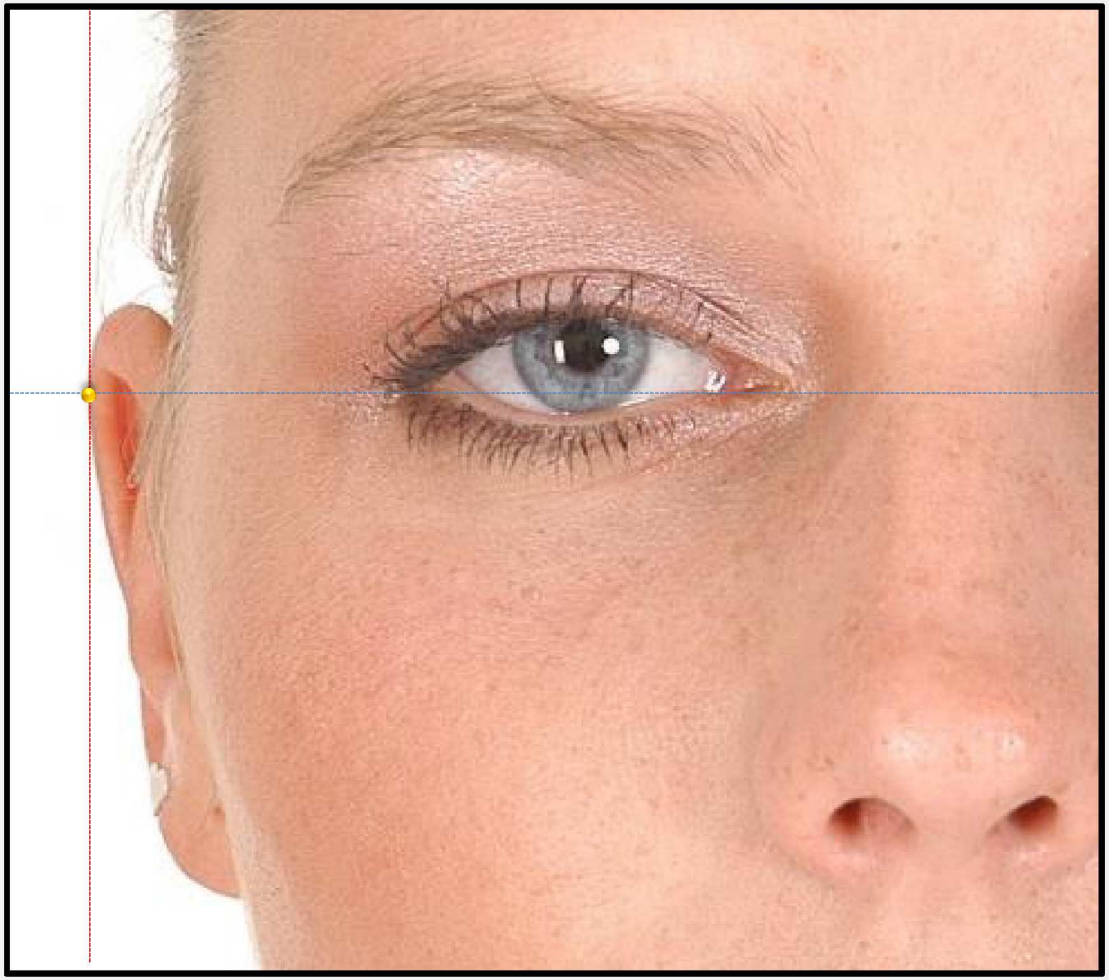

PHOTO-ANTHROPOMETRIC ANALYSIS: MANUAL LANDMARKING 58

31. SUBAURALE

Number	Landmark name	Laterality	Abbreviation
31	Subaurale	Bilateral	Sba_R / Sba_L

Photo-anthropometric definition

The lowermost landmark of the earlobe.

SAFF-2D landmarking procedures

Image approximation (Zoom):
External ear region.

References:
Earlobe.
Facial lateral contour (in the presence of adhered lobes).

Auxiliary lines:
Horizontal and Vertical.

Procedure:
Mark this landmark on the lowest position of the earlobe. The horizontal reference line can be moved from bottom to top until the line is tangential to the lowest portion of the ear. Follow the same procedure for landmarking the contralateral point.

Observation:
In cases of adhered lobes, this landmark should be marked where the lowest portion of the lobe meets the most lateral portion of the face.

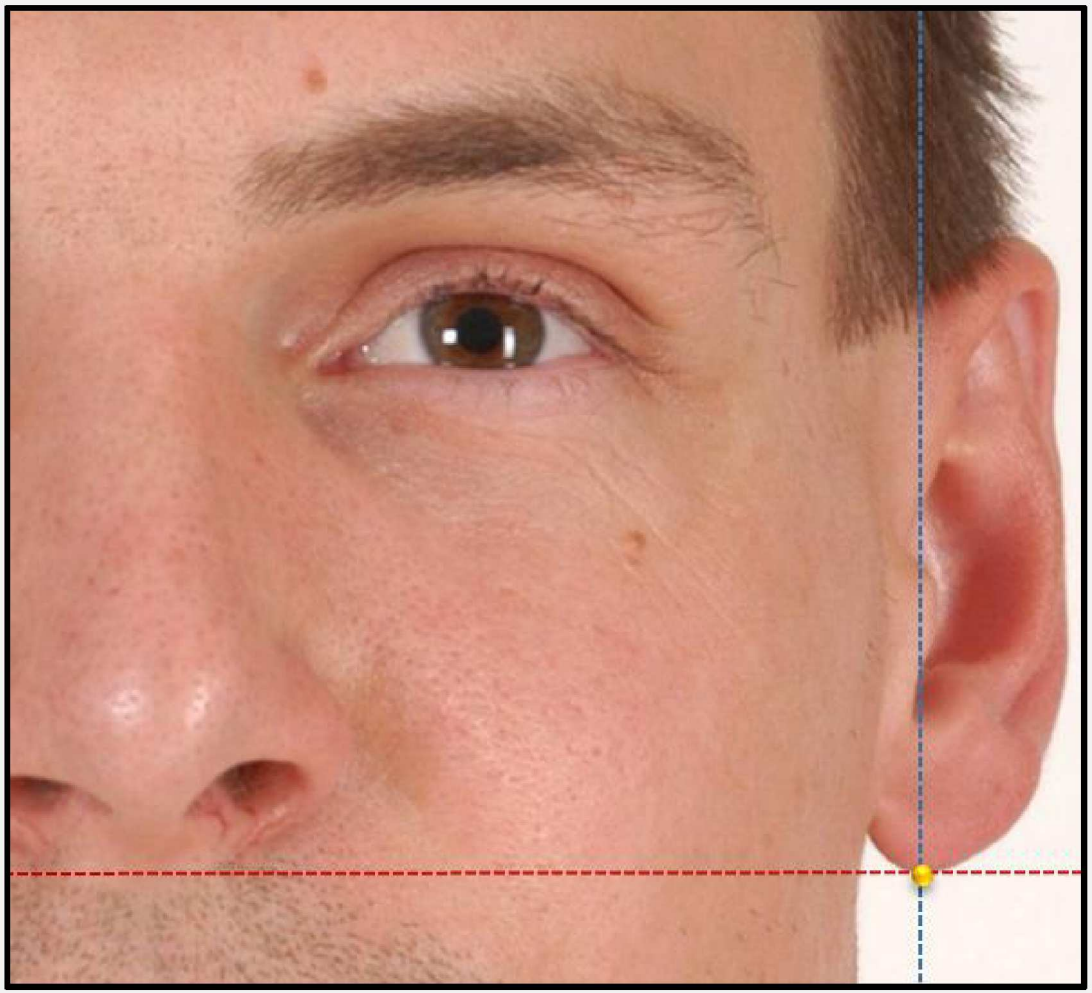

SUBAURALE: Observation

59

In cases of **adhered lobes**, this landmark should be marked where the lowest portion of the lobe meets the most lateral portion of the face.

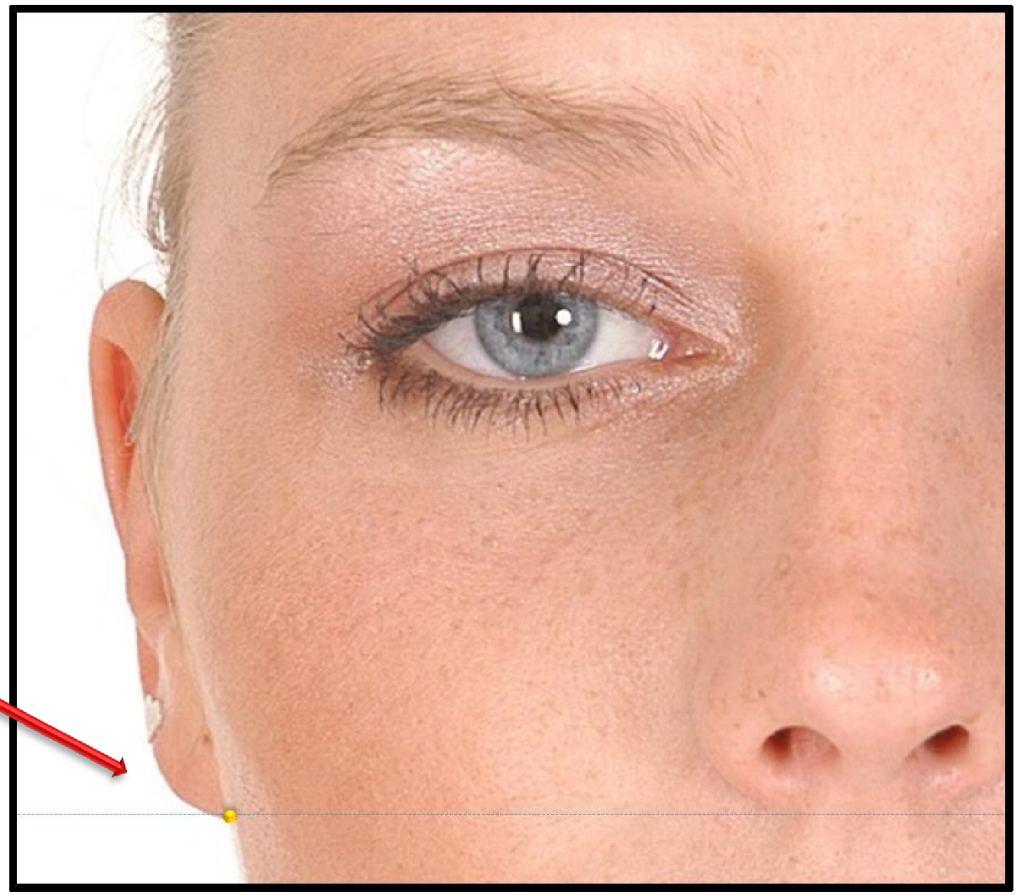

Marking of *Subaurale* landmark in the case of attached lobe

Number	Landmark name	Laterality	Abbreviation
31	Subaurale	Bilateral	Sba_R / Sba_L

PHOTO-ANTHROPOMETRIC ANALYSIS: MANUAL LANDMARKING 60

32. SUPRALOBULARE

Number	Landmark name	Laterality	Abbreviation
32	Supralobulare	Bilateral	Slb_R / Slb_L

Photo-anthropometric definition

Visually inferior landmark of the intertragic incisure of the external ear.

SAFF-2D landmarking procedures

Image approximation (Zoom):
External ear region.

References:
Earlobe.
Pinna (external ear).

Auxiliary lines:
Horizontal and Vertical.

Procedure:
Mark this landmark on the lowest portion of the cleft of the external ear (intertragic incisure), located between the tragus and the antitragus. Horizontal and vertical reference lines can be used to better visualize the lowest portion of the intertragic incisure, visualized by the difference in coloration (depth). Follow the same procedure for marking the contralateral point.

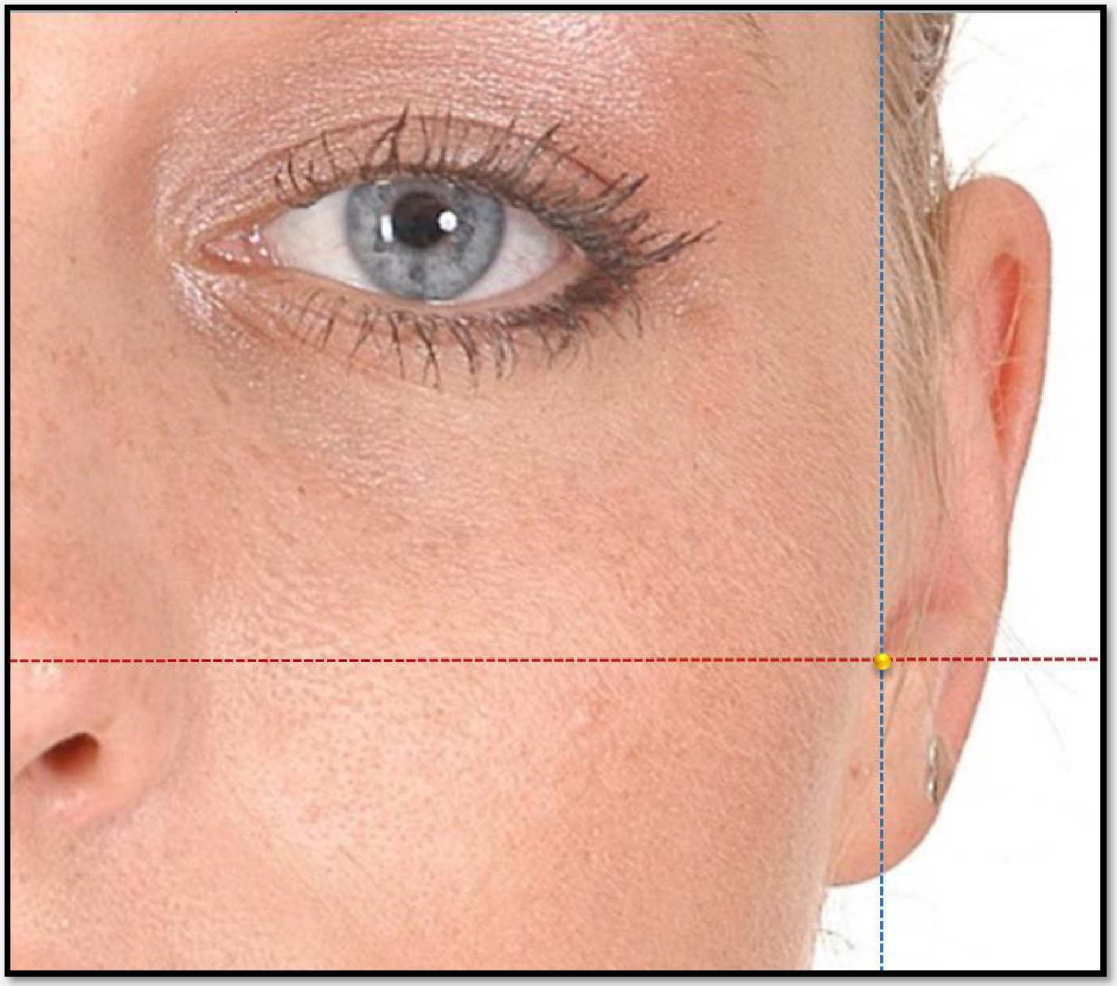

SUPRALOBULARE: Observation 1

61

Observe the anatomical position of the intertragic incisure, located between the tragus and the antitragus. In frontal normalized images, this structure can be located by a colour difference, with darkness being a function of depth in relation to the surrounding anatomical structures (i.e. darkness increases with depth).

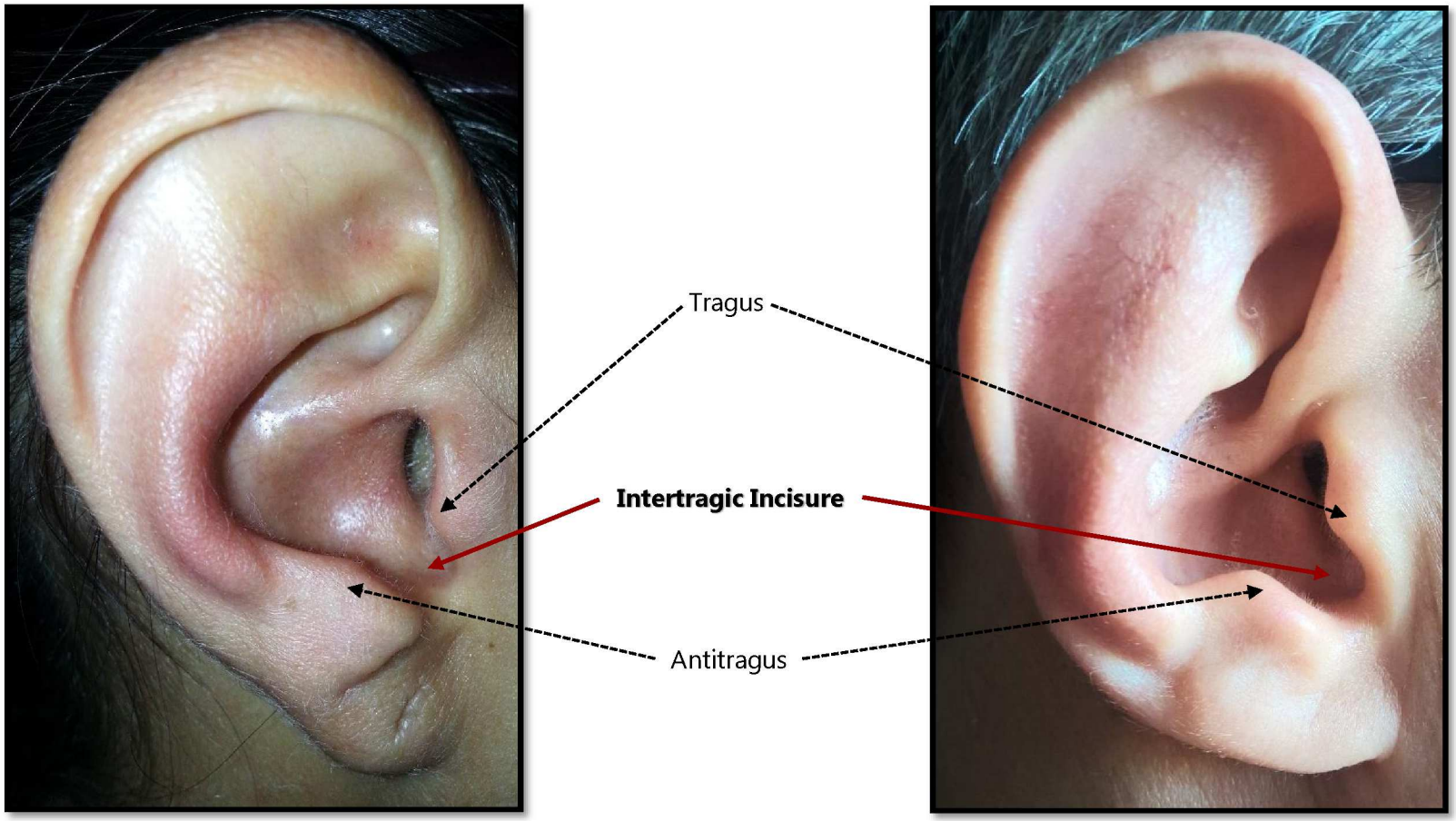

Number	Landmark name	Laterality	Abbreviation
32	Supralobulare	Bilateral	Slb_R / Slb_L

SUPRALOBULARE: Observation 1

62

When it is not possible to visualize it, do not mark this landmark and describe observation in the SAFF-2D specific field. Note that not visualizing this landmark in one of the external ears does not compromise the marking of the contralateral point.

Number	Landmark name	Laterality	Abbreviation
32	Supralobulare	Bilateral	Slb_R / Slb_L

PHOTO-ANTHROPOMETRIC ANALYSIS: AUTOMATED LANDMARKING 63

1. MIDNASALE

Number	Landmark name	Laterality	Abbreviation
a1	Midnasale	Median	Mid

Photo-anthropometric definition

Landmark on the orbital midline with reference to the height of the *Ectocanthions*.

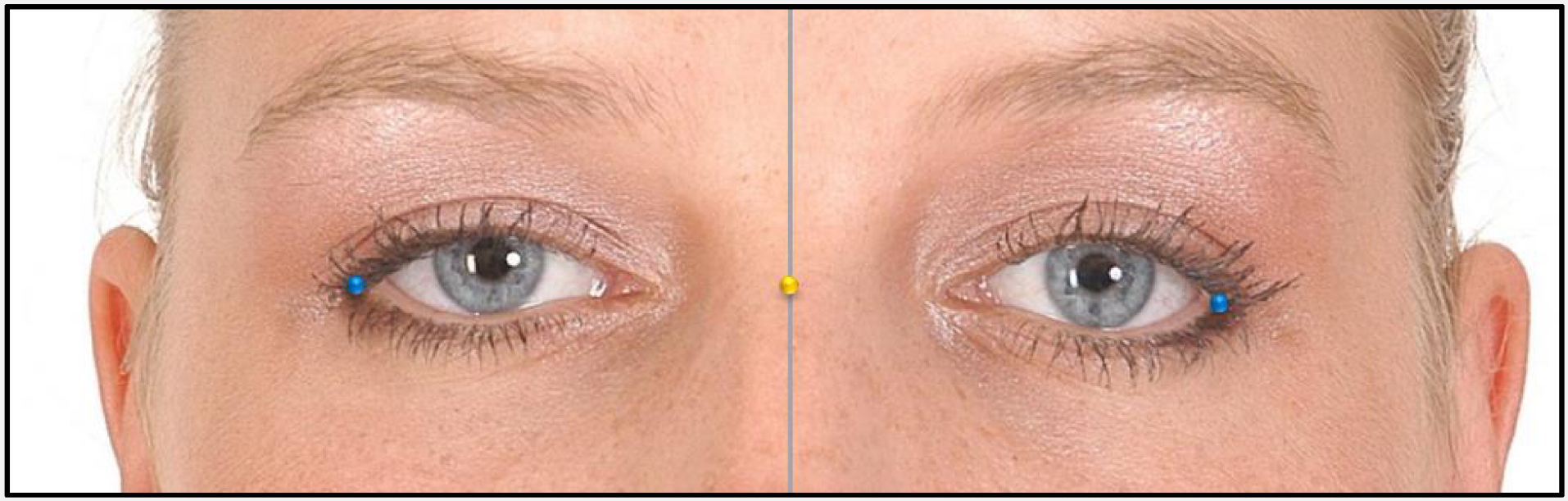

2. PUPIL

Number	Landmark name	Laterality	Abbreviation
a2	Pupil	Bilateral	Pu_R / Pu_L

Photo-anthropometric definition

Central landmark of iridian circumference (see Appendix).

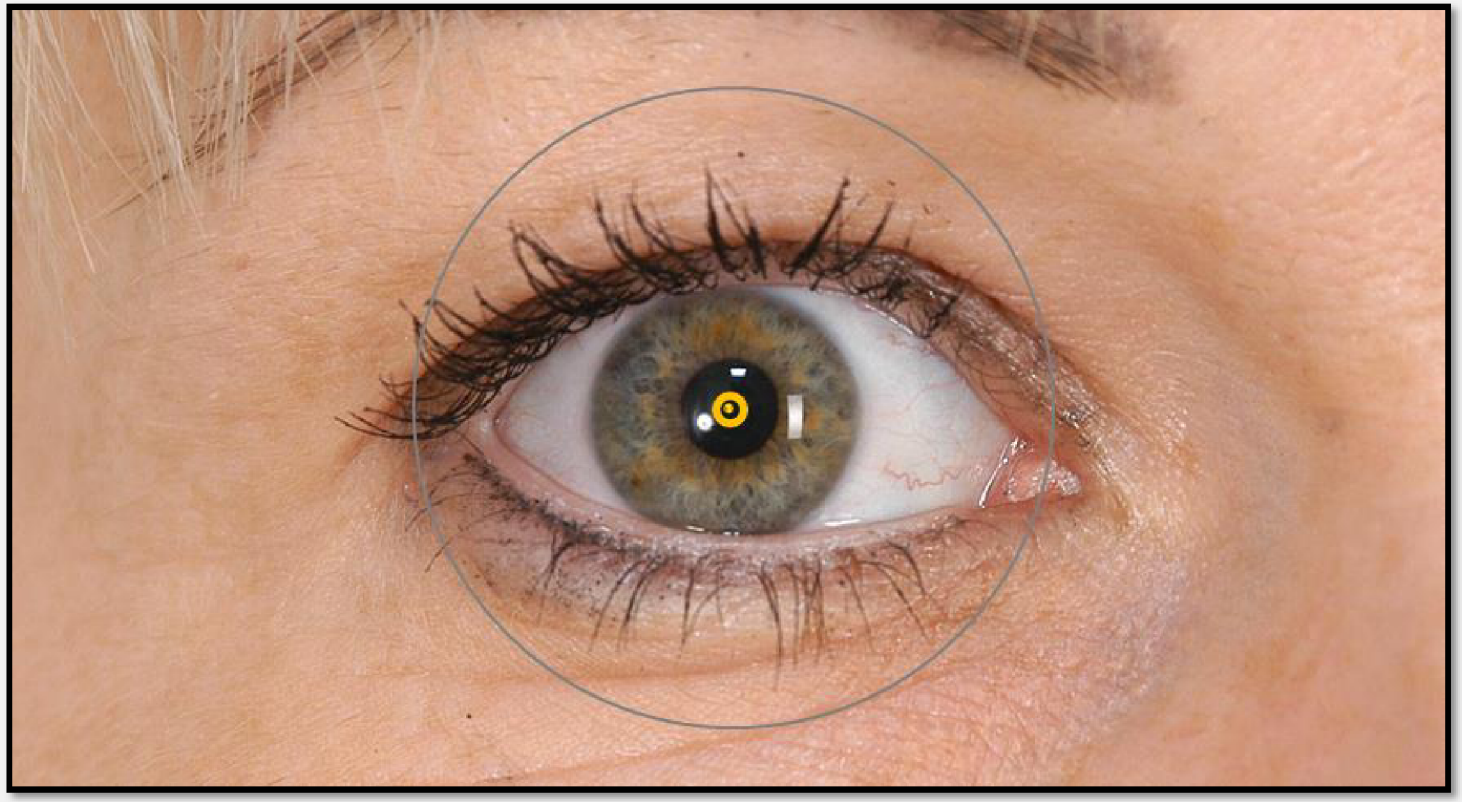

3. GLABELLA

Number	Landmark name	Laterality	Abbreviation
a3	Glabella	Median	G

Photo-anthropometric definition

Intersection between the orbital midline and the horizontal line that intersects the upper edge of the orbital circumferences (automated).

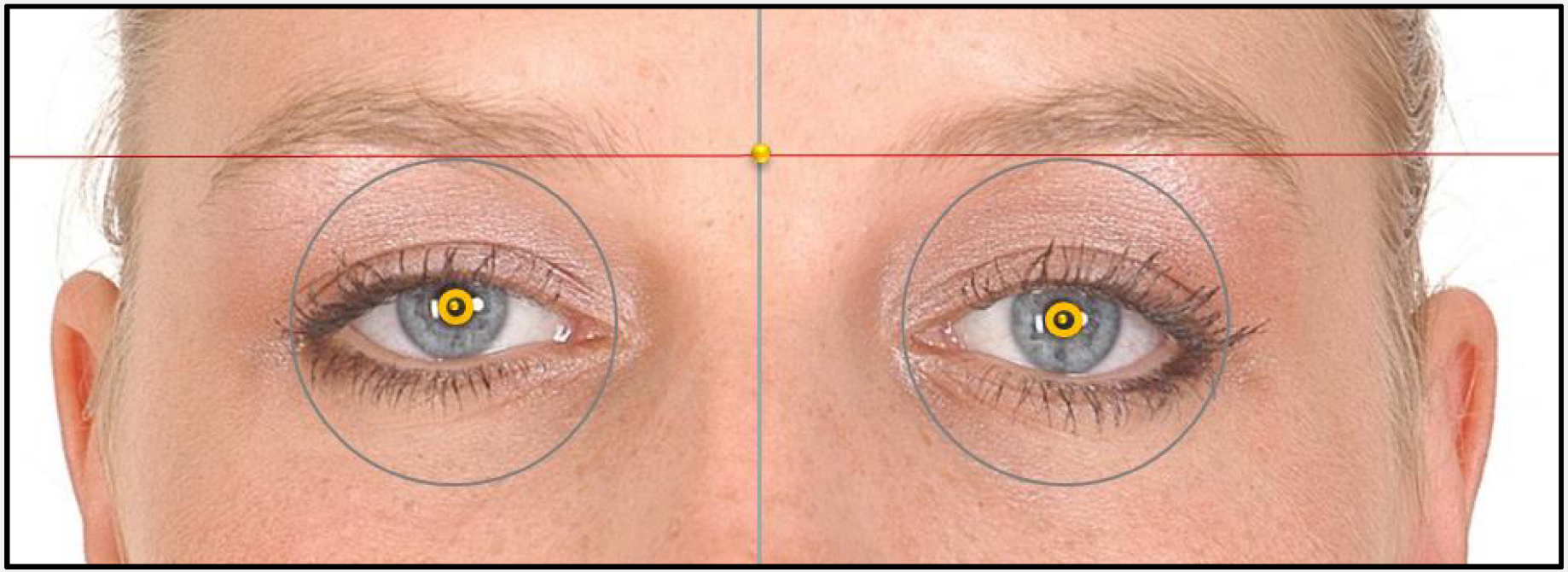

4. Nasion

Number	Landmark name	Laterality	Abbreviation
a4	Nasion	Median	N

Photo-anthropometric definition

Intersection of orbital midline with the horizontal line that passes through the upper palpebral grooves at their approximate mean height.

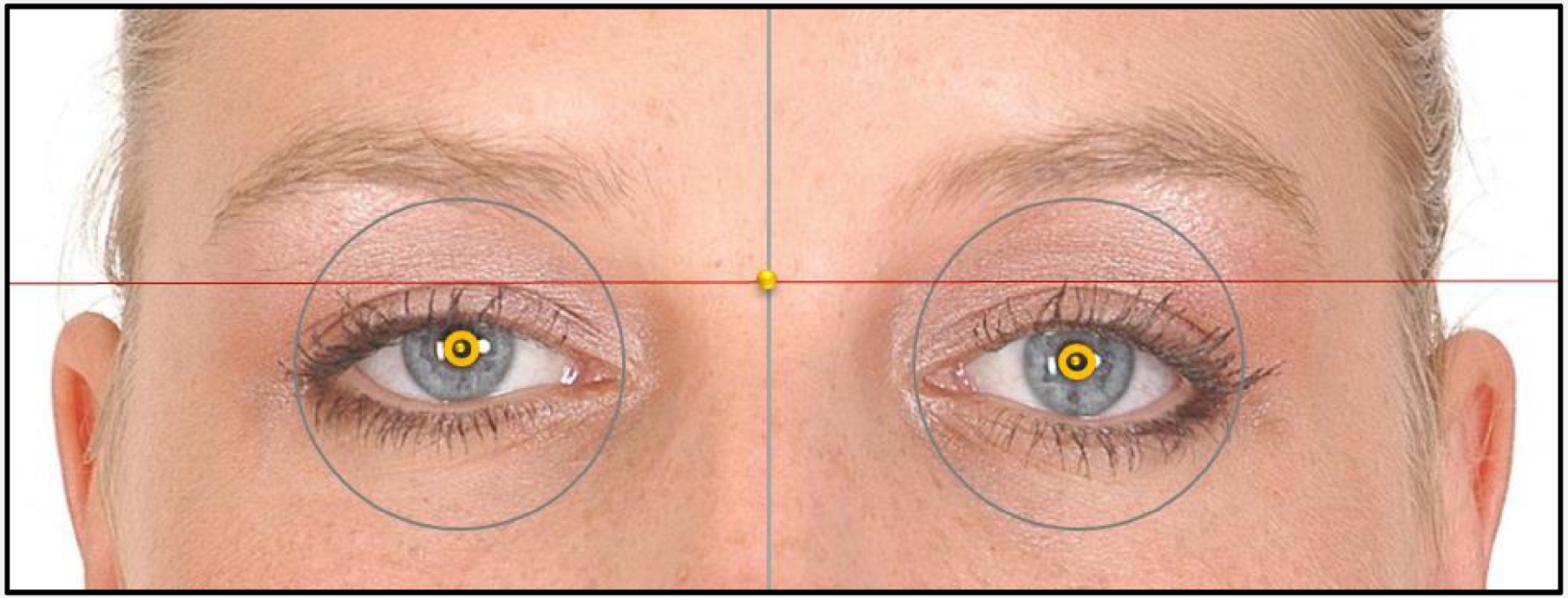

APPENDIX 67

ORBITAL MIDLINE

REFERENCE DEFINITION

Fixed vertical reference line that appears after determination of *Endocanthion* and *Ectocanthion* landmarks of both hemifaces (right and left). This line was defined as the union of the two points formed by the intersection of two circumferences, each having, as center, the *Ectocanthion* landmark of the respective facial side and, as radius, the distance from this landmark to the *Endocanthion* landmark of the contralateral hemiface.

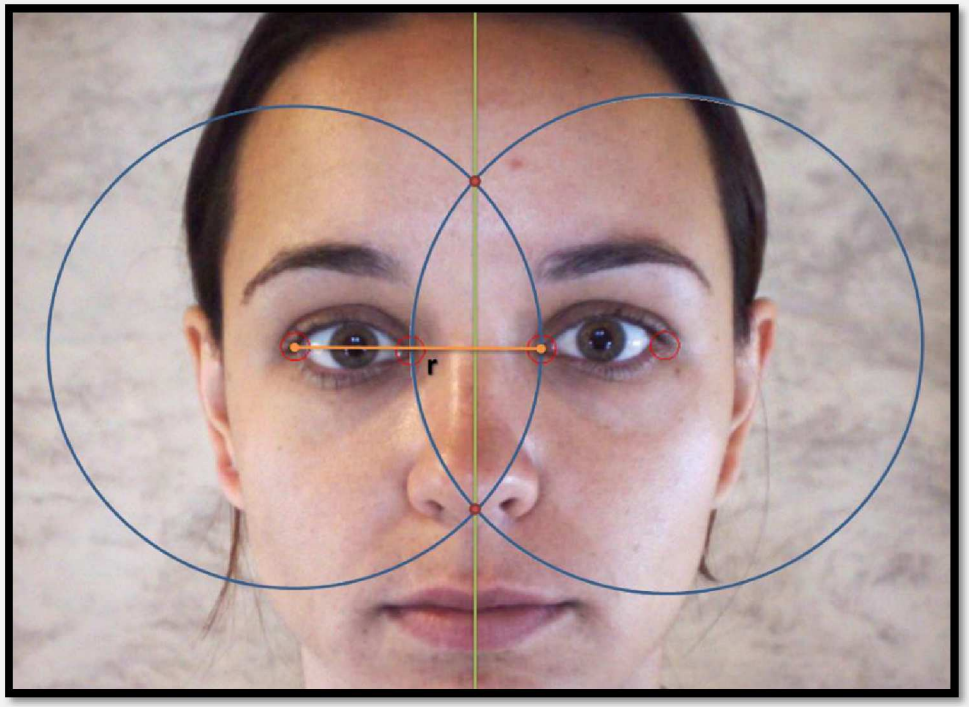

Representation of the orbital midline (green line) arising from the reference circumference of each hemiface (represented in blue), which have, as centers, the *Ectocanthions* points, and, as radii (r), the contralateral *Ectocanthion* - *Endocanthion* distances (represented in orange). The intersection points of the two circumferences (red dots) determine the orbital midline.

APPENDIX

68

PUPIL CENTER

REFERENCE DEFINITION

Ocular reference landmark that appears after the determination of four *Iridions* landmarks (two from each hemiface), being defined as the mid-landmark of the line drawn between the lateral and ipsilateral *Iridions*. The centers of pupils may vary in "y" (ordinate of Cartesian coordinate plane) as a function of variation in position of these reference points. A mean “y” of representative lines of these distances between the ipsilateral points of each hemiface is automatically defined by the software to obtain the center of the pupil reference (which has the same position in "y" for both hemifaces).

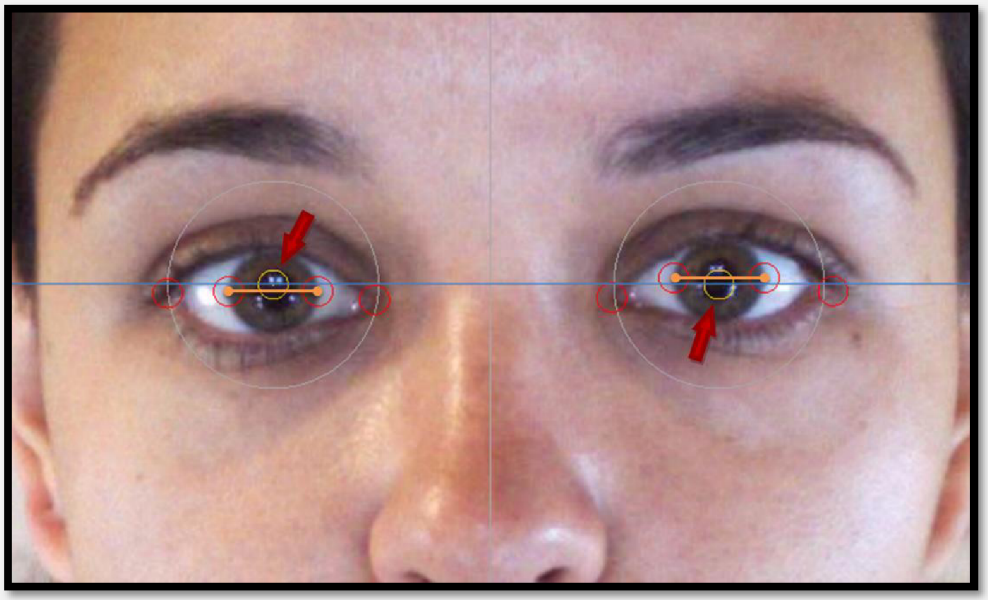

Representation of pupil centers (arrow in red). They are determined horizontally by the average of distances between the ipsilateral *Iridions Mediale* and *Laterale* landmarks (straight in orange). Vertically, they are obtained by the average of the line positions defined by these points. Note that the line representing the distance between the *Mediale* and *Laterale Iridions* on the right side is positioned above the same straight line on the left side. The computer averages the two ‘’y’’ distances to determine the central pupil position on the same line and therefore in the same y-position (shown in blue).

APPENDIX 69

OCULAR CIRCUMFERENCE

REFERENCE DEFINITION

Circumference is defined after the determination of the landmarks *Iridion Laterale* and *Iridion Mediale* of both hemifaces, determined as the circumference with a radius from the center of the pupil to the *Endocanthion*. As the radius can appear different in each hemiface, the average between the two values is calculated automatically by the software, determining the final radius of the reference circumference.

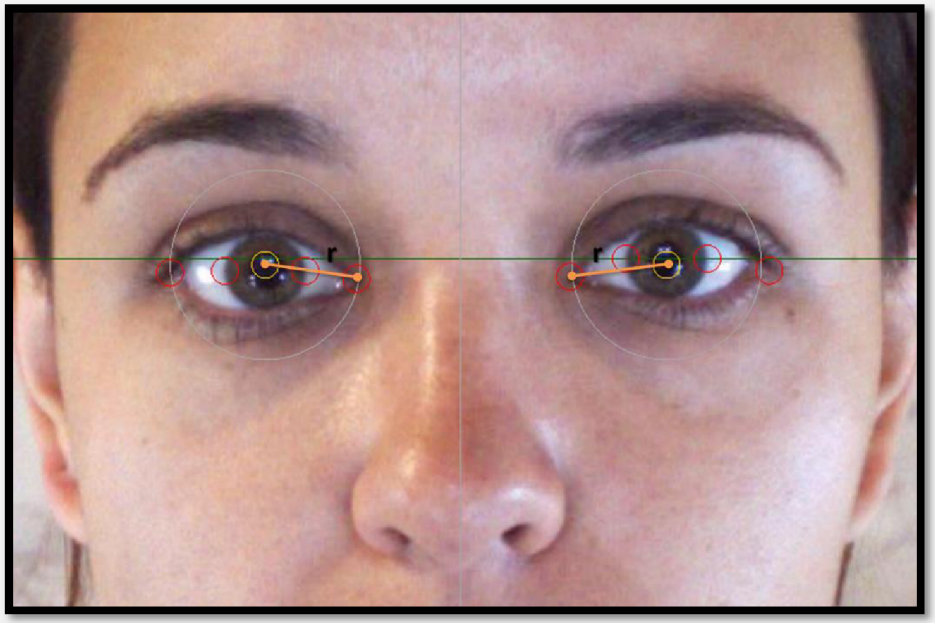

Representation of ocular circumferences (lines in gray). They are defined from the pupil center and have as radius (r) the distance of the center of the pupil to the ipsilateral *Endocanthion* (represented by the orange line). Since these distances may be different in each hemiface, the final circumference will be defined by the radius mean.

REFERENCES

70

1. BULUT, O.; SEVIM, A. The efficiency of anthropological examinations in forensic facial analysis. PBD. 2013; 15(1): 139-158.
2. CATTANEO, C.; OBERTOVÁ, Z.; RATNAYAKE, M.; MARASCIUOLO, L.; TUTKUVIENE, J.; POPPA, P.; GIBELLI, D.; GABRIEL, P.; RITZ-TIMME, S. Can facial proportions taken from images be of use for ageing in cases of suspected child pornography? A pilot study. Int J Legal Med. 2012; 126: 139–144.
3. DAVIS, J.P.; VALENTINE, T.; DAVIS, R.E. Computer assisted photo-anthropometric analyses of full-face and profile facial images. Forensic Sci Int. 2010; 200: 165-176.
4. FISWIG. FACIAL IDENTIFICATION SCIENTIFIC WORKING GROUP. Guidelines for Facial Comparison Methods. 2012. Disponível em: http://www.fiswg.org/FISWG_GuidelinesforFacialComparisonMethods_v1.0_2012_02_02.pdf. [Acesso em 10 mar 2014].
5. FARKAS, J.G.; DEUTSCH, C.K. Anthropometric Determination of Craniofacial Morphology. American Journal of Medical Genetics. 1996; 65: 1-4.
6. FARKAS, L.G. Accuracy of Anthropometric Measurements: Past, Present, and Future. Cleft Palate-Craniovacial Journal. 1996; 33: 10-22.
7. GEORGE, R.M. Facial Geometry: Graphic Facial Analysis for Forensic Artists. Springfield: Charles C Thomas Publisher LTD; 2007.
8. İŞCAN, M.Y. Introduction to techniques for photographic comparison: potentials and problems. In M. Y. İşcan and R. P. Helmer, Forensic Analysis of the Skull: Craniofacial Analysis, Reconstruction, and Identification. New York: Wiley-Liss. 1993: 57–70.
9. KLEINBERG, K.F.; PHARM, B.; VANESIZ, P.; BURTON, M.A. Failure of anthropometry as a facial identification technique using high quality photographs, J. Forensic Sci. 2007; 52(4): 779–783.
10. KLEINBERG, K.F. Facial anthropometry as an evidential tool in forensic image comparison. PhD thesis. University of Glasgow. 2008.
11. KOLAR, J.C.; SALTER, E.M. Craniofacial anthropometry: practical measurement of the head and face for clinical, surgical, and research use. Springfield: Charles C Thomas Publisher LTD; 1997.
12. KRISHAN, K.; KANCHAN, T. Anthropometric and Anthroposcopic Analysis of Face in Forensic Identification-Some Essential. Considerations Medico-Legal Update. 2012; 12(1).
13. MORECROPT, L.; FIELLER, N.R.J.; EVISON, M.P. Investigation of Anthropometric Landmarking in 2D. In: Computer-Aided Forensic Facial Comparison. CRC Press: Boca Raton, FL. 2010: 71-87.
14. MORETON, R.; MORLEY, J. Investigation into the use of photoanthropometry in facial image comparison. Forensic Sci Int. 2011; 212(1): 231-237.
15. PORTER, G.; DORAN, G. An anatomical and photographic technique for forensic facial identification. Forensic Sci Int. 2000; 114(2): 97-105.
16. PURKAIT, R. Anthropometric landmarks: How reliable are they? Anthropometric landmarks. Med Leg Update. 2004;4(4):133-40.
17. ROELOFSE, M.; STEYN, M.; BECKER, P. Photo identification: Facial metrical and morphological features in South African males. Forensic Sci Int. 2008; 177: 168-175.
18. STAVRIANOS, C.; PAPADOPOULOS, C.; PANTELIDOU, O.; EMMANOUIL, J.; PENTALOTIS, N.; TATSIS, D. The use of photo-anthropometry in facial mapping. Research Journal of Medical Sciences. 2012; 6(4): 166-169.
19. STEELE, J. Face to face. Analysis and Comparison of Facial Features to authenticate identities of people in photographs. 2nd Ed. United States of America (Washington): Joelle Steele Interprises, 2013.
20. ZIMBLER, M.S.; HAM, J. Aesthetic Facial Analysis. Otolaryngology-Head and Neck Surgery, Cummings Editor, 4a ed, 2005. Mosby.